<u>A GEOSPATIAL FRAMEWORK TO ESTIMATE DEPTH OF SCOUR UNDER BUILDINGS DUE TO STORM SURGE IN COASTAL AREAS</u>

by

Mariamawit Borga
A Thesis
Submitted to the
Graduate Faculty
of
George Mason University
in Partial Fulfillment of
The Requirements for the Degree
of
Master of Science
Civil and Infrastructure Engineering

Committee:

___________________________________	Dr. Burak F. Tanyu, Thesis Director
___________________________________	Dr. Celso Ferreira, Thesis Co-director
___________________________________	Dr. Viviana Maggioni, Committee Member
___________________________________	Dr. Liza W. Durant, Department Chair
___________________________________	Dr. Kenneth S. Ball, Dean, Volgenau School of Engineering
Date: ______________________________	Spring Semester 2016 George Mason University Fairfax, VA

A Geospatial Framework to Estimate Depth of Scour under Buildings Due to Storm Surge in Coastal Areas

A Thesis submitted in partial fulfillment of the requirements for the degree of Master of Science at George Mason University

by

Mariamawit Borga
Bachelor of Science
Jackson State University, 2014

Director: Burak F. Tanyu, Assistant Professor
Co-Director: Celso Ferreira, Assistant Professor
Department of Civil and Infrastructure Engineering

Spring Semester 2016
George Mason University
Fairfax, VA

DEDICATION

This is dedicated to my family and friends for their unconditional support.

ACKNOWLEDGEMENTS

First I would like to thank God. Then, I would like to express my gratitude to my advisor Dr. Burak Tanyu and co-advisor Dr. Celso Ferreira for their guidance and support throughout these two years. I would also like to sincerely acknowledge Juan Luis Garzon and Mike Onufrychuk for their contributions in data gathering and assistance, SGI research group for their suggestions and support, my friends for their support and finally I would like to thank the committee members for taking their time and giving feedback.

TABLE OF CONTENTS

LIST OF TABLES

LIST OF FIGURES

LIST OF EQUATIONS

ABSTRACT

A GEOSPATIAL FRAMEWORK TO ESTIMATE DEPTH OF SCOUR UNDER BUILDINGS DUE TO STORM SURGE IN COASTAL AREAS

Mariamawit Borga, M.S.

George Mason University, 2016

Thesis Director: Dr. Burak F. Tanyu

Thesis Co-Director: Dr. Celso Ferreira

Hurricanes and tropical storms represent one of the major hazards in coastal communities. Storm surge generated by strong winds and low pressure from these systems have the potential to bring extensive flooding in coastal areas. In many cases, the damage caused by the storm surge may exceed the damage from the wind resulting in the total collapse of buildings. Therefore, in coastal areas, one of the sources for major structural damage could be due to scour, where the soil below the building that serves as the foundation is swept away by the movement of the water. The existing methodologies to forecast hurricane flood damage do not differentiate between the different damage mechanisms (e.g., inundation vs. scour). Currently, there are no tools available that predominantly focus on forecasting scour related damage for buildings. Such a tool could provide significant advantages for planning and/or preparing emergency responses. Therefore the focus of this study was to develop a methodology to predict possible scour depth due to hurricane storm surges using an automated ArcGIS tool that incorporates the expected hurricane conditions (flow depth, velocity, and flood duration), site-specific building information, and the associated soil types for the foundation. A case study from Monmouth County (NJ), where the scour damages from 2012 Hurricane Sandy were recorded after the storm, was used to evaluate the accuracy of the developed forecasting tool and to relate the scour depth to potential scour damage. The results indicate that the developed tool provides relatively consistent results with the field observations.

1 INTRODUCTION

Storm surge is considered as one of the major causes of coastal inundation (Wolf 2009). Each year, there is an estimated 6 billion dollars' worth of damage caused by floods in the United States (Hallegatte 2013). A more recent example of hurricane surge and inundation is Hurricane Sandy, which impacted the east coast of the U.S. in 2012, creating damage due to flooding and strong winds (Hatzikyriakou et al. 2015). Although the storm was classified as category 1, at the time of the landfall based on the Saffir-Simpson Hurricane Scale, approximately 37,000 primary residences in New Jersey suffered from damages brought by hurricane (FEMA 2013).

Accurately estimating hurricane induced flood damage is essential to long term coastal resilience planning, support recovery efforts, and insurance purposes. While significant progress has been made in documenting damage after the occurrence of natural hazards (e.g., IPET 2007; FEMA 2013), forecasting damage due to hurricane storm surge to different infrastructure types is still subject of many active research (Kreibich et al. 2010; Nadal et al. 2010; Liu et al. 2012; Jongman et al. 2012; Banks et al. 2014; Tate et al. 2014; Xian et al. 2015; Wagenaar et al. 2015). Although correct damage estimation may not be able to directly prevent the total damage, it can support emergency management actions before the hazard and avoid fatalities. Additionally, it provides an important tool for planning purposes to help with decision making before designing residential areas along the coastlines. The most commonly used flood damage estimation approaches are based on relating the estimation of flow depth to the building damage based on previous observations in other areas (Kreibich et al. 2010; Nadal et al 2010; Jongman et al. 2012). Current research in this area has led many different countries to develop their own unique models based on publicly available data and the type of flooding observed such as the Multi-Coloured Manual (MCM) for the United Kingdom (Penning Roswell et al. 2005) and Flood Loss Estimation Model (FLEMO) in Germany (Kreibich et al. 2010). In the United States, HAZUS is the most commonly used damage estimation model for floods, developed by the Federal Emergency Management Agency (FEMA) (Scawthorn et al. 2006; FEMA 2009; and Wagenaar et al. 2015). HAZUS is a multi-hazard (MH) model that includes the estimation of damages due to high winds and earthquakes. The coastal flood model incorporated in HAZUS-MH is often used to assist flood damage estimation in the United States. It utilizes the location, building inventory and properties (such as first floor elevation, age of the structure, and presence of basements), and flooding characteristics to estimate damage and associated replacement cost. Although this model is commonly used, it has two major limitations for this study: (a) the estimated damage is for individual census block and do not differentiate the damage loss per building, and (b) flood damage estimation is based on the empirically developed depth-damage curves from previous hurricanes and the damage type is not differentiated specifically (FEMA 2009; Nadal et al. 2010). The major factors that contribute to HAZUS-MH flood model are flow depth, velocity, and flood duration, which is more comprehensive than other flood models such as FLEMO and MCM as these models are solely based on flow depth (Wagenaar 2015). The damage value for FLEMO is estimated based on the replacement cost, while the damage value for MCM is based on depreciated values. In HAZUS-MH the user can choose either to use the replacement value or depreciated value (Jongman et al. 2012). However, in all of these models, the estimated damage value is specific to the country where the model was developed for, and in none of these models the damage type is differentiated.

The impact of a hurricane in buildings and infrastructures could be attributed to hydrodynamic and hydrostatic forces, waves, debris forces, lateral loading, erosion, and scour (Robertson et al. 2007). Scour is a phenomenon that removes sediments from or around piers, abutments, and building foundations by the hydrodynamic forces caused by water. Excessive scour has the ability to remove the passive resistance provided by the soil to the structure, causing a complete structural failure as recognized by others previously (Kohli and Hager 2001; Nadal et al. 2010; Chen et al. 2013; FEMA 2013; Xian et al. 2015). The interest to evaluate scour damage has been a subject to many researches throughout the years. However, these studies primarily focus on estimating scour for piers and abutments due to riverine floods and not particularly associated with hurricanes (Shen et al. 1969; Froehlich 1989; Briaud 1999; Briaud et al. 2009; Deng and Cai 2010; Arneson et al. 2012; Govindasamy et al. 2013). Estimating scour damages in rivers is relatively easier to define since around these structures, water flows within well-defined boundaries. In the case of hurricanes, often, water with high velocity may flow for a limited time in between buildings and not necessarily following within well-defined flow geometry. Also, in the case of bridge and pier scour, it is easier to estimate the ultimate scour based on the constant flow condition assumptions. In the case of hurricanes, limited inundation time plays an important role and must be carefully considered to properly estimate building scour depth (Zevenbergen 2004), adding an extra difficulty to the problem. Yet, most of the existing methods do not take into account the time and only attempt to differentiate the scour development with different soil types. Therefore, the use of bridge scour equations to estimate hurricane driven flood without modifications will lead to unreliable scour damage (Nadal et al. 2010). There is a significant gap in the literature on estimating scour for building foundations, and only few researchers have addressed this problem. In this study only two empirical equations, developed by Kohli and Hager (2001) and Nadal et al. (2010), could be found to estimate scour for building foundations located in coastal areas. These estimations took into account the effect of building geometries, detailed flow and soil characteristics, including the flood duration. An accurate estimation of the scour damage requires consideration of flow depth, velocity of the water, and flood duration (Kohli and Hager 2001, Nadal et al. 2010). These inputs for the scour damage equations can be attained from different sources such as storm surge numerical models and publicly available data.

The purpose of this research was to develop a geographic information system (GIS) based framework to forecast depth of scour within building foundations constructed in coastal areas. Therefore, an approach was established by combining existing building scour equations, storm surge model, publicly available soil and building information to create an automated GIS tool based on the ArcGIS™ platform. This methodology could be applied to any region with different soil conditions for different storms to forecast scour depth, unlike the existing flood models that are restricted to the region it was developed for. The performance of the developed framework was then evaluated by implementing it to a case study during Hurricane Sandy. Furthermore, this framework can potentially be used for risk assessment, planning and/or preparing for emergency responses to better prepare for the storm, avoid fatalities, save money by taking precautions ahead of time, and implementing mitigation plans.

2 FRAMEWORK

A tool for estimating scour depth underneath buildings was developed using the *model builder tool* in ArcGIS^{TM}. Fig. 1 shows the framework developed to create the ArcGIS based tool. The framework consisted of three components: (a) storm surge modeling to obtain hydrodynamic data such as flow depth, velocity, and flood duration, (b) accessing public database to attain building footprints and soil characteristics for the foundation and (c) implementing existing building scour equations. Details of each component are described below.

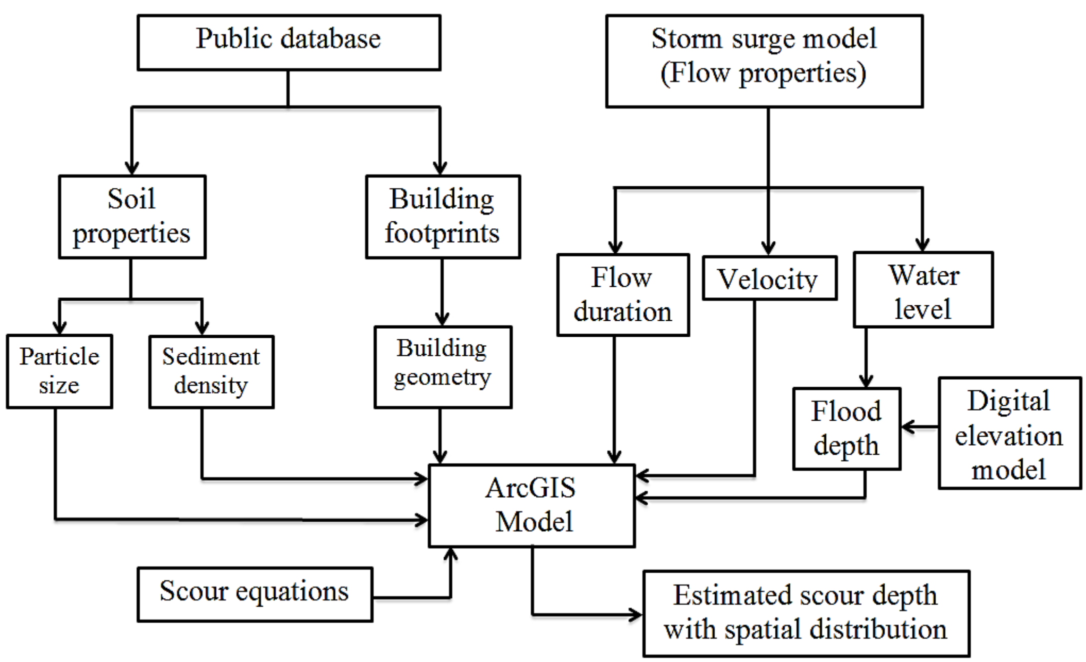

Fig. 1 Developed framework to estimate building scour depth spatially

2.1 Storm Surge

Storm surge is a potentially devastating rise in the sea surface caused by tropical or extratropical cyclones (Resio and Westerink 2008). In order to develop a realistic forecasting model, the ArcGIS based tool must incorporate the specific hydrodynamic conditions that are associated with specific storm surge caused by a hurricane scenario. Determining the hydrodynamic conditions directly from a ArcGIS platform is not possible, but there is existing public data information and numerical models such as Advance Circulation model (ADCIRC), Finite Volume Coastal Ocean Model (FVCOM), Semi-implicit Eulerian Lagrangian Finite Element Model (SELFE) specifically developed to simulate storm surge (Kerr et al. 2013).

During the last years, multiple studies have provided publicly available data for historical flood events. For instance, the FEMA Modeling Task Force (MOTF) study reported flow depth measured at different locations and at building scale after Hurricane Sandy (2012). Moreover, the North Atlantic Coast Comprehensive Study (NACCS) report of the U.S. Army Corps of Engineers (USACE) simulated maximum water elevations for historical coastal flooding events. However, these types of reports will only provide post event data at sparse locations. In order to develop a scour damage model that may be implemented in different areas, modeling the storm surge is the most viable option. Therefore, the model can simulate water levels, velocity and flood duration, and after a post processing process, this information can be used as inputs for the model used to estimate scour depth. Storm surge models have been widely used to estimate flooding in coastal areas (e.g., Bunya et al. 2010; Dietrich et al. 2010 and Ferreira et al. 2014) and they might represent a reliable tool for calculating water levels, velocity of the water, and the flood duration of the flood event. One widely used storm surge model is the Advance Circulation model (ADCIRC) (Westerink et al. 2008). ADCIRC is a finite element based model that simulates time series water levels by solving the generalized wave continuity equation and velocities by using the vertically integrated shallow water momentum equations. This model showed a high level of accuracy for estimating tides, riverine flow, and storm surge for Hurricanes Katrina and Rita (2005) (Bunya et al. 2010; Dietrich et al. 2010;). Furthermore, ADCIRC is capable of running on an unstructured mesh using a parallel communication system, allowing a high degree of scalability and integrating seamlessly the physics and numerics from ocean to floodplain (Dietrich et al 2010). Therefore for the purposes of this study, ADCIRC model is used to obtain site-specific storm surge data, which is then incorporated into the ArcGIS platform for the scour model.

Before running the storm surge model, a collection of public information dataset must be taken. This public dataset involves: (1) geographical and elevation information, (2) land cover information, (3) astronomical tidal constituent's information, and (4) meteorological information. (1) For the geographical and elevation information, the numerical model needs an unstructured mesh to perform the simulations, and it consists of a group of triangular elements and nodes, defined by its longitude, latitude and elevation. Currently there is a wide available source of numerical grids or also, the user could build a numerical grid for the study region based on topography data, which is available from variety of sources (Digital elevation model U.S. Geological Survey

(USGS), USGS National Elevation Dataset (NED) elevation data and bathymetry data (NOAA ETOPO2v2), data from US Department of Commerce 2006, Coastal Relief Model, Shoaling Waves Experiment, etc.). (2) For the land cover information, surface roughness associated to a given land cover is an important factor as it causes loss of energy in the movement of the water. Resio and Westerink (2008) emphasized that surface roughness might have a significant impact on storm surge wave propagation over water ways and over land areas. The two most widely used land cover data set are USGS National Land Cover Data (NLCD) and USGS National Gap Analysis Program (GAP). (3) Tides (driven by the movement of the Sun, Moon, and planets) play an important role in storm surge. The global ocean tide model of Le Provost et al. (1994) contains astronomical tidal constituent's data essential to properly run the storm surge model. (4) Meteorological agencies such as NOAA release a wide source of meteorological products, which are indispensable to generate storm surge. Some of these products are part of the Best Track database from National Hurricane Center (NHC) or North American Model (NAM) from National Center for Environmental Prediction (NCEP).

As it is mentioned previously, the storm surge model outputs need to be processed to be incorporated into the scour model, which is discussed in the subsequent sections of this manuscript. This post processing requires land surface elevation information, as for example determined from the Digital Elevation Model (DEM) dataset. DEM can be downloaded from National Elevation Dataset (NED) provided by the U.S. Geological Survey (USGS).

2.2 Available Public Data

In the United States, specific building footprints and soil characteristics are publicly available. In addition, the flow depth data from FEMA MOTF might also exist after the event. Public databases for building footprints may be obtained from the state or county building database. The data provided will typically include a shape file of the building footprints and this information may be incorporated into ArcGIS platform to obtain the building geometry.

Soil characteristics of an area may be extracted from soil maps and surveys available from the soil survey geographic database or county/state databases. This information is used to obtain the soil inputs (particle sizes and sediment density) for the scour damage model. The most common source for this information in the U.S. is the Soil Survey Geographic (SSURGO) database that is managed by the National Cooperative Soil Survey. This dataset includes soil classification and for the purposes of developing an ArcGIS based tool, utilizing the grain size distribution is essential to identify the median particle size (d_{50}) and particle size that corresponds to 90% of the particles to be finer (d_{90}). The definitions of how to obtain d_{50} and d_{90} from the soil data are readily available in many soil mechanics textbooks (Das and Sobhan 2006, Coduto et al. 2011). The sediment density range for the soils can also be obtained from books and different studies (Hillel 1980; Blake and Hartge 1985; Boyd 1995; Avnimelech et al. 2001). Sediment density is defined as the ratio of soil mass to the volume of the soil (Avinmelech et al. 2001).

2.3 Building Scour Equations

Currently there are only two empirical equations (Kohli and Hager 2001; Nadal et al. 2010) found that specifically estimate scour at building foundations based on specific flow velocity, flood duration, flow depth, building geometry, and soil characteristics. For the purposes of this study, both empirical equations are coded into the ArcGIS platform to estimate scour.

2.3.1 Kohli and Hager Equation

Kohli and Hager (2001) developed an equation to describe building scour based on an experimental study, which accounted for flow characteristics, building geometry, and soil characteristics. About 60 experiments were conducted in a flume simulating a horizontal floodplain. The experiments were conducted with cohesionless soils with particle sizes ranging between 1.3 and 2.74 mm, building widths between 0.05 and 0.4 m, and flow depths between 40 and 150 mm. These conditions simulated based on a Froude similarity law.

The equation developed by Kohli and Hager (2001) to estimate scour depth (z) for building foundations is presented below:

$$z = \underbrace{\left(\frac{1}{10}\overbrace{\left(\frac{\mathrm{V}}{\left(\underbrace{\left[\frac{(\rho s-\rho)}{\rho}\mathrm{g}\right]}_{g'}\mathrm{d90}\right)^{0.5}}\right)}^{Fd^2}{}^{2}\log_{10}\left(\frac{1}{10}\left(\underbrace{\frac{\left(\overbrace{\left[\frac{(\rho s-\rho)}{\rho}\mathrm{g}\right]}^{g'}\mathrm{d90}\right)^{0.5}}{\mathrm{ho}} * \mathrm{t}}_{T}\right)\right)\right)}_{Z}(\mathrm{b}\times\mathrm{ho})^{0.5} \qquad (1)$$

where:

z = scour depth (m)

F_d = densimetric particle Froude number

g' = reduced gravitational acceleration (m/s^2)

T = non-dimensional time

Z = dimensionless scour depth

b = building width (m)

h_o = flow depth (m)

t = flood duration (hour)

V = velocity (m/s)

d_{90} = 90% finer particle size (m)

ρ = fluid density (1 g/cm^3)

ρ_s = sediment density (g/cm^3)

g = gravitational acceleration (9.81 m/s^2)

2.3.2 Nadal et al. Equation

Nadal et al. (2010) developed an equation to analyze building scour by modifying the existing equations (Colorado State University and Barkdoll 2000) that were previously developed to analyze bridge piers and abutments. The equation developed by Nadal et al. (2010) account for the time-effect from the flow and a parameter to simulate the scour phenomena occurring on the corners of the buildings. The equation proposed by Nadal et al. (2010) is primarily based on the evolution of the scour equation developed by Colorado State University and time-scale factor developed by Barkdoll (2000). The modified Colorado State University (CSU) scour equation is for piers, and incorporates the flow and soil characteristics as well as the pier geometry including square shapes (Jones 1983; Richardson and Davis 2001). However, this equation does not take into account the flood duration. To account for the flood duration, Nadal et al. (2010) incorporated the time scale factor that was developed by Barkdoll (2000) into the scour equation. The time-scale factor developed by Barkdoll (2000) is based on combination of the laboratory data generated by the researcher from circular and non-circular piers and data generated by Melville and Chiew's (1999), which was limited for cylindrical bridge piers.

The methodology developed by Nadal et al. (2010) incorporates the CSU equation with the correction factor to account for the square shape condition as well as half of the building width. The building width is taken as half of the building width because of scour developing on the corners of the building instead of developing in the middle which is the case with bridge piers and the time-scale factor presented by Barkdoll (2000) to account for flood duration.

The equation developed by Nadal et al. (2010) to estimate scour depth (Zt) at a building foundation is presented below:

$$\mathbf{z} = \left(\underbrace{\left(\mathbf{2.2}\left[\frac{\mathbf{bf}}{\mathbf{ho}}\right]^{\mathbf{0.65}}\right) \times \left(\frac{\mathbf{V}}{\underbrace{(\mathbf{g}\times\mathbf{ho})^{\mathbf{0.5}}}_{Fr}}\right)^{\mathbf{0.43}} \times \mathbf{ho}}_{Zt}\right) \underbrace{\times\, (\mathbf{exp}\left\{-\,\mathbf{0.25}\,.\left|\frac{\overbrace{\left(\mu\mathbf{c}\times\left(\mathbf{5.75\,log}\left(\mathbf{5.53}\frac{\mathbf{ho}}{\mathbf{d50}}\right)\right)\right)}^{Vc}}{\mathbf{V}}\,\mathbf{ln}\left(\frac{\mathbf{tf}}{\underbrace{\mathbf{51.95}\times\frac{\mathbf{bf}}{\mathbf{V}}\left(\frac{\mathbf{V}}{\mathbf{Vc}}-\mathbf{0.4}\right)\left(\frac{\mathbf{ho}}{\mathbf{bf}}\right)^{\mathbf{0.25}}}_{tu}}\right)\right|\right\})}_{Kt} \tag{2}$$

where:

z_t = scour depth at a building foundation (m)

z = Final scour depth (m)

b_f = one half width of building in the direction of the flow (m)

h_o = flow depth (m)

F_r = Froude number

V = Flood water velocity (m/s)

g = gravitational acceleration (9.81 m/s^2)

K_t = time scale correction factor

t_f = flood duration (hour)

t_u = time required for development of maximum scour depth (hour)

V_c = critical floodwater velocity (m/s)

d_{50} = median particle size (mm)

μ_c = critical shear velocity (m/s)

($\mu c = 0.0115 + 0.0125\ (d50^{1.4})$ for $0.1\ \text{mm} < d50 \leq 1\ \text{mm}$ and

$\mu c = 0.0305 d50^{0.5} - 0.0065\ (d50^{-1.0})$ for $1\ \text{mm} < d50 \leq 100\ \text{mm}$)

(Note: The critical shear velocity equation (μ_c) requires d_{50} in mm)

2.3.3 Similarities and Limitations of these Equations

Both building scour equations developed by Kohli and Hager (2001) and Nadal et al. (2010) account for building geometry, flow characteristics such as flow depth, flood duration and velocity, and soil characteristics. However, both equations have limitations that should be recognized when using these equations to estimate building scour damage.

Kohli and Hager (2001) have stated that their equation is only applicable:

- for cohesionless soils,
- soil particles sizes (d_{90}) greater than 0.5 mm,
- flow depth larger than 25mm,
- dimensionless time between 10 and 10^6,
- densimetric Froude number up to about 3,
- building width of the intermediate range ($1 \leq b/h_o \leq 25$) and

Nadal et al. (2010) scour equation only applies to:

- for cohesionless soils,
- soil particle sizes (d_{50}) between 0.1mm and 100 mm,
- Conditions where the ratio of velocity to critical velocity (V/V_c) greater than 0.4 and less than or equal to1.

Eq. 1 is primarily based on experimental study and Eq. 2 is based of modifying existing equations. To the best of the author's knowledge the scour depths estimated from both of these equations have never been compared before with real time observed conditions.

2.3.4 Sensitivity Analyses

Before implementing the building scour equations in the ArcGIS based geospatial model, the existing scour equations were evaluated for their sensitivity to changes on input parameters related to flow, soil, and building characteristics. Altogether 73 analyses were performed using Eqs.1 and 2. Table 1 displays a range of parameters and magnitudes considered for the analyses. The selected range of parameters for building widths and particle sizes are based on the dataset obtained from Monmouth County, for flood duration, velocity, and flow depth are from a storm surge model simulated for the study region, and for sediment density is based on Hillel (1980) and Avnimelech et al (2001).

Table 1 Range of parameters and magnitudes used for sensitivity analyses

Parameters	Magnitudes
Building width- b(m)	10, 20, 30, 40, 50, 60
Flow depth- h_o (m)	0.06, 0.46, 0.86, 1.26, 1.66, 2.06, 2.46, 2.86, 3.26, 3.66
Velocity- V (m/s)	0.0001, 0.23, 0.46, 0.55, 0.69, 0.71, 0.88, 0.92, 1.04, 1.15, 1.21, 1.37, 1.54, 1.61, 1.7, 1.84, 1.87, 2
Median particle size- d_{50} (m)	0.00017, 0.00019, 0.00021, 0.00025, 0.0003, 0.0004, 0.00043, 0.00052, 0.00061, 0.00063
90% finer particle size- d_{90} (m)	0.00053, 0.0006, 0.0012, 0.0014, 0.0015, 0.0017, 0.0018, 0.0025, 0.003, 0.0035
Sediment density- ρ_s (g/cm^3)	2.6, 2.65, 2.7
Flow duration - t (hours)	1, 12, 18, 24, 48, 72, 96, 120, 144, 162

The sensitivity analyses were performed by altering a single parameter while keeping the other parameters constant. For example, the effect of flow depth was analyzed by changing the flow depth incrementally from min. to max. values (i.e., 0.06 to 3.66 m) while keeping the building width, velocity, particle size, sediment density, and flood duration constant. Each scenario was evaluated for six different building widths ranging from 10 to 60 m as obtained from the Monmouth county database.

Fig. 2 presents the sensitivity analyses results based on average range of parameters for the study region for each building width. The trends observed in Fig. 2 also very similar to the trends observed in all analyses. As shown on Fig. 2, the estimated scour magnitude increased on both scour equations with increase in flow depth, velocity, flood duration, and building width. Arneson et al. (2012) also stated that scour depth increases with an increase in velocity and flow depth. Also, for both scour equations the estimated scour depth decreased as the soil particles became coarser (larger). The observed sensitivity based on particle size is consistent with other studies such as by Ettema (1980) and Arneson et al. (2012). Based on the analyses, velocity, particle size and flow depth are the most sensitive parameters for Eq. 1, and velocity, and flood duration for Eq. 2. However for both equations, velocity appears to be the most important parameter. For Eq. 1, the scour depth was not drastically affected by the changes of sediment density.

Overall results from the sensitivity analysis indicate that there is a difference in estimated scour depth magnitudes between Eq. 1 and 2. This difference is further discussed in the subsequent sections.

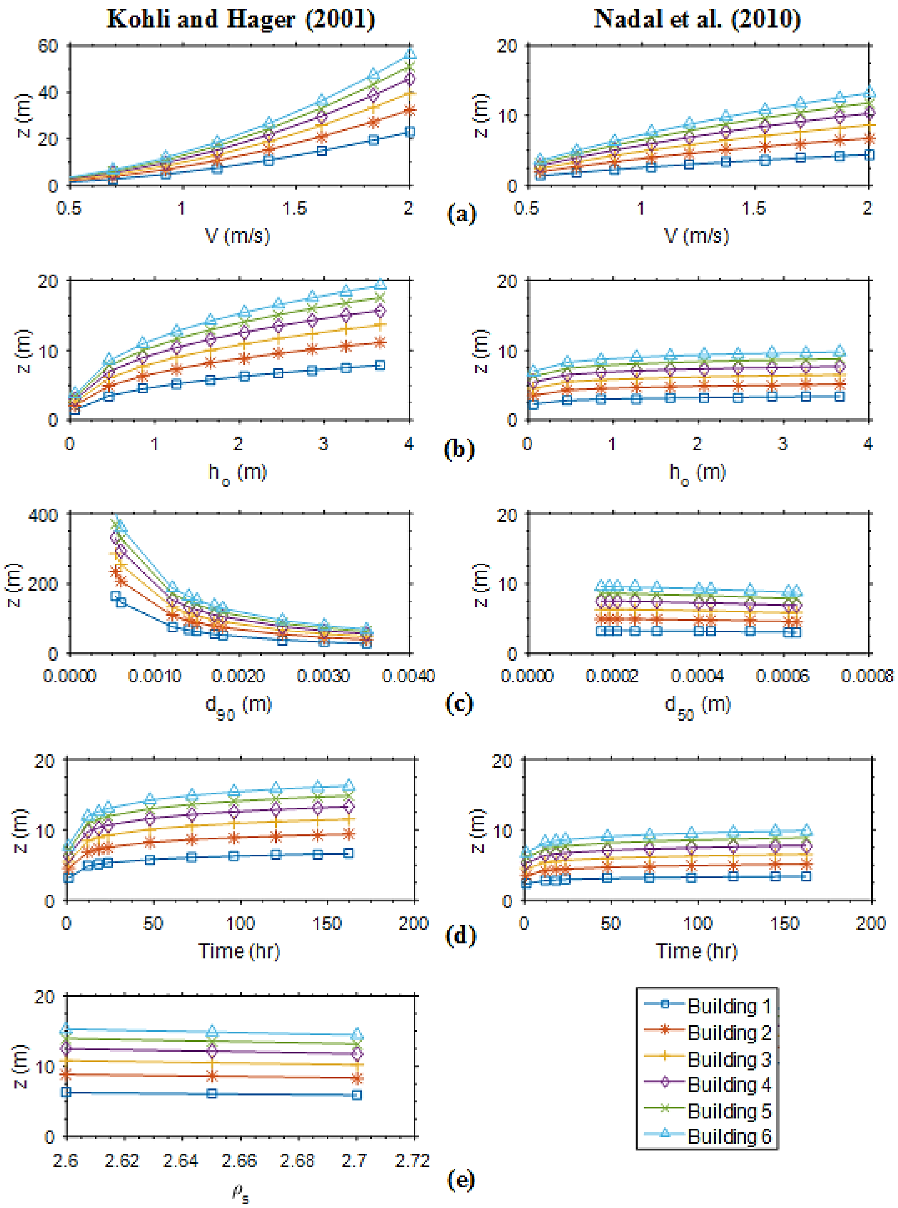

Note: All results shown above were based on average flow depth, flood duration, velocity and for Kohli and Hager (2001) average d_{90} and sediment density and for Nadal et al. (2010) average d_{50}

Fig. 2 Variation of scour depth *(z)* against: **a** velocity *(V)*; **b** flow depth *(h_o)*; **c** particle size *(d_{50}, d_{90})*; **d** flood duration *(time)*; **e** sediment density *(ρ_s)*.

2.4 Automated GIS Tool

To create an ArcGIS tool, the input parameters for the scour equations such as the hydrodynamic data, building geometry and soil information needs to be extracted. The steps to extract building geometry, soil and hydrodynamic data is discussed below.

2.4.1 Building data collection

The *model builder tool* in ArcGIS (Schaller J, Mattos C 2001) was used to develop a tool to seamlessly estimate scour damage in buildings. This tool requires specific parameters that can be obtained from the components discussed above. The building shapefile obtained from the state databases usually lacks the coordinate information for the building footprints. Therefore, it is necessary to simplify and define the geometry of each building (width), as well as their orientations. Fig. 3 illustrates the steps to create building geometry database in ArcGIS model in order to obtain building width and direction of the width. As shown on Fig. 3, first the shape file obtained from the public database is added to ArcGIS and the *simplify building tool* found in ArcGIS to simplify the building footprint is applied by removing majority of vertices and leaving most of the buildings with four vertices. Secondly, the *feature to line tool* also found in ArcGIS is applied to convert the building polygons to lines and apply *split line at vertices tool* to split the lines at the vertices into four separate features. Thirdly, after the building width is divided at the vertices, the distance of the building widths are estimated by applying *calculate geometry tool* found on ArcGIS. Next the angle of the building width is calculated by applying *field calculator* as shown on Fig. 3. Finally, the direction of the building width based on the angle is calculated and by using *field calculator* the building width is assigned north if the angle of the width lies between 0 - 45° and 315 - 360°, South 135 - 225°, East 45 - 135° or West 225 - 315°. The code used to calculate the building angles and to assign the building width is given in Appendix B.

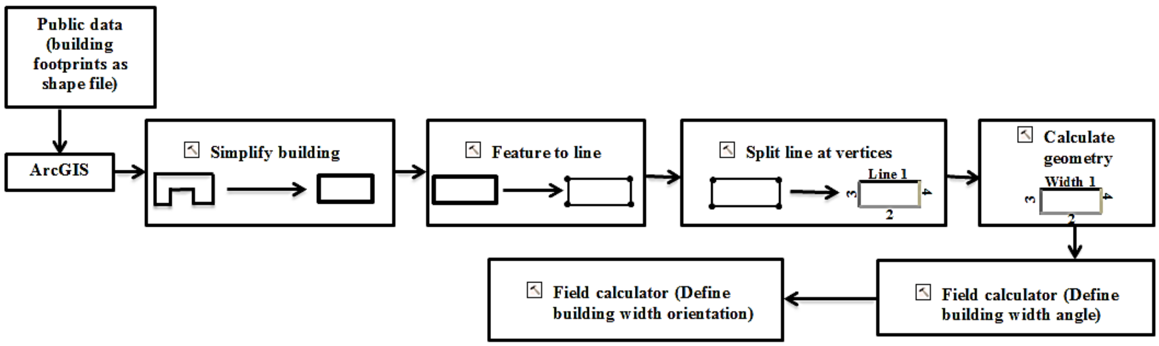

Fig. 3 Flow chart for creating building database in ArcGIS

2.4.2 Hydrodynamic data collection

The steps to process the hydrodynamic data from the storm surge model and incorporate them into the scour damage model at individual building scale are shown on Fig. 4. There are two different components involved: (1) maximum velocity and flood duration that will be obtained by using fishnet points (points at the center of each fishnet cell), and (2) the flood depth that will be obtained by an interpolation. Therefore, first fishnet points for the study region must be created by using *create fishnet tool* found in ArcGIS. Each created point comes with a unique feature id (FID) number and x and y coordinates must be added using the *add XY coordinate tool* on ArcGIS. This information is used to record stations where the model will provide maximum velocities at x and y directions, and water level time series. Thus, the flood duration is extracted from these water level time series. To integrate flood duration and maximum velocity into the ArcGIS tool, these parameters must be joined and assigned to each fishnet point based on their FID number. Conversely, the process to obtain flow depth, as it is shown in Fig. 4, is significantly different. Maximum water levels are estimated by the model on a discrete number of locations (nodes of the numerical grid) as the model results are not spatially continuous. Therefore, first it is necessary to transit from maximum water levels at specific locations to a spatially continuous map (the entire study region) by using an interpolation scheme (i.e., *spline)*. Second, in order to obtain a flood depth map, the elevation from a digital elevation model (DEM) must be subtracted from the maximum water levels map created in the previous step. It is very important both maps have the same vertical datum. In the case descried in this manuscript, the vertical datum was NAVD 88. An example of fishnet points and the steps to obtain the flood duration and maximum velocity within those points are presented in Appendix C.

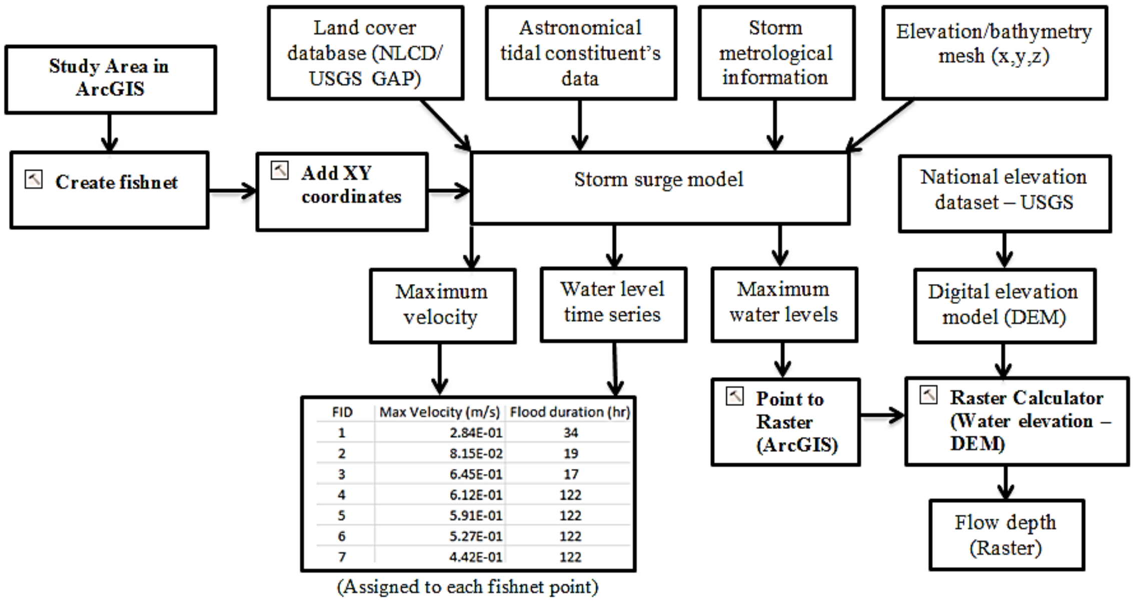

Fig. 4 Flow chart to create hydrodynamic database in ArcGIS

2.4.3 Soil data collection

The soil data obtained from state or county database comes in the form of ArcGIS layer and usually lacks d_{50}, d_{90}, and ρ_s values for the soil type. Therefore, plotting the grain size distribution curve is important to determine the particle sizes (d_{50}, d_{90}) and also, to assume sediment density values, which are then joined to the soil map using *join tool* in ArcGIS as shown on Fig. 5. The grain size distribution, particle sizes for all soils found in the study area and an example how to determine the particle sizes (d_{50}, d_{90}) and assign the sediment density is presented in Appendix D.

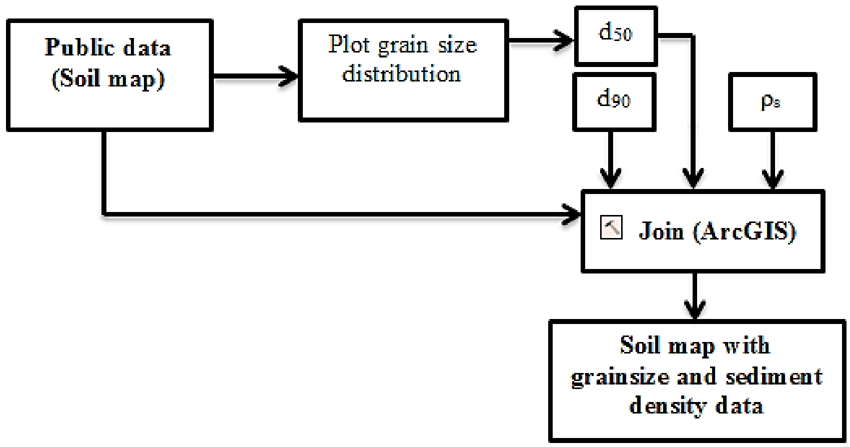

Fig. 5 Flow chart to create soil database in ArcGIS

2.4.4 Data processing

Fig. 6 illustrates the steps to join the input parameters (hydrodynamic and soil) data with the building geometry data. First, the building geometry data is merged with the fishnet point, which contains the storm surge data (maximum velocity and flood duration) using *spatial join tool*. Therefore, the data from the storm surge model (flood duration and maximum velocities) must be associated to each building based on the lowest distance between a fishnet point and those buildings. Second, the flow depth value must be assigned to each building by using the *extract tool* to extract the values based on the building polygon location. Then, the soil data must be joined with the building data using the *intersect tool*. The input parameters required to estimate scour depth for both scour equations are in the building geometry polygon.

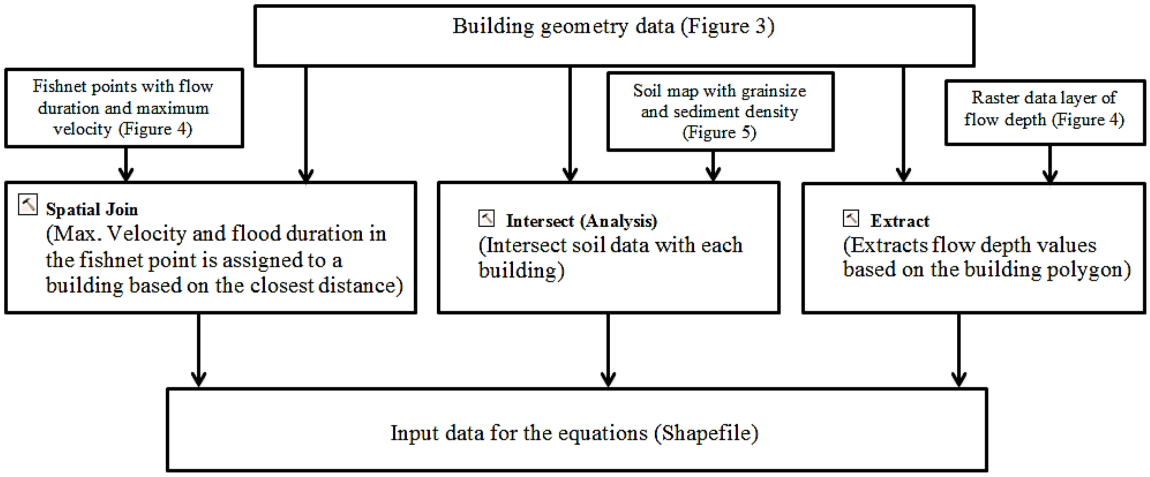

Fig. 6 Flow chart data processing for scour damage estimation in ArcGIS

Subsequently, two models are created in the *model builder tool*: Kohli and Hager (2001) Eq. (1) model and Nadal et al. (2010) Eq. (2) model as shown on Fig. 7. Furthermore, a scale factor should be applied to Eq. (1) to find relationship with Eq. (2). This is important because ranges of the scour depth for these equations are different as observed on the sensitivity analyses. Therefore the scale factor is needed to create a scour range to apply one damage classification for both equations and also for comparison. Finally the outputs obtained from Eq. (1 and 2) have to be evaluated based on the limitations of the equations used to predict scour as depicted on Fig. 7. Thus, conditional statements that contain the limitations of both Eq. (1 and 2) are subjected to the scour estimates. These constraints will ensure that the scour estimates satisfy the limitations of the equations. If the limitations are not satisfied, there will be no scour prediction. If the limitations are satisfied, the ArcGIS tool will be able to estimate scour depth with spatial distribution at a building scale.

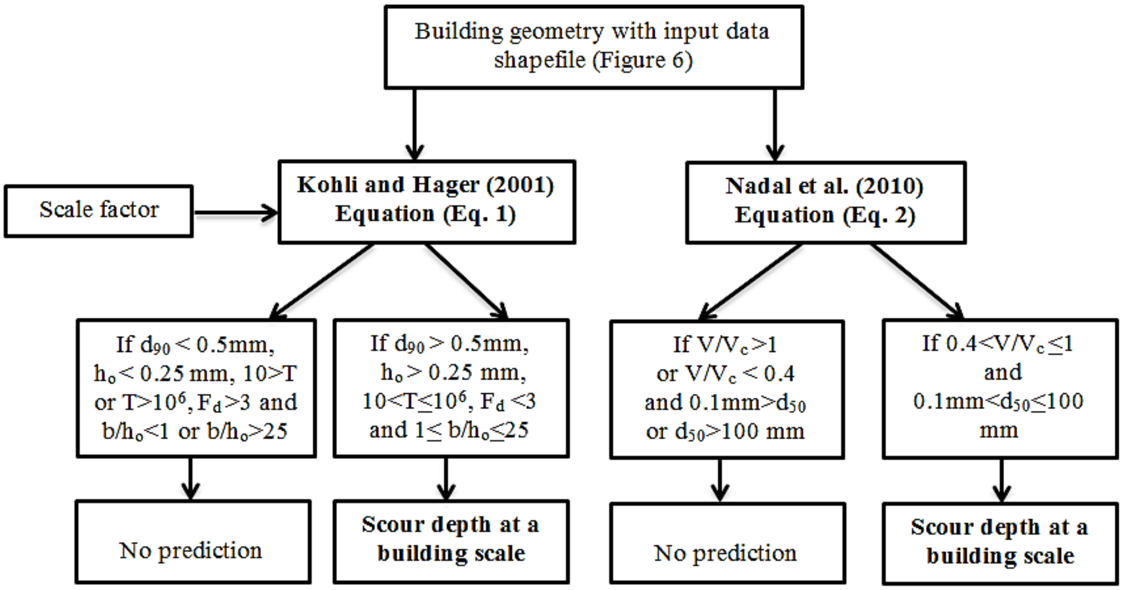

Fig. 7 Integration of scour equations into ArcGIS model for spatial distribution

3 CASE STUDY: APPLICATION TO HURRICANE SANDY

The developed ArcGIS framework can be implemented to forecast scour depths within the foundation under the building due to storm surge flooding an area. To test and demonstrate the developed framework, the ArcGIS tool was implemented to a known hurricane event in the New Jersey area to predict the scour depth. Furthermore, outputs of ArcGIS tool were compared with the observed damage in the field to relate the estimated scour depth to scour damage and to evaluate the consistency of the tool.

3.1 Study Region

Monmouth County (NJ) was selected to implement the ArcGIS framework (Fig. 8).This area was selected as the region of interest because there are publicly available flood damage reports from FEMA after Hurricane Sandy and, in addition, the authors had the opportunity to visit the site before and after the hurricane. The authors surveyed some areas in the study region and documented the observed damage by taking photographs of buildings. Area 5 shown on Fig. 8 is the fifth area observed by the authors that consists of 223 buildings. It was observed that there were damaged buildings due to scour and inundation in this area. This area was selected due to the availability of field photos that show scour and inundation damage. Also, the soils in this area are primarily cohesionless, which is an important factor for the available building scour equations.

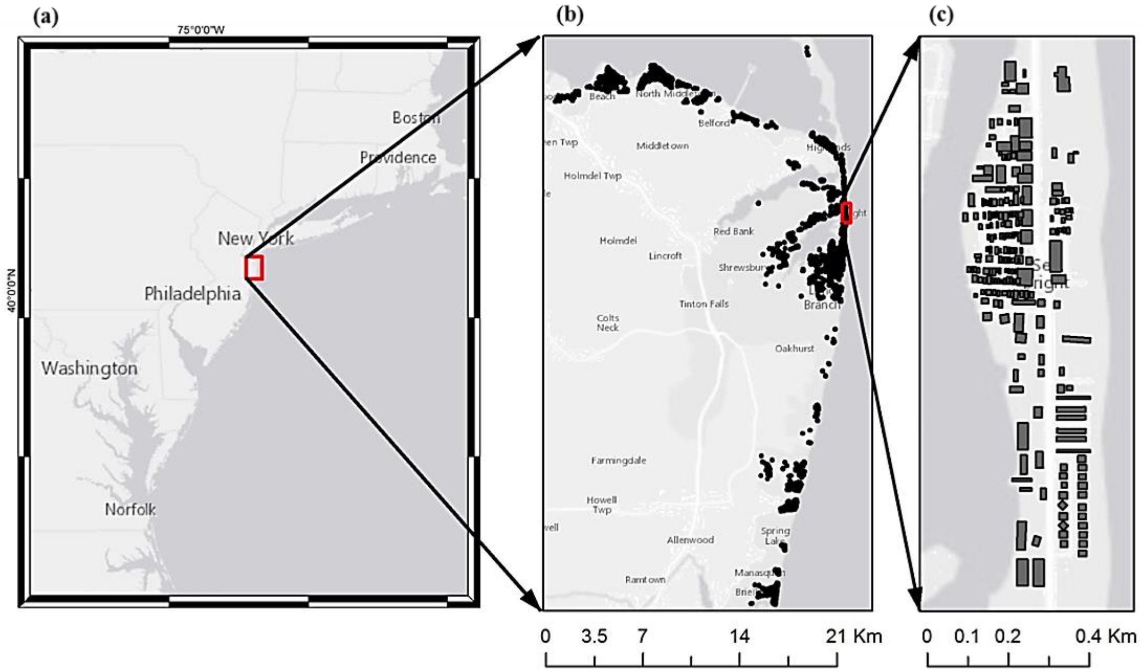

Fig. 8 Overview of study region **a** geographical location; **b** location of the buildings in the study region; **c** location of area 5 with field photos (the 5th area visited)

3.2 Available Public Data

Before Hurricane Sandy made landfall, the U.S. Geological Survey (USGS) deployed a wide number of surge sensors. Additionally, after this event, high water marks in this area were reported. The information gathered was used to update the modeled surge inundation with physical field observations (FEMA MOTF 2014). Using the support from Civil Air Patrol and NOAA imagery, FEMA MOTF was able to develop a database for each building in the area. The flow depth was determined by subtracting the high water marks and surge sensor records from a digital elevation map (DEM). The key attributes to the building points included the damage level based on the combination of visible imagery, flow depth estimated at each structure point based on the FEMA-MOTF observed inundation products, presence or absence of inundation based on visible aerial imagery, and the depth in feet of inundation at each structure point relative to the ground surface (FEMA MOTF 2014). For this particular study, the focus was only on the inundation damage; therefore, inundation damage was extracted from this data.

Buildings that are found within the study region were obtained from the county building database. However, the coordinate information for the building footprints was not available in this database. Therefore, the ArcGIS tool and the method discussed above were used to simplify the buildings, measure the width of each building, and direction associated to this width (north, south, east, and west).

An ArcGIS soil map and soil survey of Monmouth County (NJ) was also obtained from Monmouth County Division of Planning. The grain size distribution of each soil type was graphically summarized for each soil type observed from the database. Soils in the study region primarily consisted of sand with fines. Grain size distributions for each soil type were used to obtain the corresponding particle sizes that pass through 50% (d_{50}) and 90% (d_{90}) finer maximum particle sizes, which varied from fine to medium size sand and from medium to coarse sand respectively. There were also pockets of areas where the soils had 5 to 35% fines content (particles smaller than 0.075 mm, primarily characterized as silt and clays). However, (as one of the limitations) this information is not incorporated in the analyses as the scour depth equations are only based on d_{50} and d_{90} particle size values of the soils, which in the study region primarily consisted of sand sized particles (particles greater than 0.075 mm in size). In addition to the particle sizes, Eq. 1 also requires the input of the sediment density, which is assumed as 2.65 g/cm^3 for the soils found in this area. This assumption was made because sediment density is typically taken as 2.65 g/cm^3 (Blake and Hartge 1985; Boyd 1995; Avnimelech et al. 2001).

3.3 Damage Classification for Study Area: FEMA MOTF Hurricane Sandy Impact Analysis and Field Scour Observations

Damage level reported from FEMA MOTF as it relates to inundation damage is categorized into the following three groups: *affected* (field verified flow depth or storm surge greater than 0 up to 0.6 m), *minor* (0.6 to 1.5 m), and *major* (greater than 1.5 m) (FEMA MOTF 2014). The precision of the values is based on the reported values by FEMA. However, for the purpose of this study they were rounded to the nearest decimal. Fig. 9 is created to depict the spatial distribution of the reported inundation damage in the study area based on the FEMA categorizations as a function of measured flow depths by FEMA (i.e., *affected* (flow depth of 0 to 0.6 m), *minor* (0.6 to 1.5 m), and *major* (greater than 1.5 m)).

Independently from FEMA, during the site visit, the authors noted the damaged buildings due to inundation and scour. For the purposes of this study, each building was given a rating based on the scour damage and the selected four scour photos are shown on Fig. 9. The ratings were divided into no damage, minor, and major damage based on observed scour damage. Buildings are rated as *major*, if it appears to have significant damage due to the removal of soil that caused a complete structural failure as shown on Fig. 9a. Buildings are rated as *minor*, if it appears to have *minor damage* due to soils washed away but no major scour damage to the building was observed as shown on Fig.

9c. Buildings are rated as *no damage*, if it appears to have inundation but no visible to very minor scour damage observed as shown on Fig. 9b and d. Each damaged building location was identified with an associated latitude and longitude and verified on Google Earth and Google Street View. Using Imagery provided by ESRI, building points were plotted on ArcGIS and then attributed with the damage rating along with the picture ID.

The building points were used to compare these field observations (photos) to the ones compiled by FEMA during their study and analysis of Hurricane Sandy for area 5 as shown on Fig. 9. It was established that there were differences between the damage analysis and the field photos that were taken after the disaster by the researchers and damage categorized by FEMA based on inundation damage analysis. Out of the 4 photos, 3 of them (Fig. 9a, b, and c) display an agreement between what was observed in the field and FEMA's inundation damage analysis. In two of these locations scour damage was also observed (Fig. 9a and c). In the other location (Fig. 9d), the FEMA inundation analysis stated *minor damage* but *no damage* was not observed in the field. FEMA's damage analyses match quite well with the observations from the field because FEMA's analyses were performed after the Hurricane with the measured flow depths. However, the developed inundation damage analyses do not differentiate between the damages observed and therefore, it sometimes captures the areas with scour and sometimes does not. Therefore, if the specific interest was to determine the scour damage, FEMA's analyses do not provide sufficient information, and a better assessment is needed to determine damage due to scour. Furthermore, FEMA's analysis is not based on predictions, it is based on observations, and therefore it cannot be used to estimate conditions before the Hurricane struck the area.

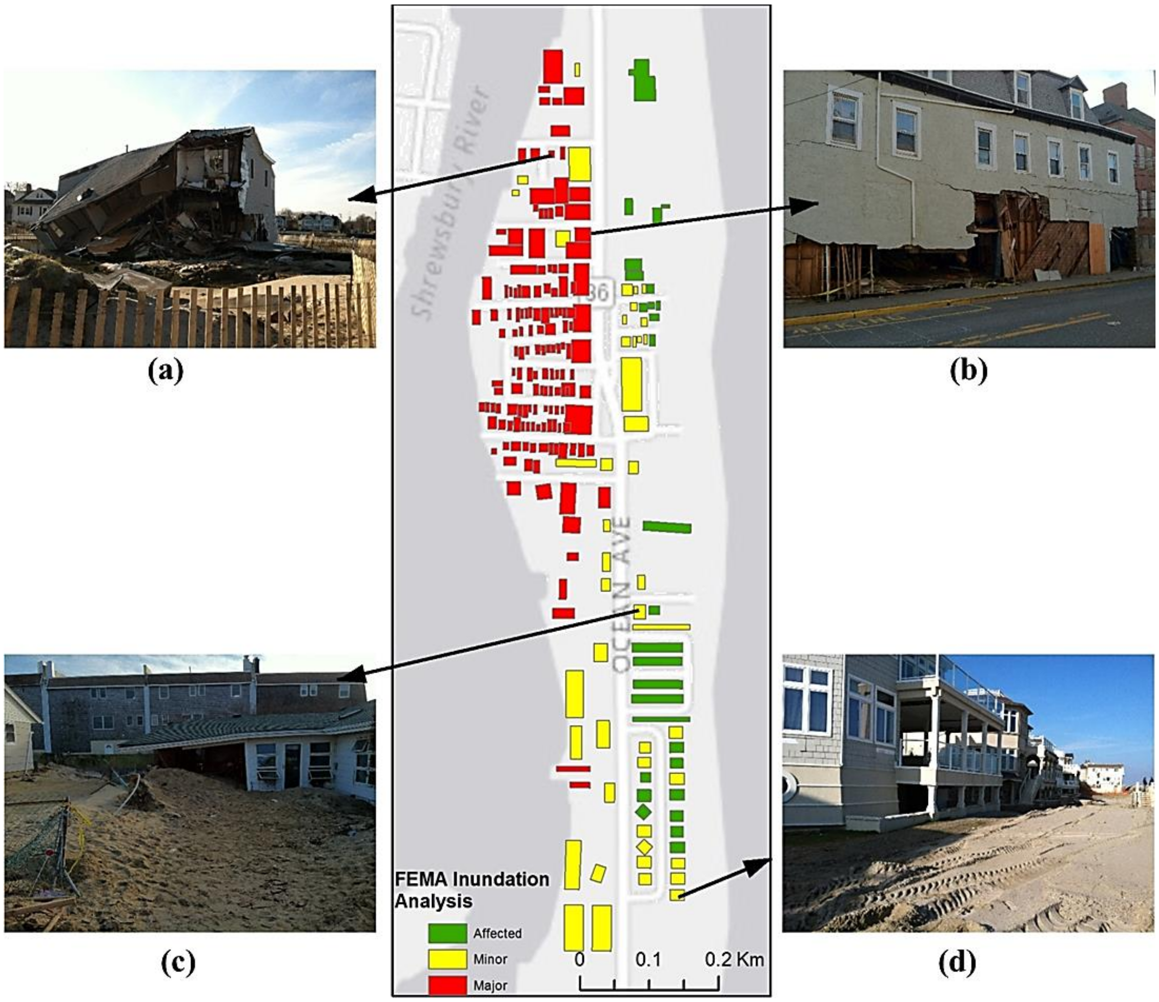

Fig. 9 Comparison of FEMA inundation damage analysis and field photos **a** *major scour damage*; **b** *no scour damage*; **c** *minor scour damage*; **d** *no damage*

3.4 Storm Surge Model: Flow Characteristics

ADCIRC model was used to simulate maximum velocity, water levels, and flood duration for this area. The simulation was performed on the numerical grid built by the United States Army Corps of Engineers (USACE) developed for the North Atlantic Coast Comprehensive Study (NACCS) (Nadal-Caraballo et al. 2015). This grid covers the western Atlantic Basin, the Gulf of Mexico, and the Caribbean Sea, and a finer resolution is observed at coastal areas in order to properly reproduce all hydrodynamic processes involved on the storm surge phenomenon. The open ocean tidally forced boundary lies on the 60ºW meridian, where the tidal wave was estimated and propagated to the shoreline based on the amplitude, phase, nodal factor, and the equilibrium argument of the eight major constituents at this region (K1, K2, O1, M2, N2, P1, Q1, and S2). That information was extracted from the Le Provost tidal database (Le Provost et al. 1994). Regarding the meteorological forcing, the wind velocity and the atmospheric pressure driven by Hurricane Sandy were calculated at exact grid node locations and coupled to ADCIRC using the asymmetric vortex formulation (Mattocks et al, 2006; Mattocks and Forbes, 2008) based on the Holland gradient wind model (Holland, 1980). Then Garratt's drag formulation (Garratt, 1977) was used to compute wind stress over water surface from the wind velocity. National Hurricane Center (NHC) tracked Hurricane Sandy from 10th October 2012 at 18:00 GMT time to 31st October 2012 at 12:00, and reported the primary parameters of the hurricane, such as, position of the eye of the storm, radius of maximum wind, minimum central pressure, maximum wind speed, radii at specific wind speeds (34, 50, 60, 100 knots), and heading direction. This information is available on the Hurricane

Data 2nd generation (HURDAT2) (Landsea et al. 2015), which is based on the Automated Tropical Cyclone Forecast (ATCF), and was employed to generate storm surge by using ADCIRC model. As an output of the storm surge model, maximum velocity, flood duration, and maximum flow depth were obtained, which are input parameters for the scour damage models (Equations 1 and 2).

3.5 Storm Surge Model Validation

The storm surge model performance was evaluated by a comparison of the model results and available historical storm surge data. This storm surge data was collected from 19 NOAA tidal gages and 487 high water marks (HWM) distributed through the east coast of the U.S. (from Virginia to New Hampshire). The validation of the HWM contributes to clarify uncertainties associated to adequate storm surge flood propagation overland, since the results of the storm surge model are used to estimate scour depths in building foundations. It is important to highlight that this comparison present some limitations (Atkinson 2011). One limitation is the unknown contribution of waves to overall water levels that is included in the observed data, but excluded in the storm surge model. Additionally, HWM contains other wave effects such as run up and overtopping. Also, HWMs are based on observations, which could be subjective. Fig. 10 shows the spatial distribution of the errors, i.e., the difference between the maximum modeled water levels and the maximum observation, through the east coast. Negative values represent under estimations and positive values denote over predictions. Those errors ranged between -2.0 m and 2.5 m; the largest over predictions were found along the coast of Long Island (NY). One of the reasons for the large difference between the flow depths measured in the field and estimated in the model could be due to the wind fields implemented in the storm surge model. Wind fields produced by Hurricane Sandy were simulated in the storm surge model considering this hurricane as a tropical cyclone. This is a common approach used in storm surge models as reported by others (Holland, 1980; Mattocks et al, 2006; Mattocks and Forbes, 2008). However, Hurricane Sandy transitioned from tropical storm to extratropical storm while the center of circulation was about 45 miles of Atlantic City, and therefore, Hurricane Sandy no longer met the definition of a tropical cyclone (Blake et al. 2013). This fact could reduce the accuracy of the wind fields, and consequently, water levels. Here, we chose to keep the simulation with the asymmetric wind model as it represents a widely used storm surge modeling framework for planning and forecast (e.g., NACCS).

To specifically understand the difference between the measured and estimated flow depths for the study region (Fig. 8), the results of this comparison are depicted on Fig. 10b. The difference (referred as errors in the Fig. 10) in this region were primarily between -0.5 m and 0.5 m. Based on this range, it is considered that the modeled results agreed moderately well with the observed data in the study region. This is because this magnitude of the errors is already expected even if the storm wind was modeled with upmost accuracy. The model has known limitations as discussed above related to modeling water circulation and what is included in the HWM data. Therefore, the storm surge model was not revised to further evaluate the changes due to modeling Hurricane Sandy as extratropical storm.

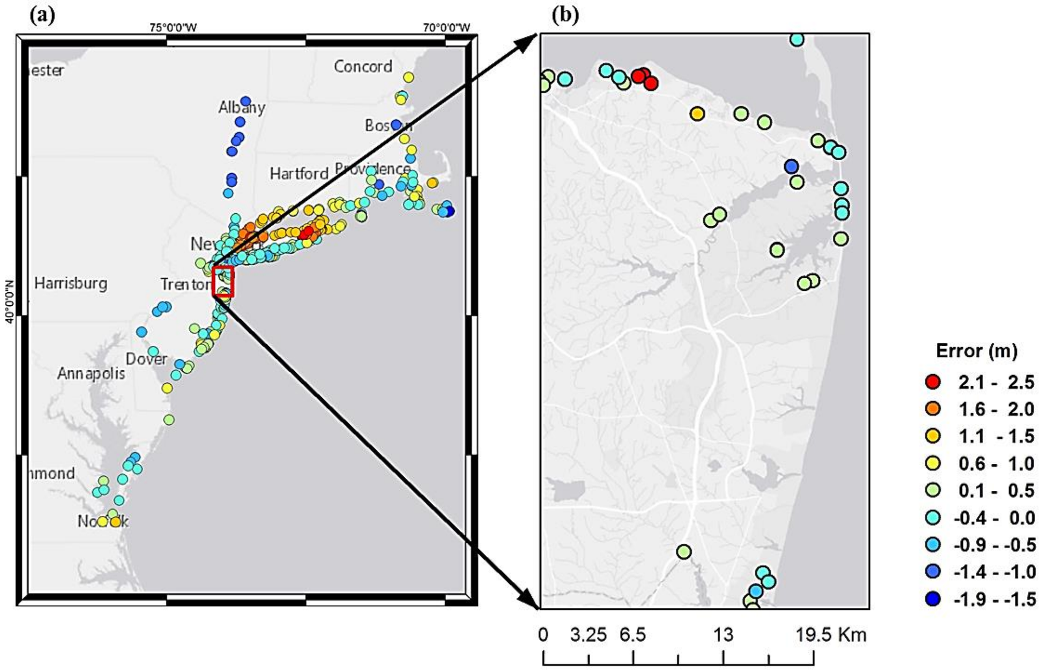

Fig. 10 Storm surge model validation (difference between the maximum modeled water levels and maximum observation) **a** spatial distribution of the errors in east coast; **b** spatial distribution of the errors in the study area

3.6 Estimated Scour Depths under Residential Buildings

The scour depth under the residential buildings was estimated based on Eq. 1 and 2 and specific features at each building location as codified in the ArcGIS tool. Based on the limitations associated with both equations, Eq. 1 provided results that covered 68% of the study region, whereas Eq. 2 covered only 14% of the study region. Due to the limitations of these equations, 30% of the study region was not covered. In addition, 12% of the region was covered with both equations. The estimated scour depth based on Eq. 1 with much better coverage ranged up to 17 m and with Eq. 2 with less coverage ranged up to 3

m. The maximum scour depths noted for these equations were not for the same buildings as the extent of the areas covered with the two equations were different. However, the results appeared to have an order of magnitude difference from each other. The primary focus of this study was to determine a tool where the estimated scour depths could be related to potential scour damage that may be used to preliminarily evaluate the susceptibility of an area against scour before a hurricane strikes. However, when the scour depth range from both equations provide very different ranges, it is difficult to develop a scour damage classification that can readily be implemented without relating the estimated values from one equation onto another.

The difference between the estimated scour depths obtained from Eq. 1 and 2 were also observed during the sensitivity analyses. Based on the field observations, for the buildings that both equations were able to compute scour, Eq. 1 appears to be significantly over estimating the magnitude of the scour than Eq. 2. For those buildings that both equations were able to compute scour, the maximum scour depth for Eq. 1 was 16.9 m and minimum was 0.8 m and for Eq. 2, the maximum scour depth computed was 1.6 m and minimum was 0.1 m. The magnitude difference between the maximum scour depths is roughly about 10 (as also observed during the sensitivity analyses). Therefore, a scale factor of 10 was applied to Eq. 1 to relate the results to the estimated scour depths from Eq. 2. Once this adjustment was made, adjusted scour depths from Eq. 1 were compared against estimated scour depths from Eq. 2. The comparison in ArcGIS model output from both equations with the scale factor showed an agreement of 90%. Consequently, a scale factor of 10 is implemented to create a range of Eq. 1 output similar to Eq. 2 output. It is envisioned that a similar scale factor may also be implemented if scour depth is estimated in other areas with other hurricane scenarios. However at this stage this is not validated yet but will be further investigated in the subsequent articles.

3.7 Relating Scour Depths to Scour Damage

Unfortunately, there is no available literature that provides a threshold to classify specific scour depth as low, medium, or high scour based on different soil types and relate these observations to building damage. Therefore, an attempt was made in this study to relate the scour depth to scour damage based on the available data. Fig. 11 depicts the estimated scour depths based on Eq. 1 with scale factor. This figure was created with the results from Eq. 1 instead of results from Eq. 2 because Eq. 1 provided a much larger coverage within the study region. These estimated scour depths were than compared against the field observations to relate the estimated scour depths to scour damage. Based on this comparison, three categories were developed to differentiate between the areas as it relates to scour (i.e., no damage, minor, and major scour). Estimated scour depths up to 45 mm (0.045 m) were considered no damage (as observed from photo d in Fig. 11 and noted in the field), depths greater than 0.045 but less than 0.4 m were considered minor damage (as observed from photo c in Fig. 11 and noted in the field), and depths greater than 0.4 m were considered major damage (as observed from photo a in Fig. 11 and noted in the field). However one of the limitations with this tool is, in the analysis, the effects of the urbanization is not accounted, meaning in all areas it is assumed that the foundation of the building is assumed to be exposed (e.g., prone to scour damage). This is not true as can be seen in Photo b in Fig. 11, where damage is observed but that is not due to scour of the building foundation. This factor will be further evaluated in the next generation of this model.

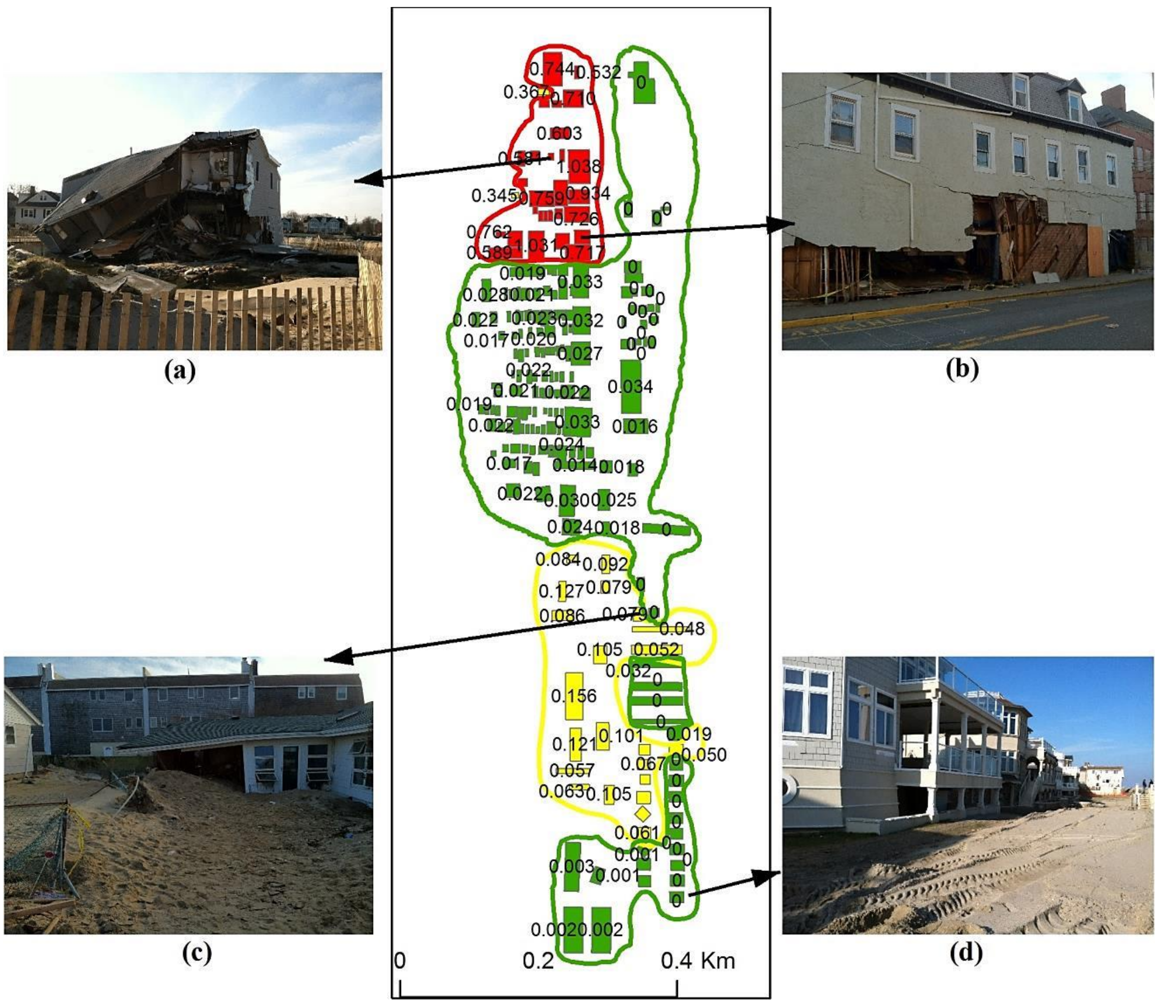

Note: Numbers in the middle figure show the estimated scour depths.

Fig. 11 Scour damage classification based on predicted scour depth

Because the scour depth results obtained from Eq. 1 were scaled down to provide a similar range as in Eq. 2, the damage category determined from Eq. 1 results were also implemented to the results obtained from Eq. 2. Fig. 12 provides a comparison between categorized scour damage in the study area based on both scour depth equations. If these results were evaluated for planning purposes, it can be stated that they are in good agreement.

Table 2 provides an overview of the comparison when this approach is expended to the entire region shown in Fig. 8b. Using Eq. 1 scour depth could be computed for 5,071 buildings out of the 7,470 in the region. Eq. 1 was not able to predict scour for the remaining 2,399 buildings due to the limitations of the equation. As shown on Table 2, 66% of the 5,071 buildings in this study region were classified as no damage, 32% for minor damage, and about 2% of the buildings for major damage. Eq. 2 computed scour damage for only 1,021 buildings out of the 7,470 buildings in the region. About 79 % of the 1,021 buildings were included in the minor damage category and 21% in major damage category. As for the scour depth comparisons, overall, among the buildings that both of these equations (Eq. 1 and 2) were able to predict scour depth, the comparison of predicted scour damage categories (no damage, minor, affected) shows an agreement of 90%. Fig. 12 is a good example for this agreement.

Table 2 Scour damage classification in the study area

Damage classification	Kohli and Hager (%)	Nadal et al. (%)
No damage	66	-
Minor	32	79
Major	2	21

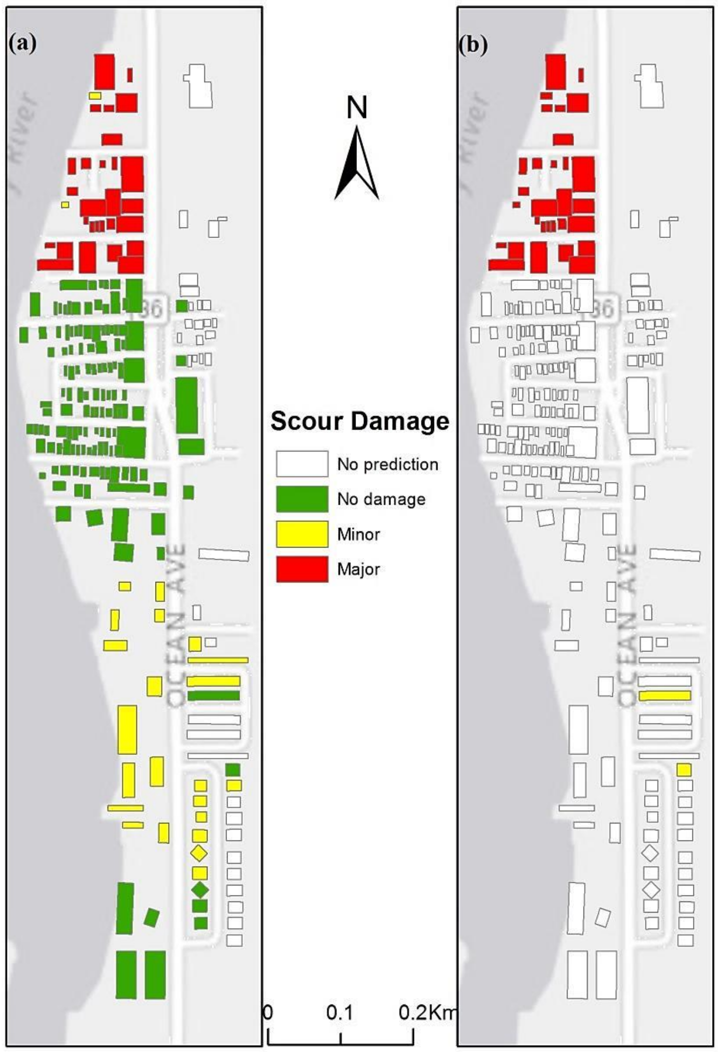

Fig. 12 Spatial distribution of buildings with estimated scour damage using **a** Kohli and Hager (2001) Eq. 1; **b** Nadal et al. (2010) Eq. 2

4 DISCUSSIONS AND CONCLUSIONS

Estimating flood induced damages are essential to long term coastal resilience planning, support recovery efforts, and insurance purposes and differentiating scour damage from this phenomenon is very important because if predicted, simple construction improvements could result in significant cost savings avoiding damages caused by scour. As a result, an ArcGIS framework has been developed in this study by combining the use of existing building scour equations, storm surge model, available building geometry and soil data to estimate scour damage. Unlike the existing flood damage models, this automated ArcGIS framework can be used to estimate building scour damages spatially for any area with different soil conditions and different storm events.

Insights drawn from the sensitivity analyses are that: (1) Scour magnitude increases when there is an increase in flow velocity, flow depth, building geometry and flood duration for Eq. 1, however there was no significant change for increasing sediment density. (2) Scour magnitude increases when there is an increase in velocity, building width and flood duration for Eq. 2, however there was no significant change for increasing flow depth. (3) Both equations were very sensitive to changes of velocity. (4) Coarser particle sizes led to a decrease on scour magnitude for both equations. (5) Eq. 1 estimates larger scour magnitudes compared to Eq. 2.

The developed ArcGIS Framework is presented and applied to a case study. This framework was used to estimate flood induced building scour damages related to the scour depth caused by Hurricane Sandy in coastal areas of Monmouth County (NJ). The results from both equations were compared and the coverage for the study region using Eq. 2 was less than the coverage using Eq. 1. However, for those buildings where both equations computed scour damage, a good agreement was observed after applying a scale factor to Eq. 1. Although the extent of the spatial coverage of these equations were different from each other, both equations provide valuable information as there were some areas where Eq. 1 was able to predict scour depth but not Eq. 2 and vice versa.

Overall, the results from this study indicate that the automated tool provide relatively consistent predictions with the field observations. Ultimately, the analyses in this study may be used by Monmouth County. Furthermore, the framework may be applied to any area by implementing the range and possible definitions of scour damage provided in this paper to make an initial estimate for scour damage before the hurricane. This tool may potentially be used for emergency responses, risk assessments, and mitigation strategies to avoid fatalities and cost savings to minimize after repairs.

5 LIMITATIONS

This ArcGIS-based tool is the alpha model and requires further improvements as it has limitations that the user must be aware of:

- The tool is based on the assumption that in all areas soil below the building is exposed. Although this provides the worst-case scenarios, in urban settings this is not a correct assumption. Further research is necessary to improve this assumption.
- The equations used to estimate scour depth have limitations as shown in Fig. 7 and in some areas do not converge because of these limitations. Additional investigations are necessary to expand the capability of estimated scour damage in areas where there are limitations.
- In this study, the range of scour depths estimated from one equation was related to the other with a scale factor. This was performed based on scour depths estimated from one hurricane event. Further comparisons are needed to confirm or revise this approach.
- An attempt was made to relate the scour depths to scour damage; however this relationship was obtained based on limited data. Further revisions will be performed to confirm or improve this range using the field observations from the next severe hurricane event.

APPENDIX A: SENSITIVITY ANALYSES

Sensitivity Analyses

The sensitivity analyses were performed to evaluate the sensitivity of the parameters of each equation. The values selected for these analyses are applied for both equations and the particle size values used for both equation is based on the same soil type since Kohli and Hager (2001) equation requires d_{50} values and Nadal et al. (2010) equation requires d_{90} values. The values used for this analysis is as shown in Table 1 in section 2.3.4 and again provided below.

Parameters	Magnitudes
Building width- b(m)	10, 20, 30, 40, 50, 60
Flow depth- h_o (m)	0.06, 0.46, 0.86, 1.26, 1.66, 2.06, 2.46, 2.86, 3.26, 3.66
Velocity- V (m/s)	0.0001, 0.23, 0.46, 0.55, 0.69, 0.71, 0.88, 0.92, 1.04, 1.15, 1.21, 1.37, 1.54, 1.61, 1.7, 1.84, 1.87, 2
Median particle size- d_{50} (m)	0.00017, 0.00019, 0.00021, 0.00025, 0.0003, 0.0004, 0.00043, 0.00052, 0.00061, 0.00063
90% finer particle size- d_{90} (m)	0.00053, 0.0006, 0.0012, 0.0014, 0.0015, 0.0017, 0.0018, 0.0025, 0.003, 0.0035
Sediment density- ρ_s (g/cm^3)	2.6, 2.65, 2.7
Flow duration - t (hours)	1, 12, 18, 24, 48, 72, 96, 120, 144, 162

The building widths used for this analysis are the ranges of buildings found in Monmouth County (NJ).

	Width (m)
Building 1	10
Building 2	20
Building 3	30
Building 4	40
Building 5	50
Building 6	60

The average values used for Kohli and Hager (2001) equation is as shown below.

Parameters	Magnitude
Flow depth- h_o (m)	1.86
Velocity- V (m/s)	1.03
90% finer particle size- d_{90} (m)	0.0018
Sediment density- ρ_s (g/cm^3)	2.65
Flow duration - t (hours)	69.7

The average values used for Nadal et al. (2010) equation is as shown below.

Parameters	Magnitude
Flow depth- h_o (m)	1.86
Velocity- V (m/s)	1.29
Median particle size- d_{50} (m)	0.0004
Flow duration - t (hours)	69.7

Note: The reason why the average velocity in Nadal et al's. equation was selected differently is because in the Kohli and Hager's equation the minimum velocity could be established as 0.0001 m/s but when the same value was used in Nadal et al's. equation, the equation was not providing any output. Therefore the minimum value used for Nadal et al. had to be adjusted. In the future, both equations can be re-checked with same minimum values such as 0.55 m/s as that was the threshold where both equations started to provide results. However, a quick check between the equations with the average values used in these sensitivity analyses indicated that the difference of the impact of using avg. 1.03 and 1.29 m/s was not drastic.

<u>Kohli and Hager (2001)</u>

45 analyses were done to evaluate the parameters for Kohli and Hager (2001) equation. The plots below shows the effects of velocity, flow depth, particle size (d_{90}), flood duration and sediment density respectively on the scour depth for a scenario when one constant is increased. (i.e analyze the effect of velocity with constant soil properties, flood duration, sediment density but varying flow depth (average, minimum and maximum flow depth).

Scenario 1 is based on average flow depth of 1.856 m, average sediment density of 2.65 g/cm^3, average flood duration of 69.7 hours and average d_{90} of 0.0018 m.

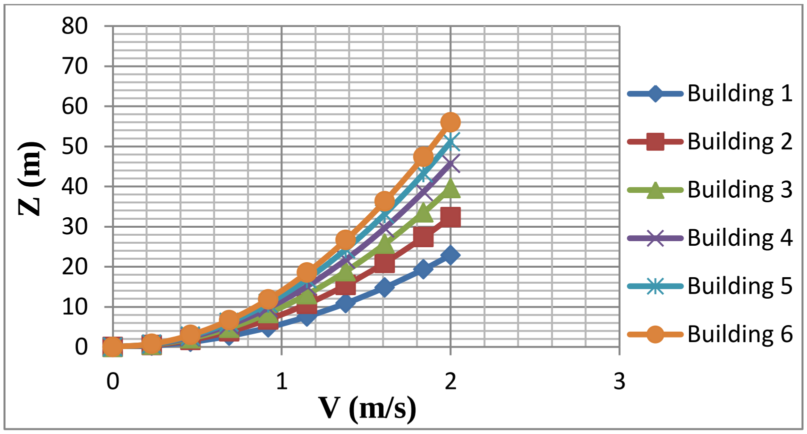

Scenario 2 below is based on minimum flow depth of 0.006 m, average sediment density of 2.65 g/cm^3, average flood duration of 69.7 hours and average d_{90} of 0.0018 m.

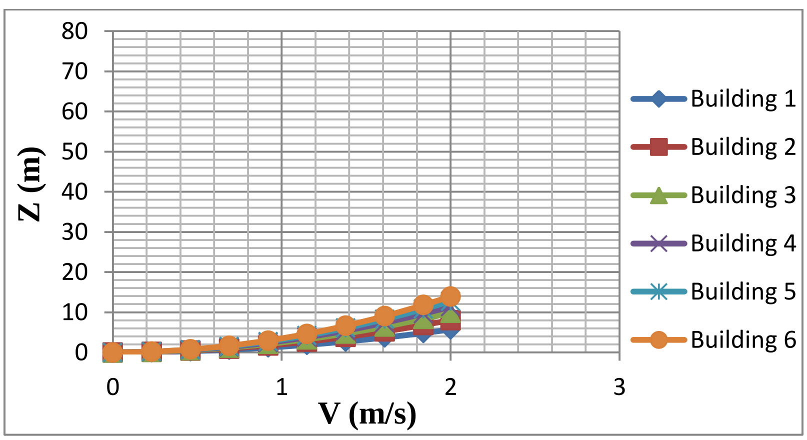

Scenario 3 below is based on maximum flow depth of 3.66 m, average sediment density of 2.65 g/cm^3, average flood duration of 69.7 hours and average d_{90} of 0.0018 m.

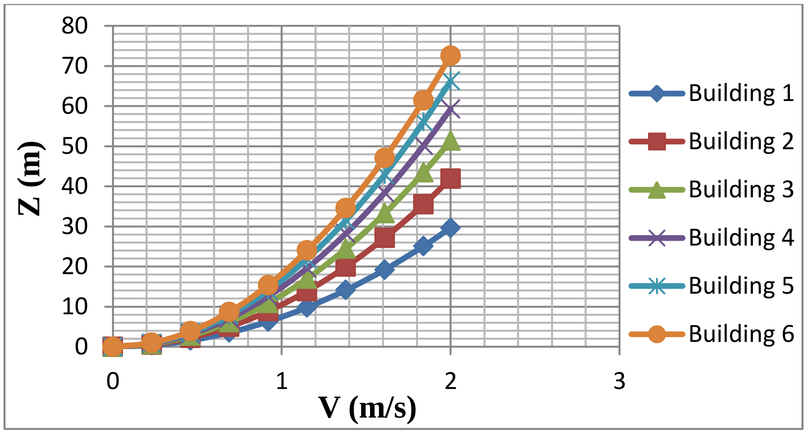

Scenario 4 below is based on average flow depth of 1.86 m, minimum sediment density of 2.6 g/cm^3, average flood duration of 69.7 hours and average d_{90} of 0.0018 m.

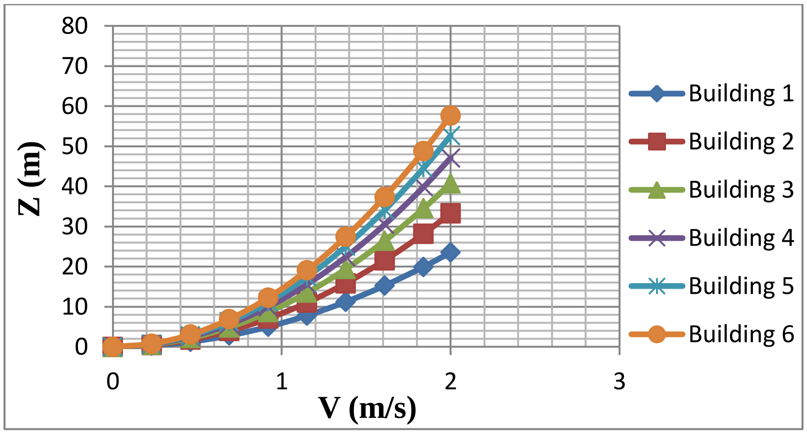

Scenario 5 below is based on average flow depth of 1.86 m, maximum sediment density of 2.7 g/cm^3, average flood duration of 69.7 hours and average d_{90} of 0.0018 m.

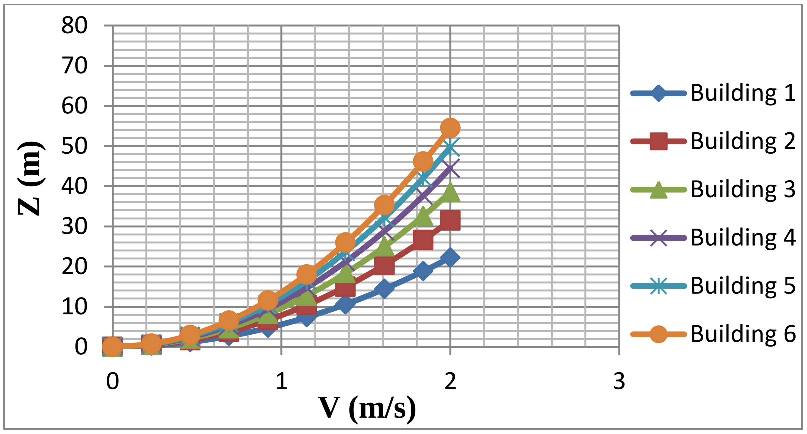

Scenario 6 below is based on average flow depth of 1.86 m, average sediment density of 2.65 g/cm^3, minimum flood duration of 1 hour and average d_{90} of 0.0018 m.

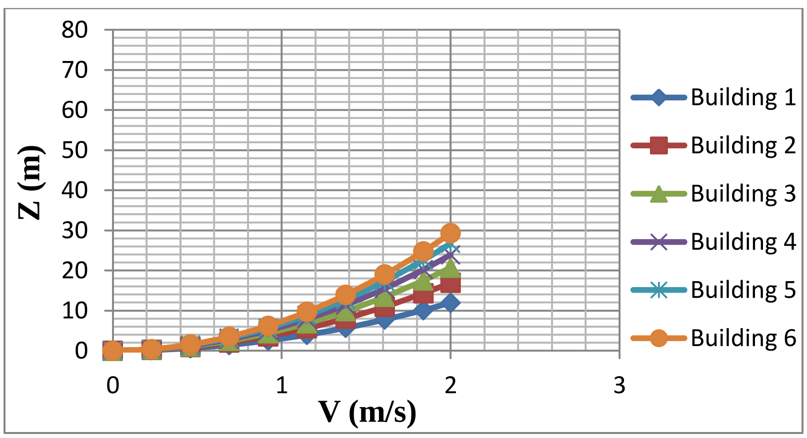

Scenario 7 below is based on average flow depth of 1.86 m, average sediment density of 2.65 g/cm^3, maximum flood duration of 162 hours and average d_{90} of 0.0018 m.

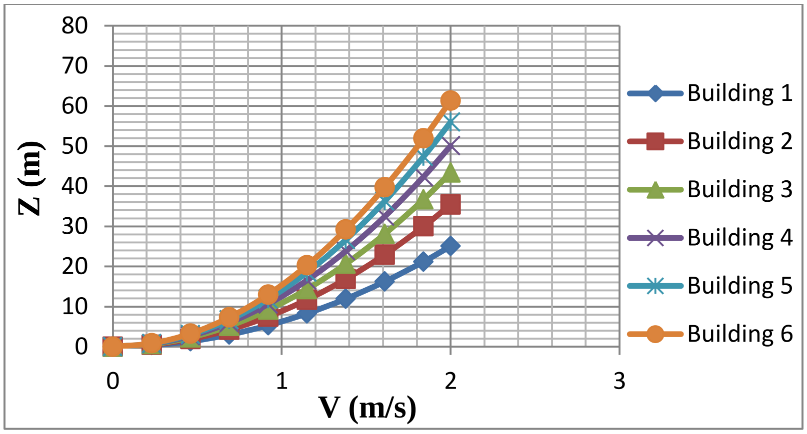

Scenario 8 below is based on average flow depth of 1.86 m, average sediment density of 2.65 g/cm^3, average flood duration of 69.7 hours and minimum d_{90} of 0.00053 m.

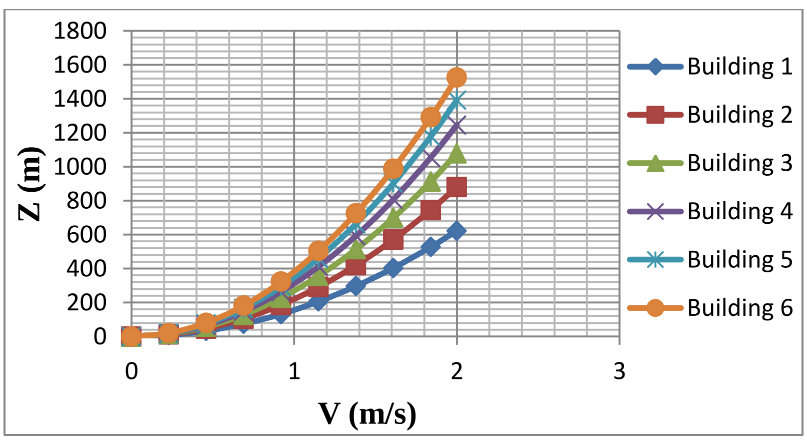

Scenario 9 below is based on average flow depth of 1.86 m, average sediment density of 2.65 g/cm^3, average flood duration of 69.7 hours and maximum d_{90} of 0.0035 m.

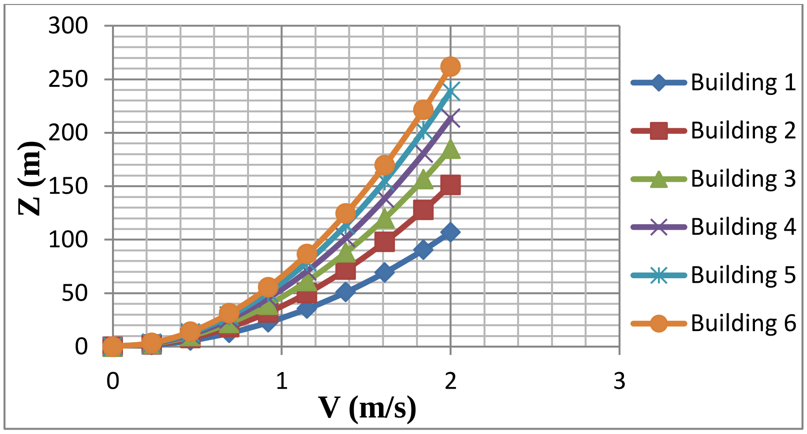

Based on this plots it can be seen that scour depth magnitude increases for increasing velocity significantly. And when the constant values were increased such as the flow depth and flood duration the scour magnitude increased while velocity is increasing. And the constant values such as the sediment density and particle size decreased the scour magnitude as the velocity increases. However the sediment density is not that sensitive. The significant increase of the scour magnitude is due to the limitations of the equations such as densimetric Froude number limitation.

Scenario 10 below is based on average velocity of 1.03 m/s, average sediment density of 2.65 g/cm^3, average flood duration of 69.7 hours and average d_{90} of 0.018 m.

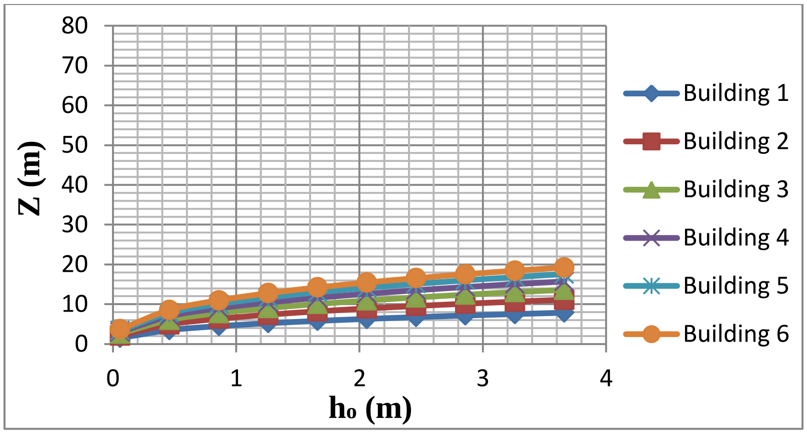

Scenario 11 below is based on minimum velocity of 0.0001 m/s, average sediment density of 2.65 g/cm^3, average flood duration of 69.7 hours and average d_{90} of 0.018 m.

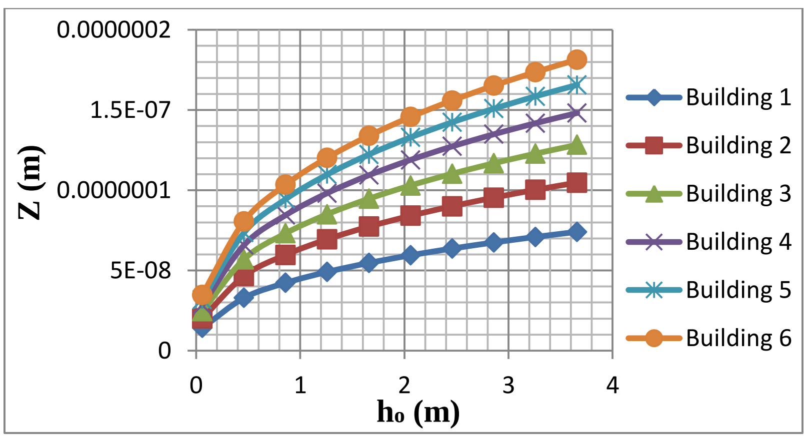

Scenario 12 below is based on maximum velocity of 2 m/s, average sediment density of 2.65 g/cm^3, average flood duration of 69.7 hours and average d_{90} of 0.018 m.

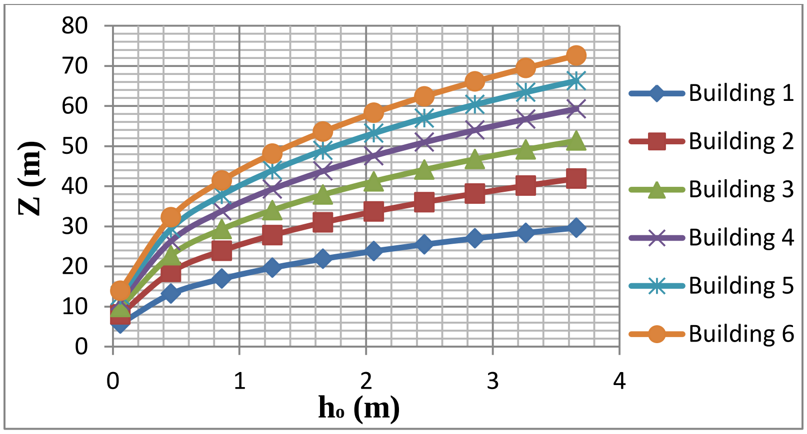

Scenario 13 below is based on average velocity of 1.03 m/s, minimum sediment density of 2.6 g/cm^3, average flood duration of 69.7 hours and average d_{90} of 0.018 m.

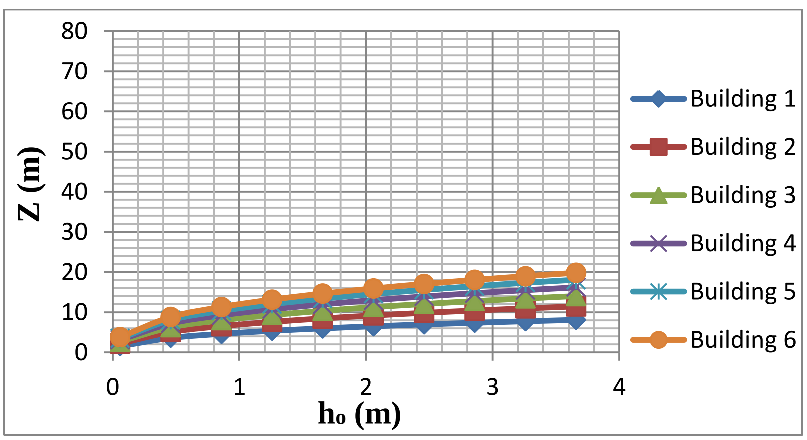

Scenario 14 below is based on average velocity of 1.03 m/s, maximum sediment density of 2.7 g/cm^3, average flood duration of 69.7 hours and average d_{90} of 0.018 m.

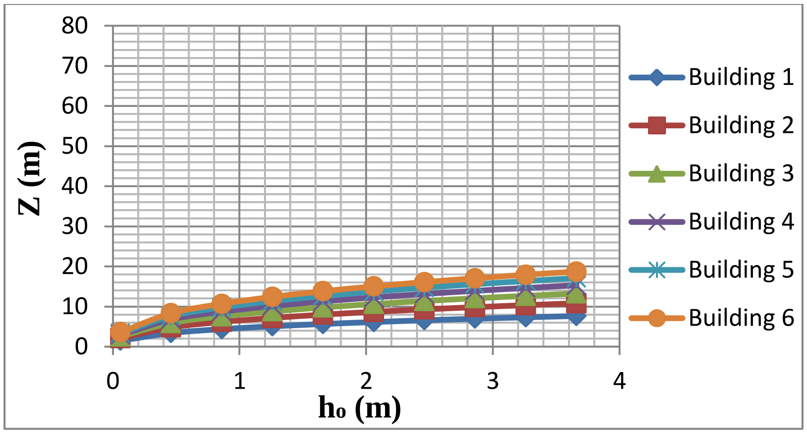

Scenario 15 below is based on average velocity of 1.03 m/s, average sediment density of 2.65 g/cm^3, minimum flood duration of 1 hour and average d_{90} of 0.018 m.

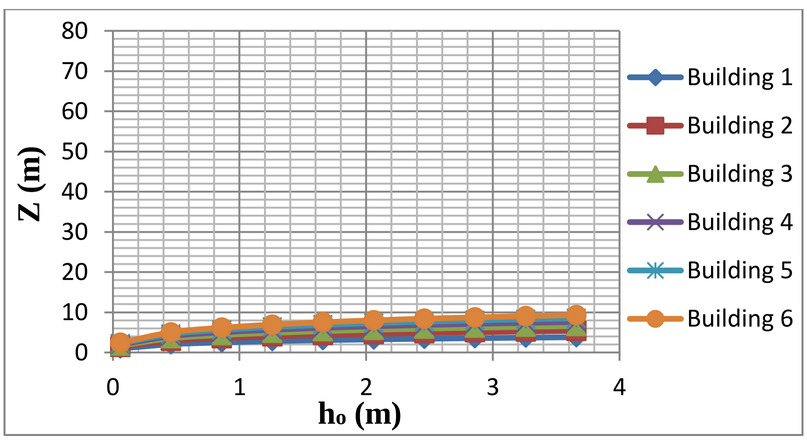

Scenario 16 below is based on average velocity of 1.03 m/s, average sediment density of 2.65 g/cm^3, maximum flood duration of 162 hours and average d_{90} of 0.018 m.

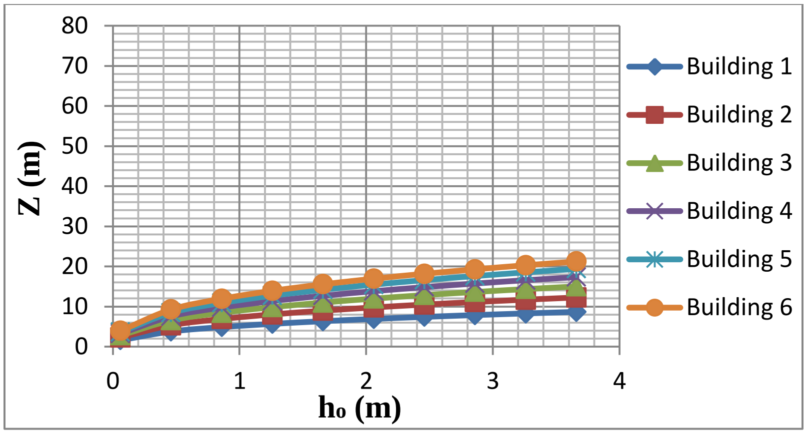

Scenario 17 below is based on average velocity of 1.03 m/s, average sediment density of 2.65 g/cm^3, average flood duration of 69.7 hours and minimum d_{90} of 0.00053 m.

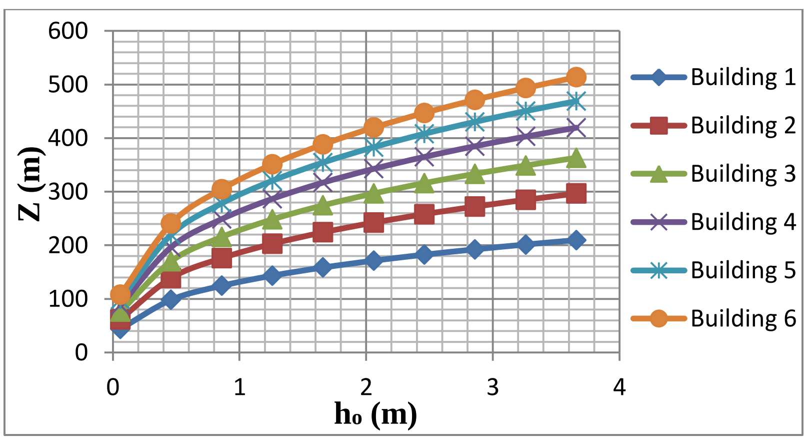

Scenario 18 below is based on average velocity of 1.03 m/s, average sediment density of 2.65 g/cm^3, average flood duration of 69.7 hours and maximum d_{90} of 0.0035 m.

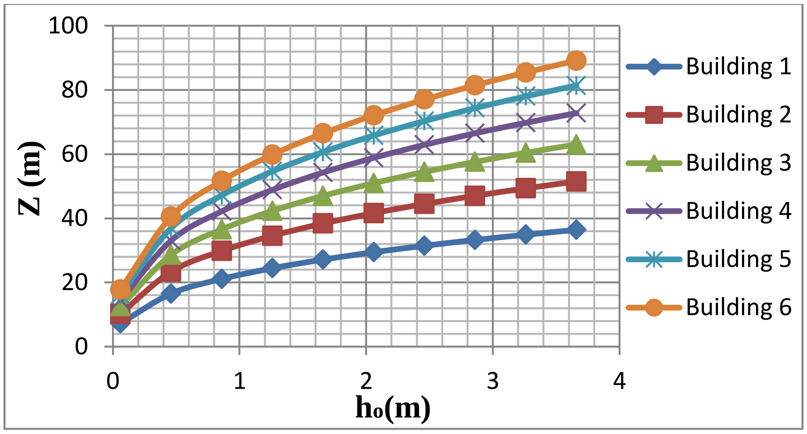

Based on this plots it can be seen that scour depth magnitude increases for increasing flow depth. And an increase of the constant values such as the velocity and flood duration increased the scour magnitude. And the constant values such as the sediment density and particle size decreased the scour magnitude. The significant increase of the scour magnitude is due to the limitations of the equations such as densimetric Froude number limitation.

Scenario 19 below is based on average velocity of 1.03 m/s, average sediment density of 2.65 g/cm^3, average flood duration of 69.7 hours and average flow depth of 1.86 m.

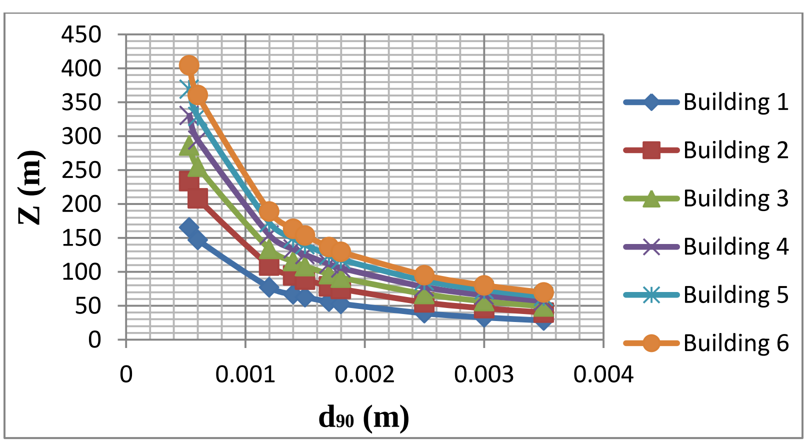

Scenario 20 below is based on minimum velocity of 0.0001 m/s, average sediment density of 2.65 g/cm^3, average flood duration of 69.7 hours and average flow depth of 1.86 m.

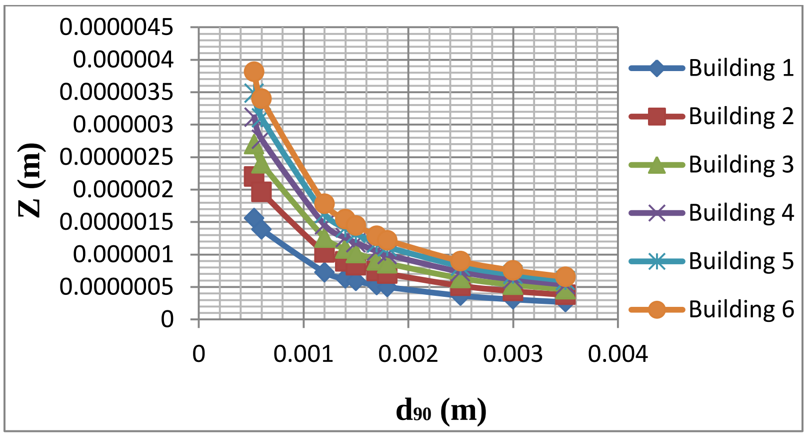

Scenario 21 below is based on maximum velocity of 2 m/s, average sediment density of 2.65 g/cm^3, average flood duration of 69.7 hours and average flow depth of 1.86 m.

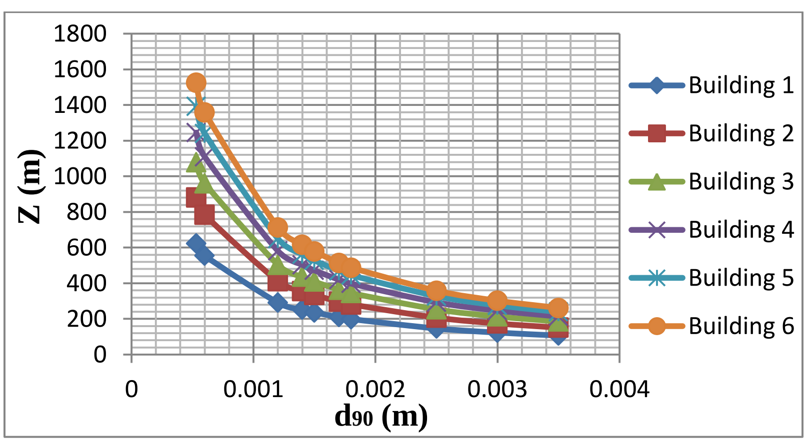

Scenario 22 below is based on average velocity of 1.03 m/s, minimum sediment density of 2.6 g/cm^3, average flood duration of 69.7 hours and average flow depth of 1.86 m.

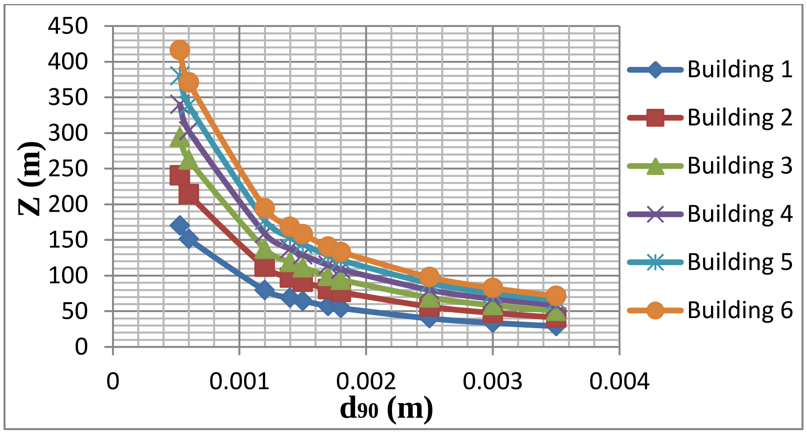

Scenario 23 below is based on average velocity of 1.03 m/s, maximum sediment density of 2.7 g/cm^3, average flood duration of 69.7 hours and average flow depth of 1.86 m.

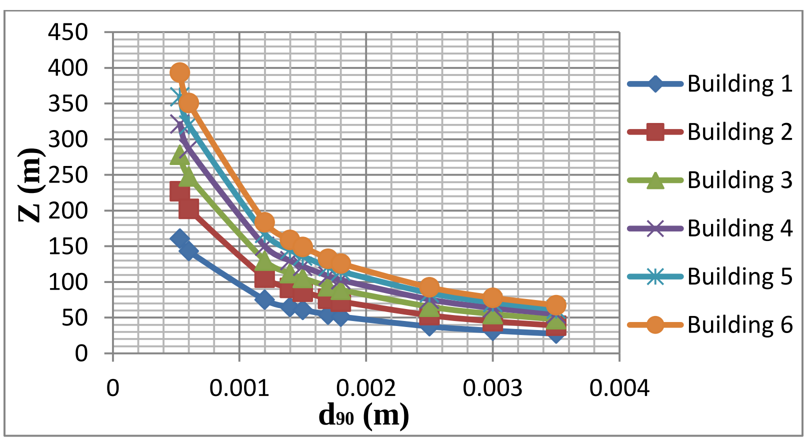

Scenario 24 below is based on average velocity of 1.03 m/s, average sediment density of 2.65 g/cm^3, minimum flood duration of 1 hour and average flow depth of 1.86 m.

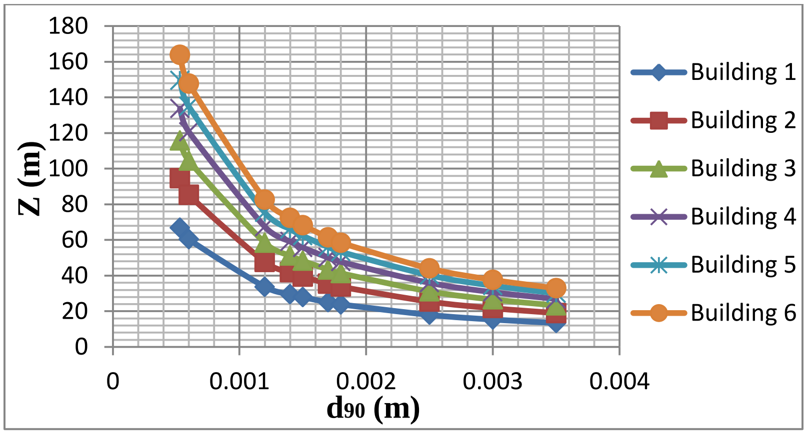

Scenario 25 below is based on average velocity of 1.03 m/s, average sediment density of 2.65 g/cm^3, minimum flood duration of 162 hours and average flow depth of 1.86 m.

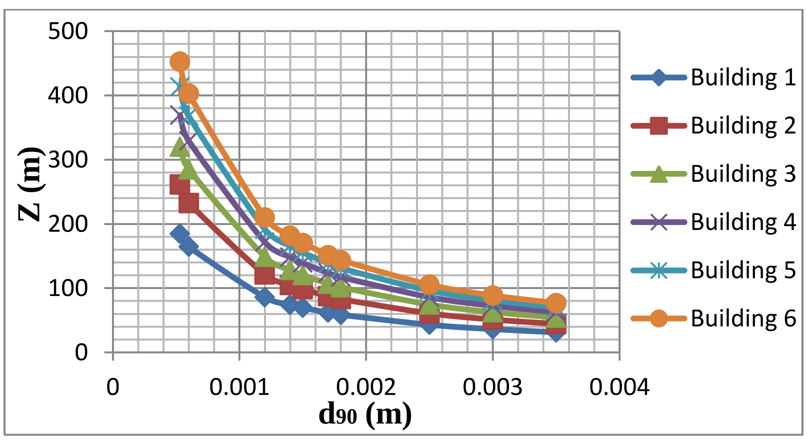

Scenario 26 below is based on average velocity of 1.03 m/s, average sediment density of 2.65 g/cm^3, average flood duration of 69.7 hours and minimum flow depth of 0.06 m.

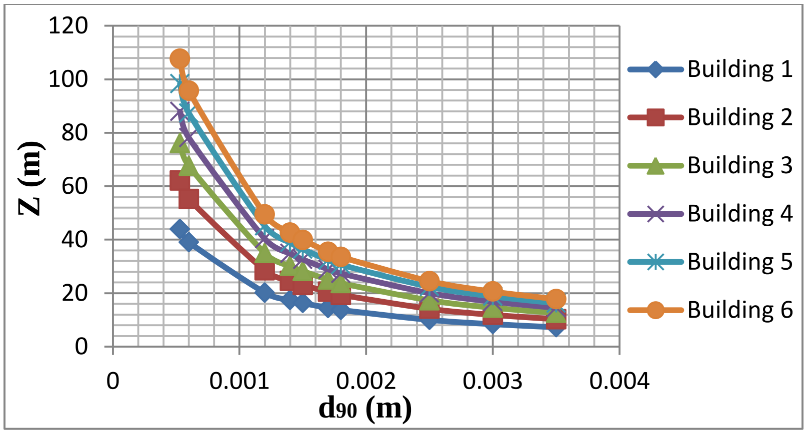

Scenario 27 below is based on average velocity of 1.03 m/s, average sediment density of 2.65 g/cm^3, average flood duration of 69.7 hours and maximum flow depth of 3.66 m.

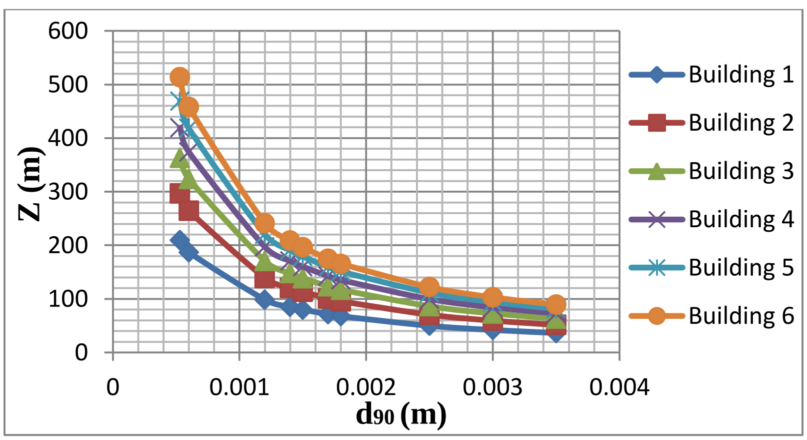

Based on the above plots it can be seen that scour depth magnitude decreases for increasing particle size (d_{90}). And an increase of the constant values such as the velocity, flow depth and flood duration increased the scour magnitude. And the constant values such as the sediment density decreased the scour magnitude. The significant increase of the scour magnitude is due to the limitations of the equations such as densimetric Froude number limitation.

Scenario 28 below is based on average velocity of 1.03 m/s, average sediment density of 2.65 g/cm^3, average d_{90} of 0.018 m and average flow depth of 1.86 m.

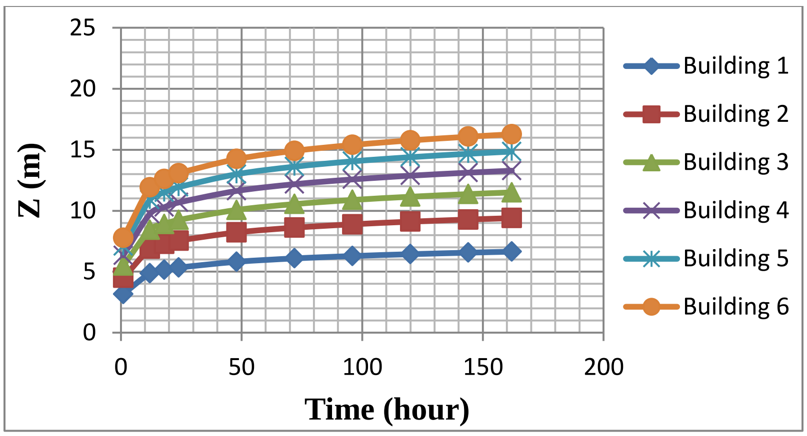

Scenario 29 below is based on minimum velocity of 0.0001 m/s, average sediment density of 2.65 g/cm^3, average d_{90} of 0.018 m and average flow depth of 1.86 m.

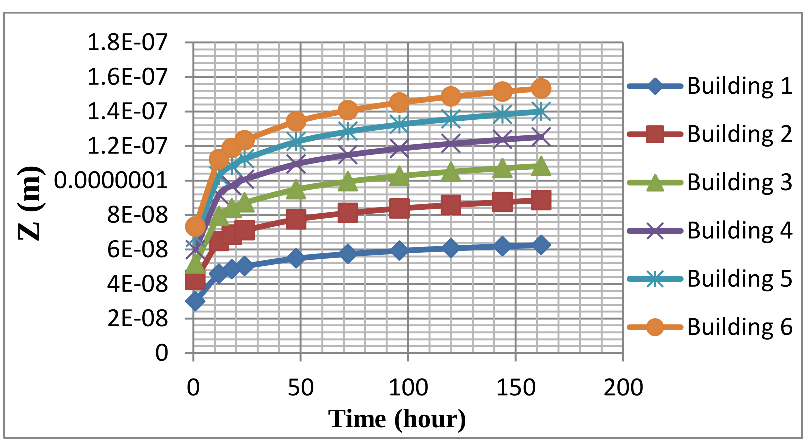

Scenario 30 below is based on maximum velocity of 2 m/s, average sediment density of 2.65 g/cm^3, average d_{90} of 0.018 m and average flow depth of 1.86 m.

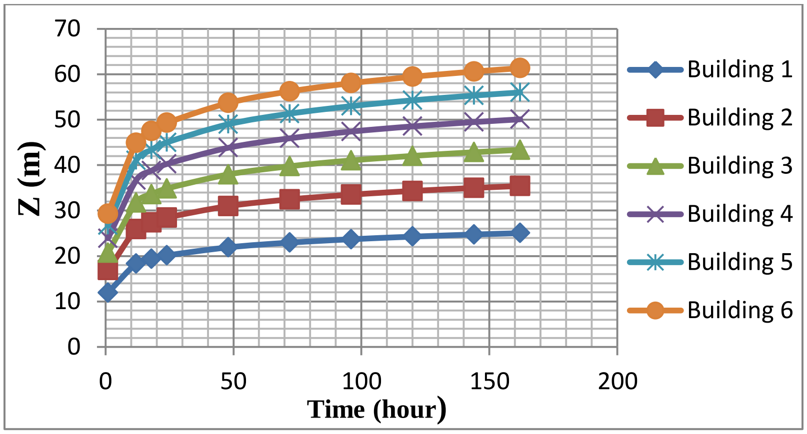

Scenario 31 below is based on average velocity of 1.03 m/s, minimum sediment density of 2.6 g/cm^3, average d_{90} of 0.018 m and average flow depth of 1.86 m.

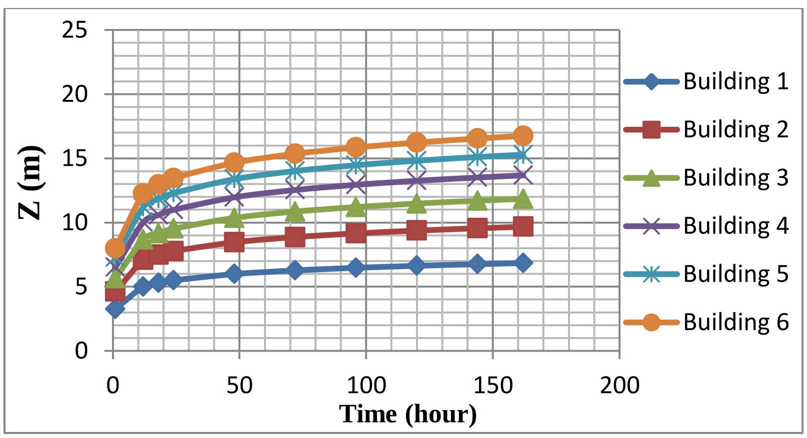

Scenario 32 below is based on average velocity of 1.03 m/s, maximum sediment density of 2.7 g/cm^3, average d_{90} of 0.018 m and average flow depth of 1.86 m.

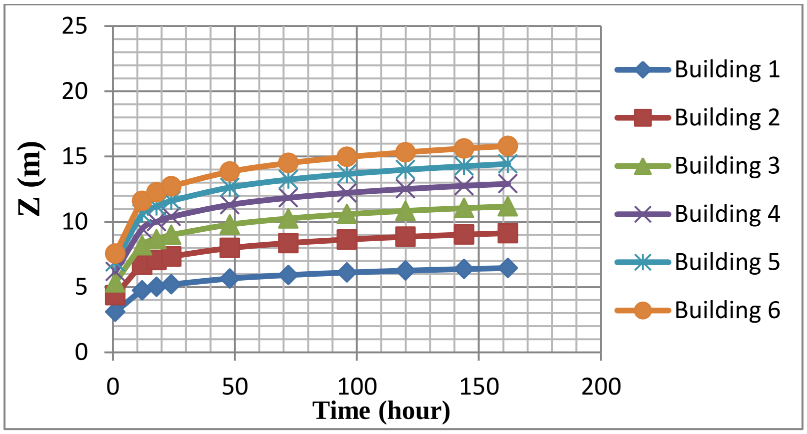

Scenario 33 below is based on average velocity of 1.03 m/s, average sediment density of 2.65 g/cm^3, minimum d_{90} of 0.00053 m and average flow depth of 1.86 m.

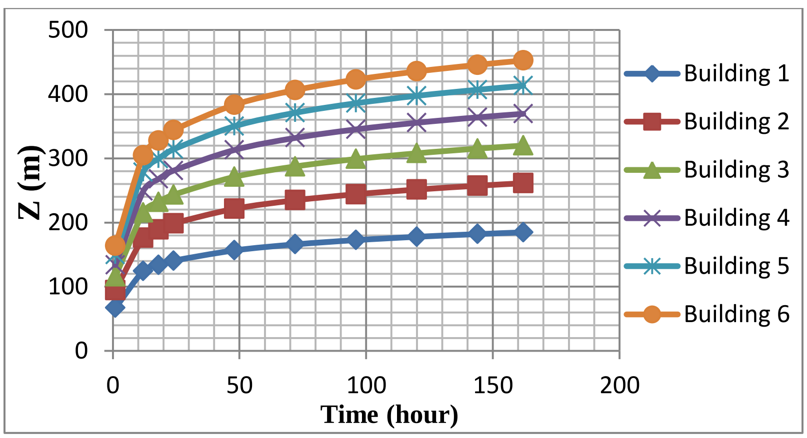

Scenario 34 below is based on average velocity of 1.03 m/s, average sediment density of 2.65 g/cm^3, maximum d_{90} of 0.0035 m and average flow depth of 1.86 m.

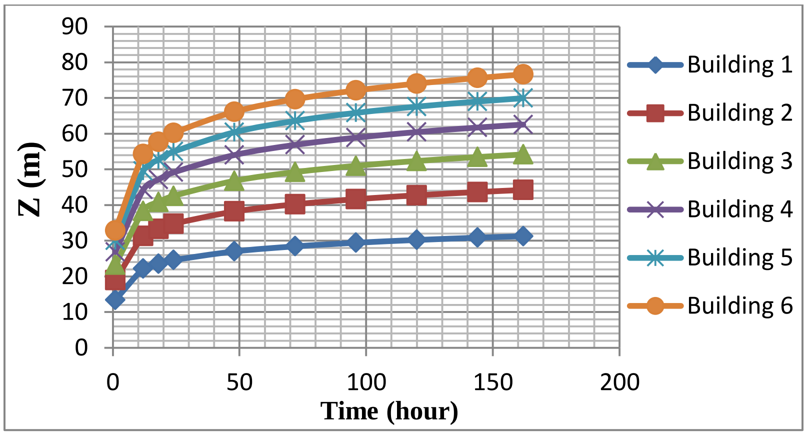

Scenario 35 below is based on average velocity of 1.03 m/s, average sediment density of 2.65 g/cm^3, average d_{90} of 0.018 m and minimum flow depth of 0.06 m.

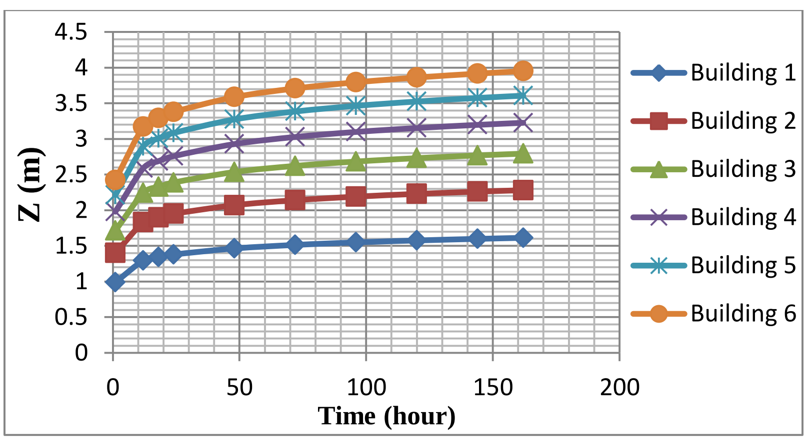

Scenario 36 below is based on average velocity of 1.03 m/s, average sediment density of 2.65 g/cm^3, average d_{90} of 0.018 m and maximum flow depth of 3.66 m.

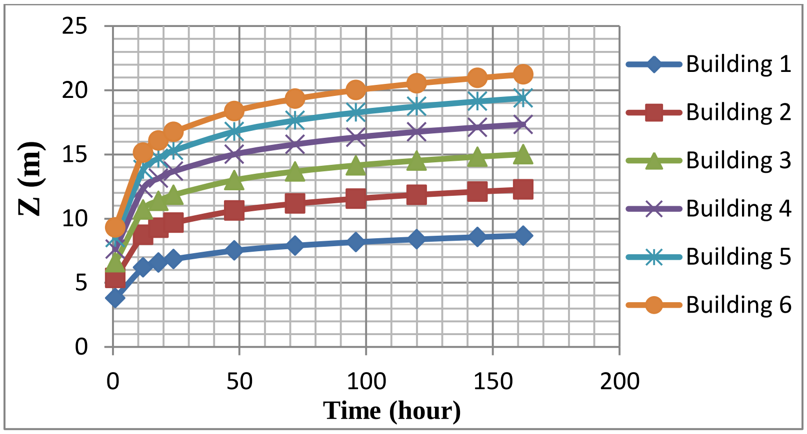

Based on the above plots it can be seen that scour depth magnitude increases for increasing flood duration. And an increase of the constant values such as the velocity, and flow depth increased the scour magnitude. And the constant values such as the sediment density and particle size (d_{90}) decreased the scour magnitude. The significant increase of the scour magnitude is due to the limitations of the equations such as densimetric Froude number limitation.

Scenario 37 below is based on average velocity of 1.03 m/s, average flood duration of 69.7 hours, average d_{90} of 0.018 m and average flow depth of 1.86 m.

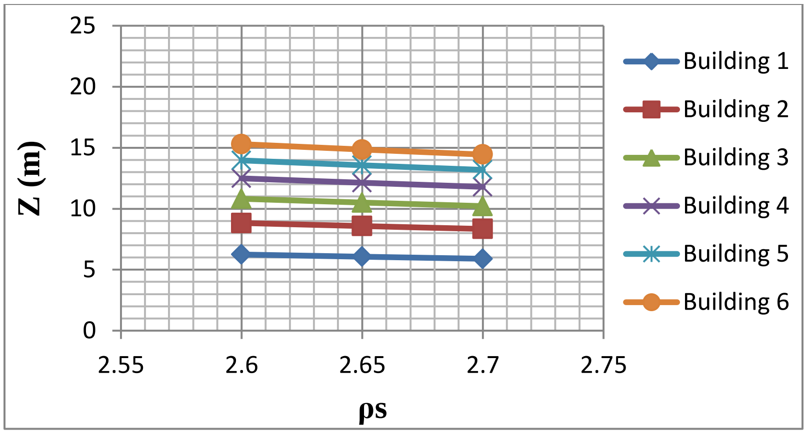

Scenario 38 below is based on minimum velocity of 0.0001 m/s, average flood duration of 69.7 hours, average d_{90} of 0.018 m and average flow depth of 1.86 m.

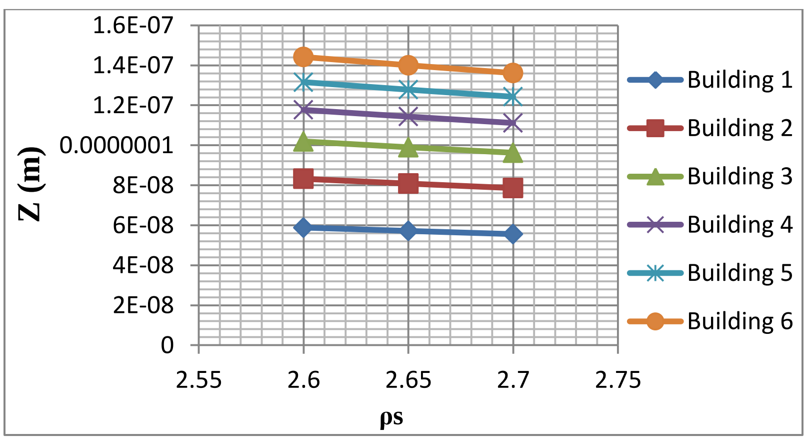

Scenario 39 below is based on maximum velocity of 2 m/s, average flood duration of 69.7 hours, average d_{90} of 0.018 m and average flow depth of 1.86 m.

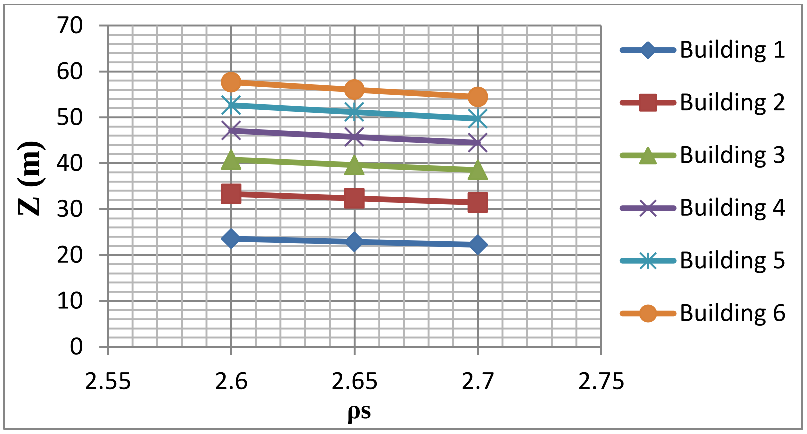

Scenario 40 below is based on average velocity of 1.03 m/s, minimum flood duration of 1 hour, average d_{90} of 0.018 m and average flow depth of 1.86 m.

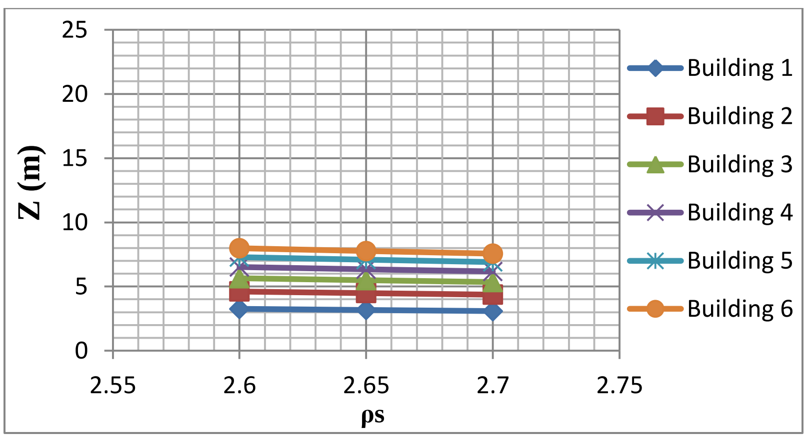

Scenario 41 below is based on average velocity of 1.03 m/s, maximum flood duration of 162 hours, average d_{90} of 0.018 m and average flow depth of 1.86 m.

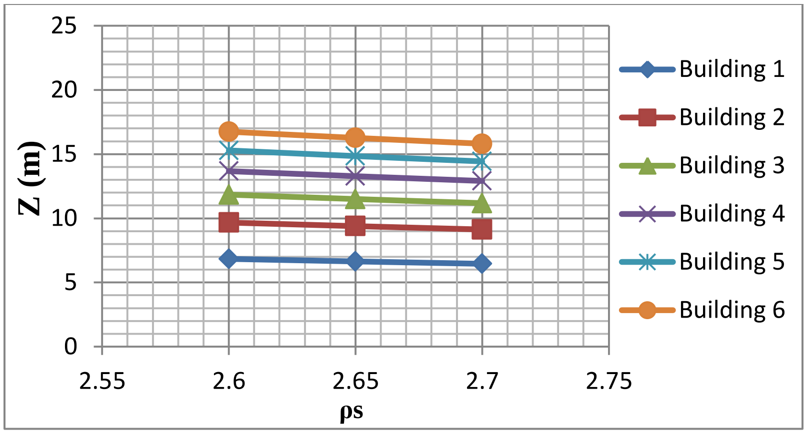

Scenario 42 below is based on average velocity of 1.03 m/s, average flood duration of 162 hours, minimum $d_{90}$of 0.00053 m and average flow depth of 1.86 m.

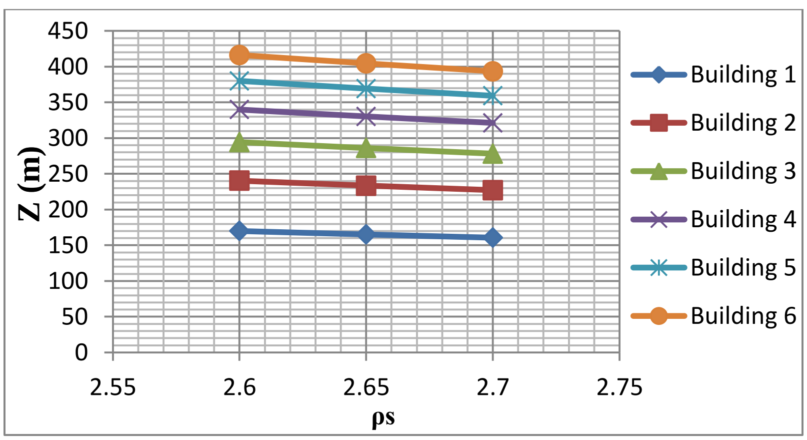

Scenario 43 below is based on average velocity of 1.03 m/s, average flood duration of 162 hours, maximum d_{90} of 0.0035 m and average flow depth of 1.86 m.

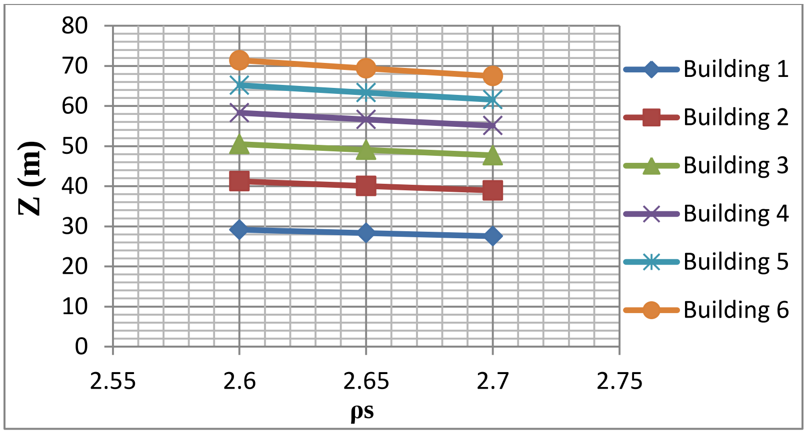

Scenario 44 below is based on average velocity of 1.03 m/s, average flood duration of 162 hours, average d_{90} of 0.0035 m and minimum flow depth of 0.06 m.

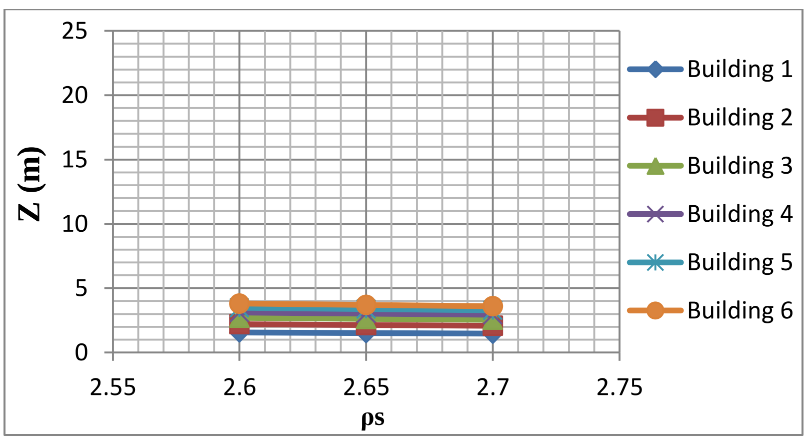

Scenario 45 below is based on average velocity of 1.03 m/s, average flood duration of 162 hours, average d_{90} of 0.0035 m and maximum flow depth of 3.66 m.

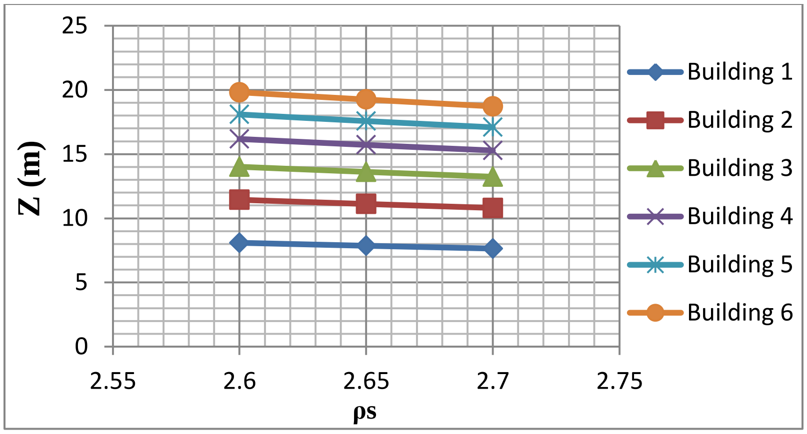

Based on the above plots it can be seen that scour depth magnitude decreases for increasing sediment density. And an increase of the constant values such as the velocity, flood duration and flow depth increased the scour magnitude. And the constant values such as the particle size (d_{90}) decreased the scour magnitude.

It can be established based on the overall results that the scour magnitude increased as the flow depth, velocity, building width and flood duration was increased. However, the scour magnitude decreased as the particle size and sediment density was increased. It can be seen that flow depth, flood duration, velocity, building width and particle size has an effect on the scour magnitude but velocity is more sensitive than the other parameters for Kohli and Hager (2001) equation. It can also be seen that sediment density is the least sensitive parameters.

Nadal et al. (2010)

28 analyses were done to evaluate the parameters for Nadal et al. (2010) equation. The plots below shows the effects of velocity, flow depth, particle size (d_{50}) and flood duration respectively on the scour depth for a scenario when one constant is increased. (i.e analyze the effect of velocity with constant soil properties, flood duration, but varying flow depth (average, minimum and maximum flow depth).

Scenario 1 below is based on average flood duration of 2.9 days, average d_{50} of 0.0004 m and average flow depth of 1.86 m.

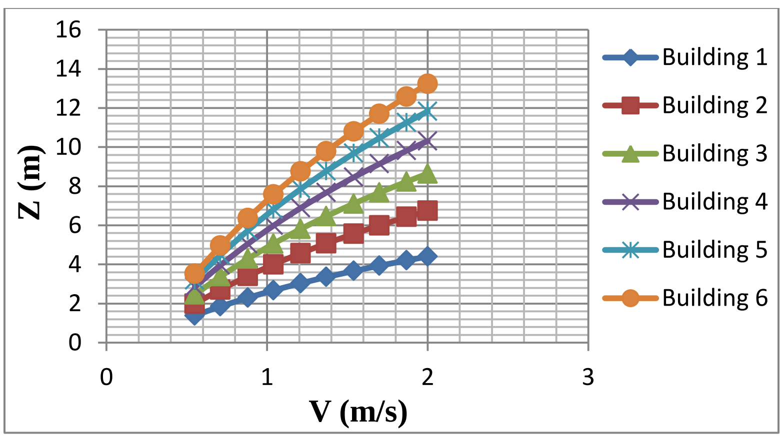

Scenario 2 below is based on average flood duration of 2.9 days, average d_{50} of 0.0004 m and minimum flow depth of 0.06 m.

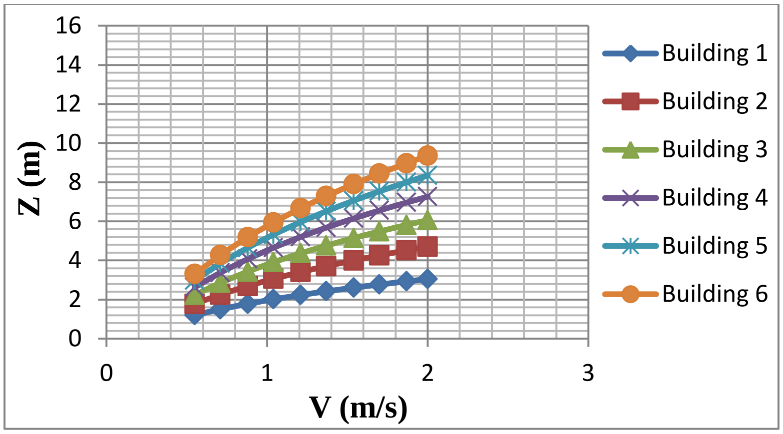

Scenario 3 below is based on average flood duration of 2.9 days, average d_{50} of 0.0004 m and maximum flow depth of 3.66 m.

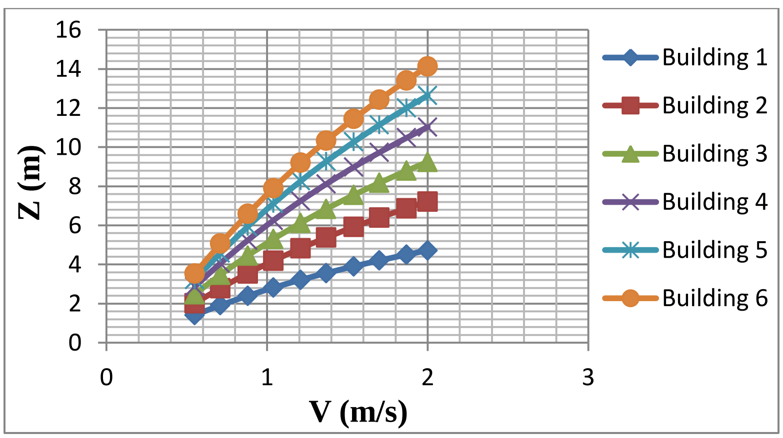

Scenario 4 below is based on minimum flood duration of 1 hour, average d_{50} of 0.0004 m and average flow depth of 1.86 m.

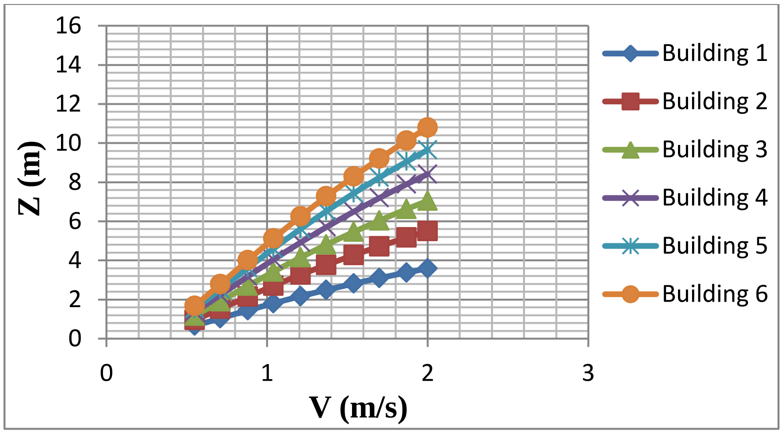

Scenario 5 below is based on maximum flood duration of 6.75 days, average d_{50} of 0.0004 m and average flow depth of 1.86 m.

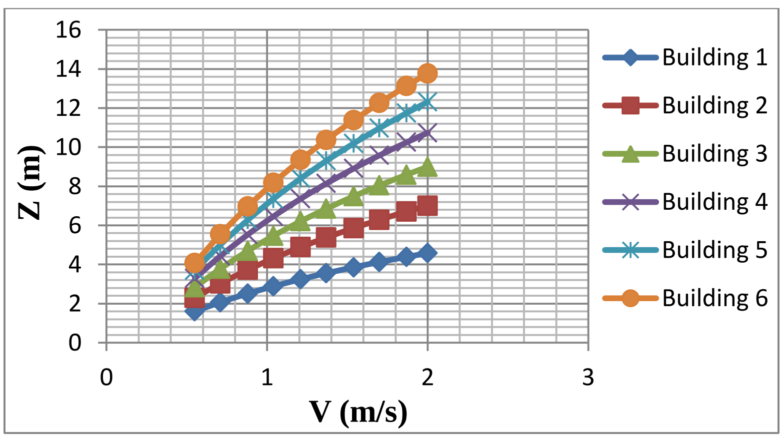

Scenario 6 below is based on average flood duration of 2.9 days, minimum d_{50} of 0.00017 m and average flow depth of 1.86 m.

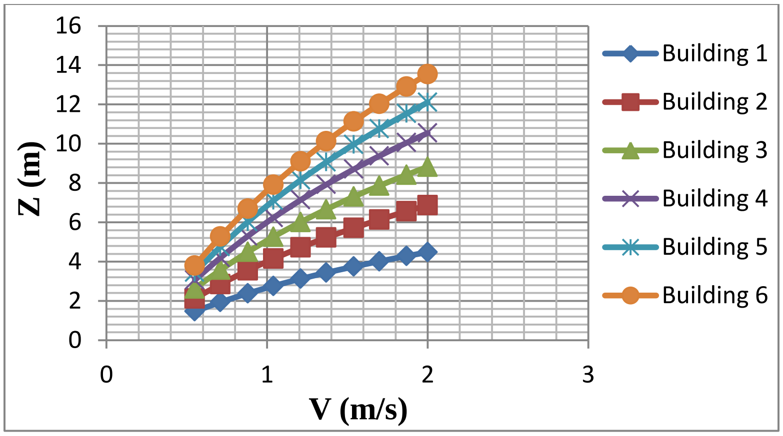

Scenario 7 below is based on average flood duration of 2.9 days, maximum d_{50} of 0.00063 m and average flow depth of 1.86 m.

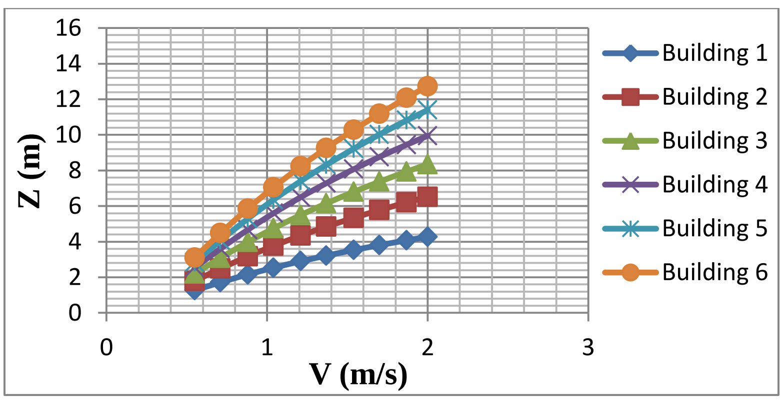

Based on this plots it can be seen that scour depth magnitude increases for increasing velocity. The scour depth is significantly increased due to the limitation of v/vc being greater than 1. And when the constant values were increased such as the flow depth and flood duration the scour magnitude increased while velocity is increasing. And the constant values such as the particle size decreased the scour magnitude as the velocity increases.

Scenario 8 below is based on average flood duration of 2.9 days, average d_{50} of 0.0004 m and average velocity of 1.29 m/s.

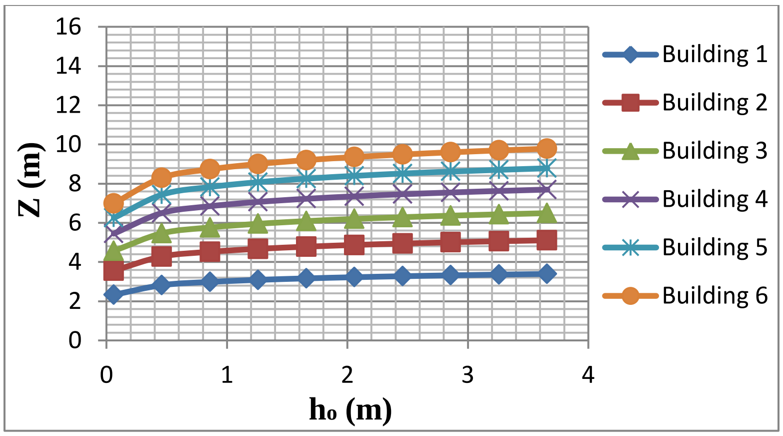

Scenario 9 below is based on average flood duration of 2.9 days, average d_{50} of 0.0004 m and minimum velocity of 0.55 m/s.

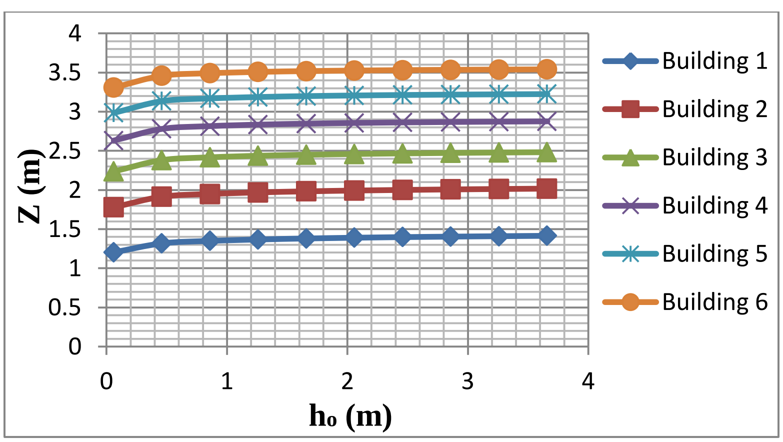

Scenario 10 below is based on average flood duration of 2.9 days, average d_{50} of 0.0004 m and maximum velocity of 2 m/s.

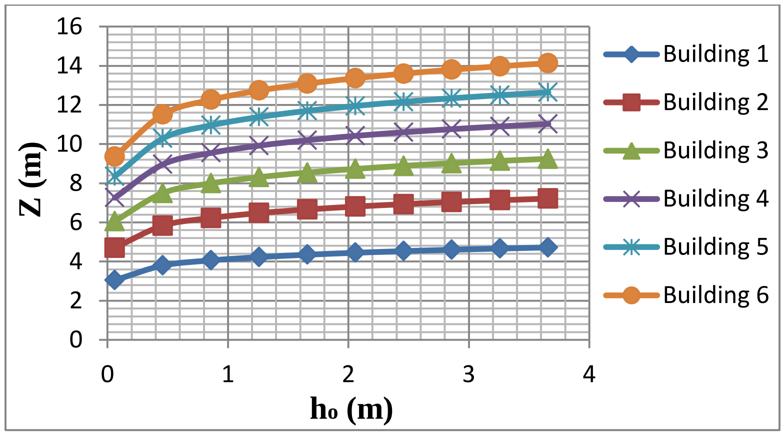

Scenario 11 below is based on minimum flood duration of 1 hour, average d_{50} of 0.0004 m and average velocity of 1.29 m/s.

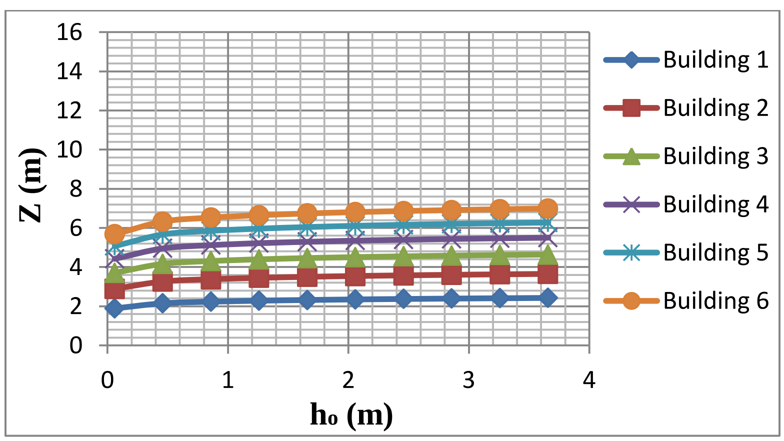

Scenario 12 below is based on maximum flood duration of 6.75 days, average d_{50} of 0.0004 m and average velocity of 1.29 m/s.

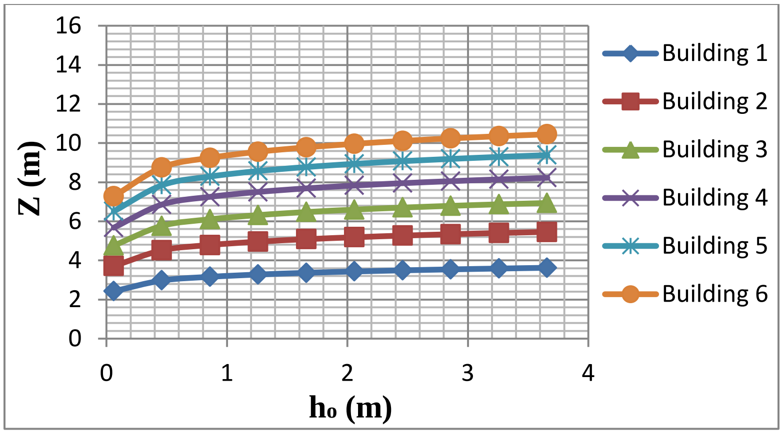

Scenario 13 below is based on average flood duration of 2.9 days, minimum d_{50} of 0.00017 m and average velocity of 1.29 m/s.

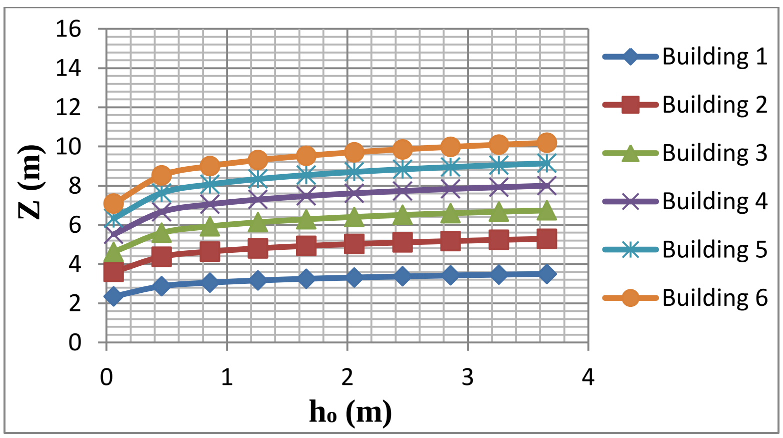

Scenario 14 below is based on average flood duration of 2.9 days, maximum d_{50} of 0.00063 m and average velocity of 1.29 m/s.

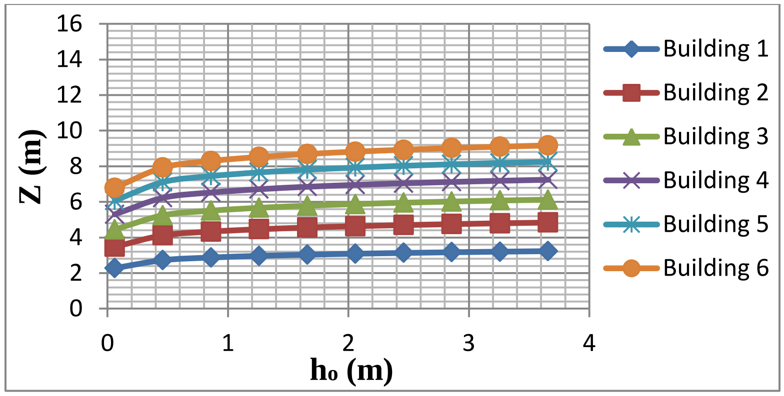

Based on this plots it can be seen that scour depth magnitude increases for increasing flow depth. The scour depth is significantly increased due to the limitation of v/vc being greater than 1. And when the constant values were increased such as the velocity and flood duration the scour magnitude increased while flow depth is increasing. And the constant values such as the particle size decreased the scour magnitude as the flow depth increases. Based on this results changing the constant velocity is very sensitive to the scour magnitude.

Scenario 15 below is based on average flood duration of 2.9 days, average flow depth 1.86 m and average velocity of 1.29 m/s.

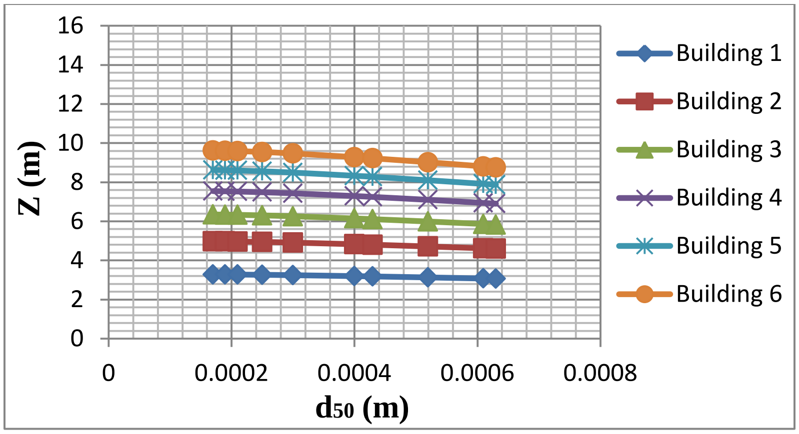

Scenario 16 below is based on average flood duration of 2.9 days, minimum flow depth 0.06 m and average velocity of 1.29 m/s.

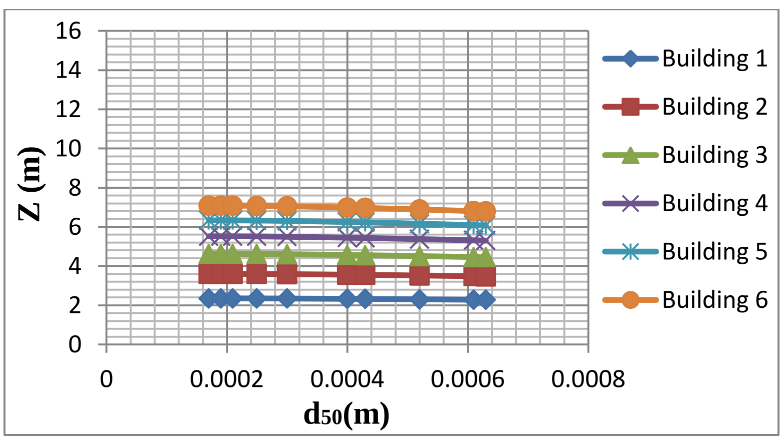

Scenario 17 below is based on average flood duration of 2.9 days, maximum flow depth 3.66 m and average velocity of 1.29 m/s.

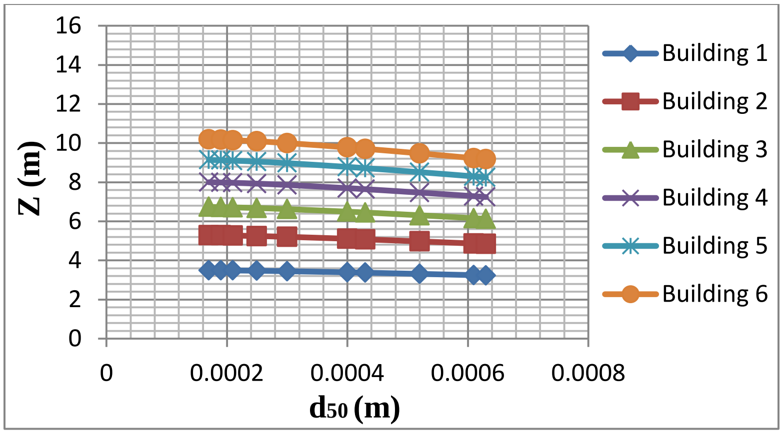

Scenario 18 below is based on minimum flood duration of 1 hour, average flow depth 1.86 m and average velocity of 1.29 m/s.

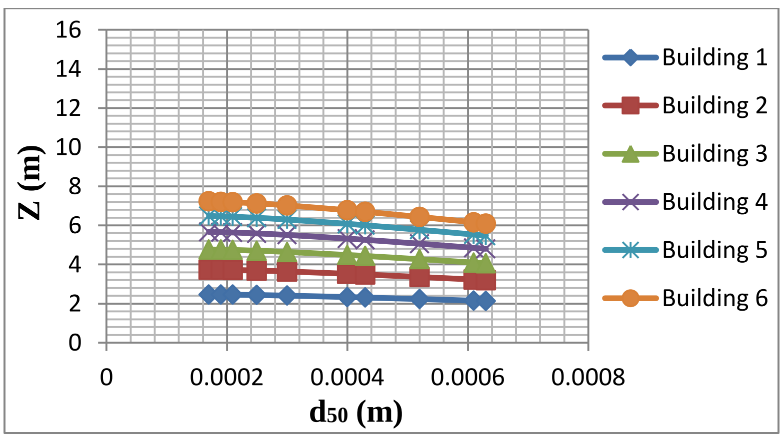

Scenario 19 below is based on maximum flood duration of 6.75 days, average flow depth 1.86 m and average velocity of 1.29 m/s.

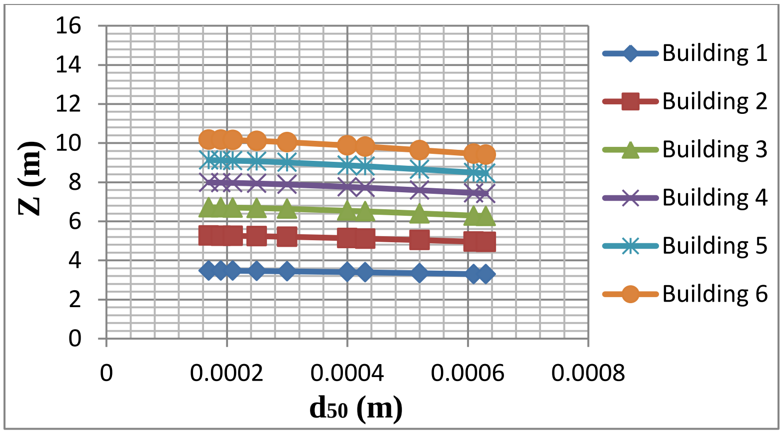

Scenario 20 below is based on average flood duration of 2.9 days, average flow depth 1.86 m and minimum velocity of 0.55 m/s.

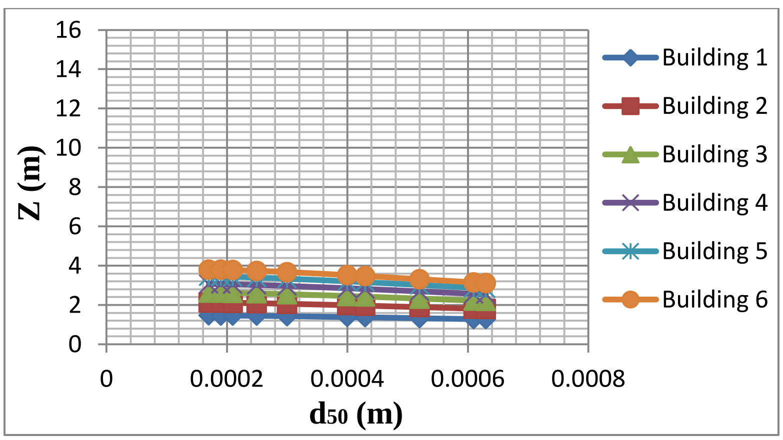

Scenario 21 below is based on average flood duration of 2.9 days, average flow depth 1.86 m and maximum velocity of 2 m/s.

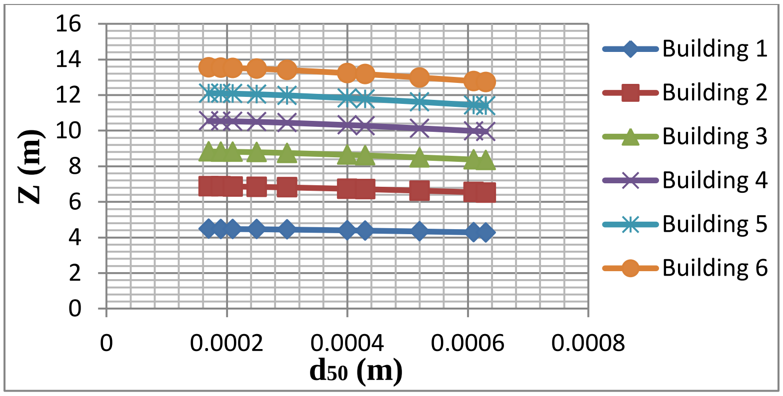

Based on this plots it can be seen that scour depth magnitude decreases for increasing particle size (d_{50}). The scour depth is significantly increased due to the limitation of v/vc being greater than 1. And when the constant values were increased such as the velocity, flow depth and flood duration the scour magnitude increased while flow depth is increasing. Based on this results changing the constant velocity is very sensitive to the scour magnitude.

Scenario 22 below is based on average flow depth 1.86 m and average velocity of 1.29 m/s and average of d_{50} of 0.0004 m.

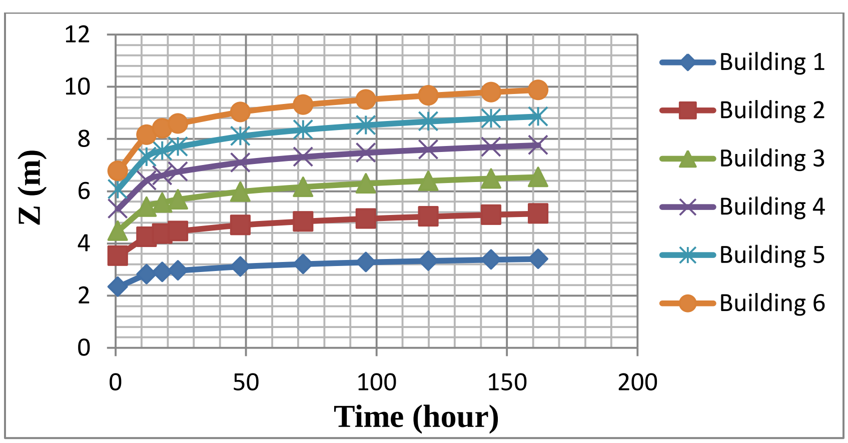

Scenario 23 below is based on minimum flow depth 0.06 m and average velocity of 1.29 m/s and average of d_{50} of 0.0004 m.

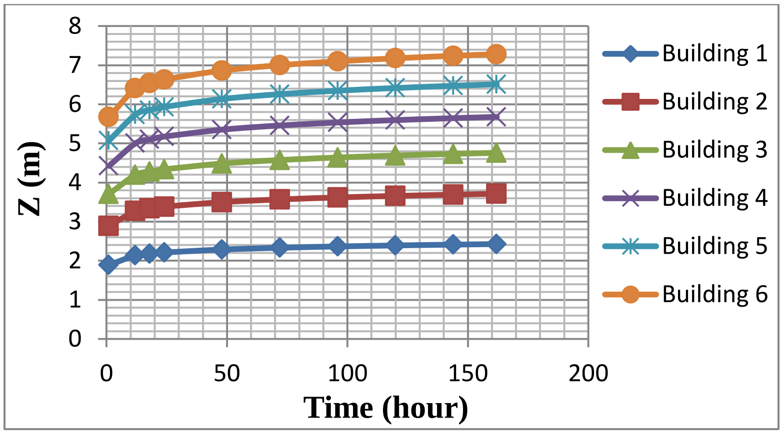

Scenario 24 below is based on maximum flow depth 3.66 m and average velocity of 1.29 m/s and average of d_{50} of 0.0004 m.

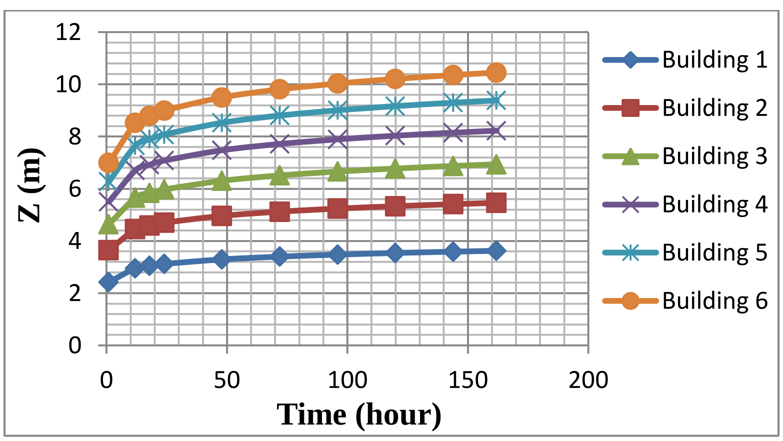

Scenario 25 below is based on average flow depth 1.86 m and minimum velocity of 0.55 m/s and average of d_{50} of 0.0004 m.

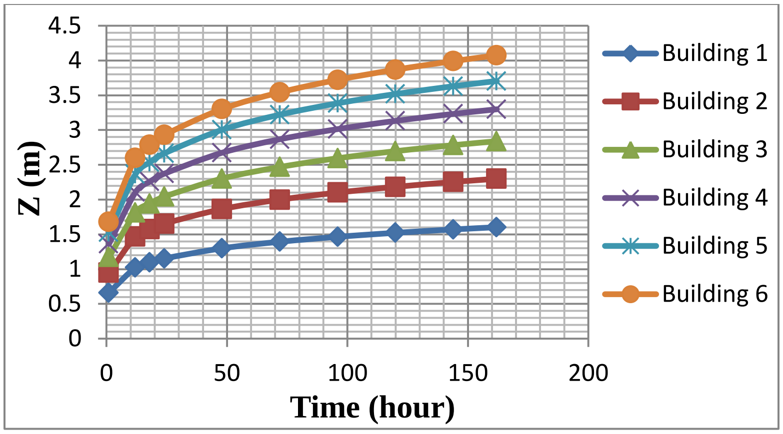

Scenario 26 below is based on average flow depth 1.86 m and maximum velocity of 2 m/s and average of d_{50} of 0.0004 m.

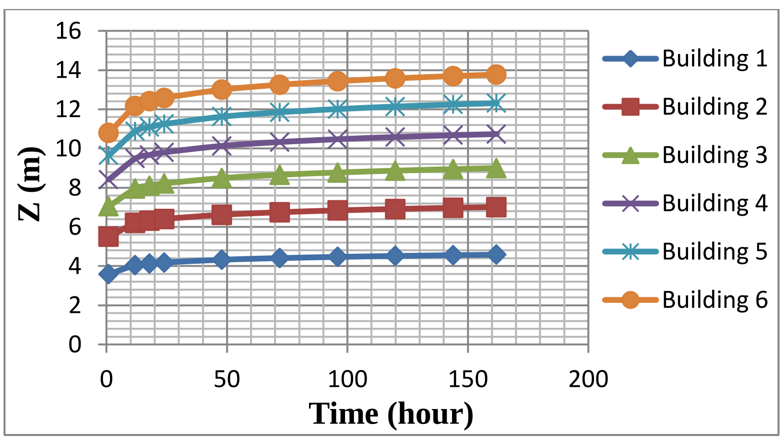

Scenario 27 below is based on average flow depth 1.86 m and average velocity of 1.29 m/s and minimum of d_{50} of 0.00017 m.

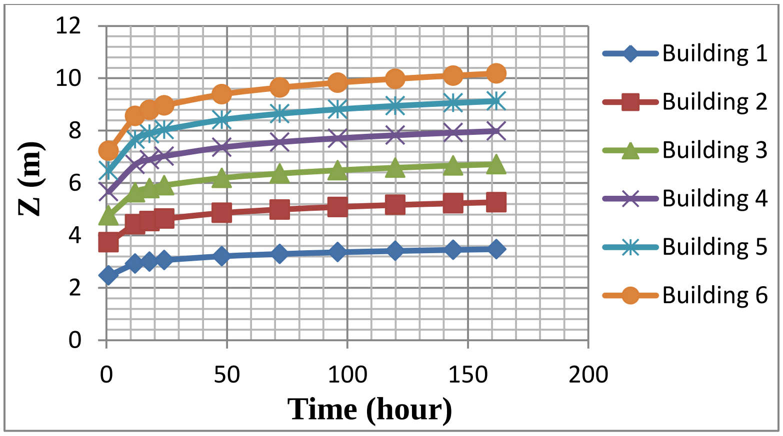

Scenario 28 below is based on average flow depth 1.86 m and average velocity of 1.29 m/s and maximum of d_{50} of 0.00063 m.

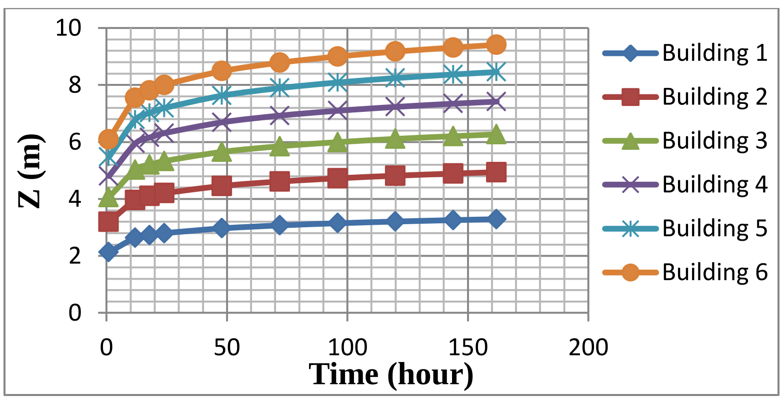

Based on the above plots it can be seen that scour depth magnitude increases for increasing flood duration. And an increase of the constant values such as the velocity and flow depth increased the scour magnitude. And the constant values such as the particle size (d_{90}) decreased the scour magnitude.

It can be established based on the overall results that the scour magnitude increased as the flow depth, velocity, building width and flood duration was increased. However, the scour magnitude decreased as the particle size was increased. It can be seen that flow depth, flood duration, velocity, building width and particle size has an effect on the scour magnitude but velocity is more sensitive than the other parameters for Nadal et al. (2010) equation. It can also be seen that particle size is the least sensitive parameters.

APPENDIX B: BUILDING INFORMATION

Obtaining Building Footprint and an example on ow to define the building angle and orientation

Building footprint for Monmouth County was obtained from Monmouth County division of planning website (https://co.monmouth.nj.us/page.aspx?ID=3866). The Monmouth County division of planning provides an access with a username and password to the file transfer protocol (FTP) site. Then the building footprint as a shapefile which can be opened in ArcGIS was downloaded from the FTP site. The footprints provided for this site lacks building geometry information therefore simplifying the building (as discussed in the paper) is important in order to obtain the missing information (building width and angle). After simplifying the building, the angle of the width is determined by using field calculator tool found on GIS and a script coded in the field calculator as shown below.

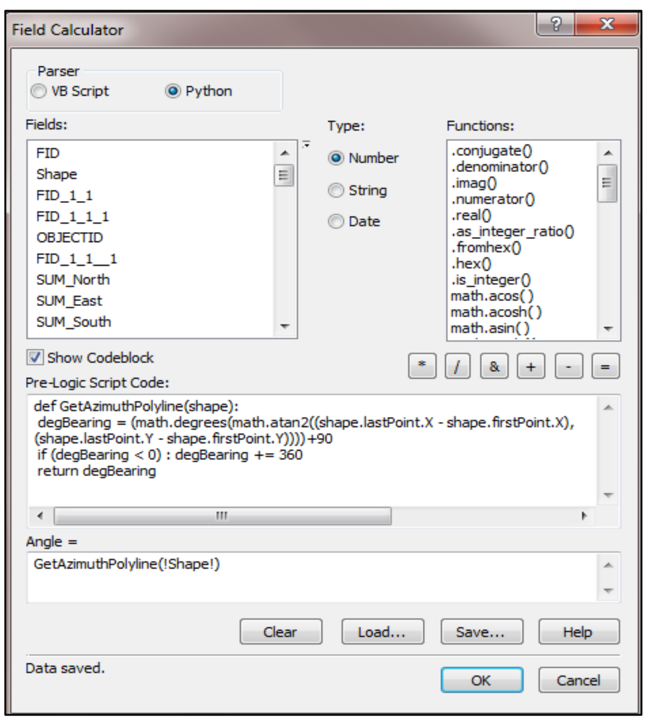

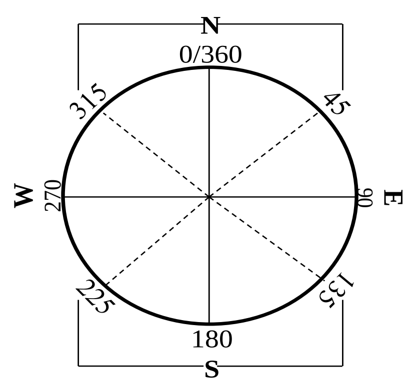

North = 0 – 45° and 315 – 360°
South = 135 – 225°
East = 45 – 135°
West = 225 – 315°

The building width angle will be defined based on the figure shown on the right side. The building width orientation is also defined by using the field calculator tool and the script code. An example on how to define the orientation is shown on the figure below. Defining the orientation is important to help select the side of the building that is perpendicular to the flow of water.

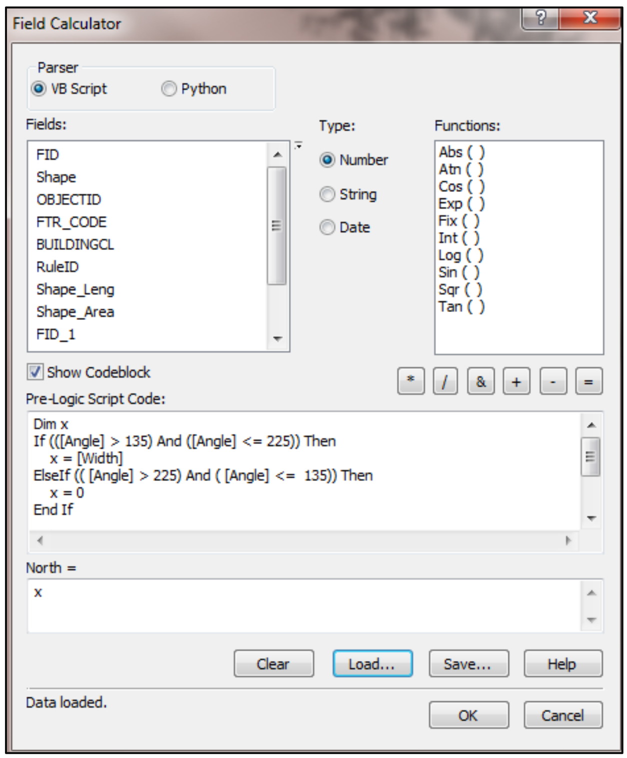

The script shown on the field calculator selects the building sides as south if the angle is between 135 and 225 degrees.

APPENDIX C: HYDRODYNAMIC DATA

How to create fishnet points to obtain flow information

Creating fishnet points are beneficial if your study area is wide and consists of numerous buildings. Fishnet points created for our study area are as shown below.

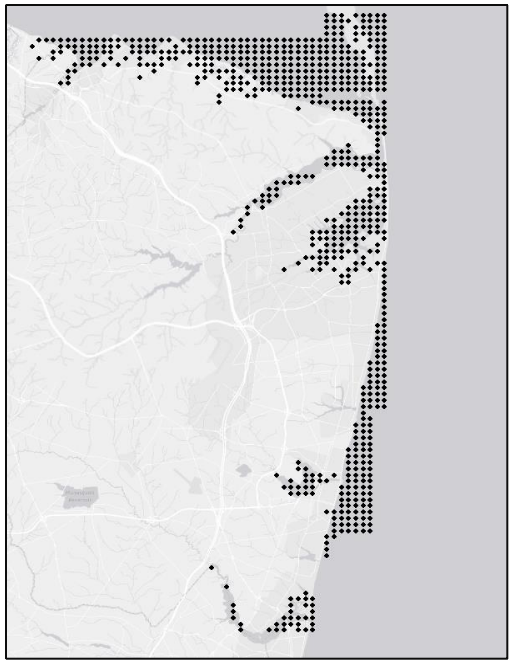

This points with feature id and x and y locations were used to obtain the water time series, and time series velocity from the storm surge model. Then the maximum velocity and the flood duration were extracted from the data obtained from the storm surge model (ADCIRC model). Then the maximum velocity and flood duration is assigned to each fishnet point based on the feature ID (FID) number. Finally, the fishnet points with the flood duration and maximum velocity were assigned to a building based on the closest distance using the spatial join tool found in GIS.

APPENDIX D: SOIL INFORMATION

Soil information and how to obtain particle size

Soil map for Monmouth County was also obtained from FTP site provided by the Monmouth County division of planning. The soil map was obtained as a shapefile which can be opened in ArcGIS. The soil map provided lacks the soil information therefore soil survey of Monmouth County, NJ was used to obtain the soil information (percentage finer for sieve number 4, 10, 40 and 200) for each soil type found in this county. The table below shows an example of the data provided from the soil map.

[The symbol < means less than; > means more than. Absence of an entry indicates that data were not estimated]

Soil name and map symbol	Depth	USDA texture	Classification		Frag-ments > 3 inches	Percentage passing sieve number--				Liquid limit	Plas-ticity index
			Unified	AASHTO		4	10	40	200		
	In				Pct					Pct	
AeA, AeB---------- Adelphia	0-8	Loam--------------	SM, SC, ML, CL	A-2-4, A-4	0	95-100	95-100	60-95	30-90	<35	NP-10
	8-38	Sandy clay loam, loam.	SM, SC, ML, CL	A-4, A-6	0	95-100	95-100	75-95	35-75	27-40	9-18
	38-60	Stratified loamy sand to sandy loam.	SM, SC, SP-SM	A-2-4, A-4	0	95-100	95-100	50-75	15-40	<23	NP-6
ALA*: Adelphia---------	0-8	Loam--------------	SM, SC, ML, CL	A-2-4, A-4	0	95-100	95-100	60-95	30-90	<35	NP-10
	8-38	Sandy clay loam, loam.	SM, SC, ML, CL	A-4, A-6	0	95-100	95-100	75-95	35-75	27-40	9-18
	38-60	Stratified loamy sand to sandy loam.	SM, SC, SP-SM	A-2-4, A-4	0	95-100	95-100	50-75	15-40	<23	NP-6
Urban land-------	0-6		---	---	---	---	---	---	---	---	---
At---------------- Atsion	0-20	Sand--------------	SP-SM, SM	A-3, A-1-B, A-2-4	0	95-100	90-100	45-80	5-35	---	NP
	20-28	Loamy sand, sand, sandy loam.	SM, SP-SM	A-2-4, A-3, A-1-B, A-4	0	95-100	85-100	40-75	5-40	---	NP
	28-38	Sand, loamy sand	SM, SM-SC, SP-SM	A-2-4, A-3, A-1-B	0	95-100	85-100	40-75	5-30	<20	NP-7
	38-60	Stratified sand to silt loam.	SM, SM-SC, SP-SM	A-2-4, A-3, A-4, A-1-B	0	95-100	70-100	35-100	5-90	<22	NP-7
Cm---------------- Colemantown	0-9	Loam--------------	SC, ML, CL	A-7, A-6	0	100	98-100	60-95	30-75	---	---
	9-36	Sandy clay, clay, clay loam.	ML, MH, SM	A-7	0	100	98-100	80-95	45-90	45-55	15-25
	36-60	Loam, clay loam, sandy loam.	SM, SC, ML, CL	A-4, A-6, A-7, A-2	0	95-100	95-100	60-95	30-80	30-45	5-20
CnB, CnC2, CnD3-- Collington	0-13	Sandy loam--------	SM, ML, SC, CL	A-2-4, A-4	0	95-100	95-100	60-95	30-85	20-30	5-10
	13-32	Sandy clay loam, sandy loam, clay loam.	SM, SC, CL, CL-ML	A-4, A-6, A-5, A-7-6	0	95-100	95-100	75-100	35-70	20-45	5-25
	32-60	Stratified sand to sandy loam.	SM, SC, SM-SC	A-2-4, A-4, A-1-B	0	95-100	95-100	50-70	10-40	<30	NP-10
CoA--------------- Collington	0-13	Loam--------------	SM, ML, SC, CL	A-2-4, A-4	0	95-100	95-100	60-95	30-85	20-30	5-10
	13-32	Sandy clay loam, sandy loam, clay loam.	SM, SC, CL, CL-ML	A-4, A-6, A-5, A-7-6	0	95-100	95-100	75-100	35-70	20-45	5-25
	32-60	Stratified sand to sandy loam.	SM, SC, SM-SC	A-2-4, A-4, A-1-B	0	95-100	95-100	50-70	10-40	<30	NP-10

Using the information obtained from the soil survey, the maximum grain size distributions were plotted for the soils that are found in the study area as presented below. The soils found in this region are sand with fine particles as discussed in the paper.

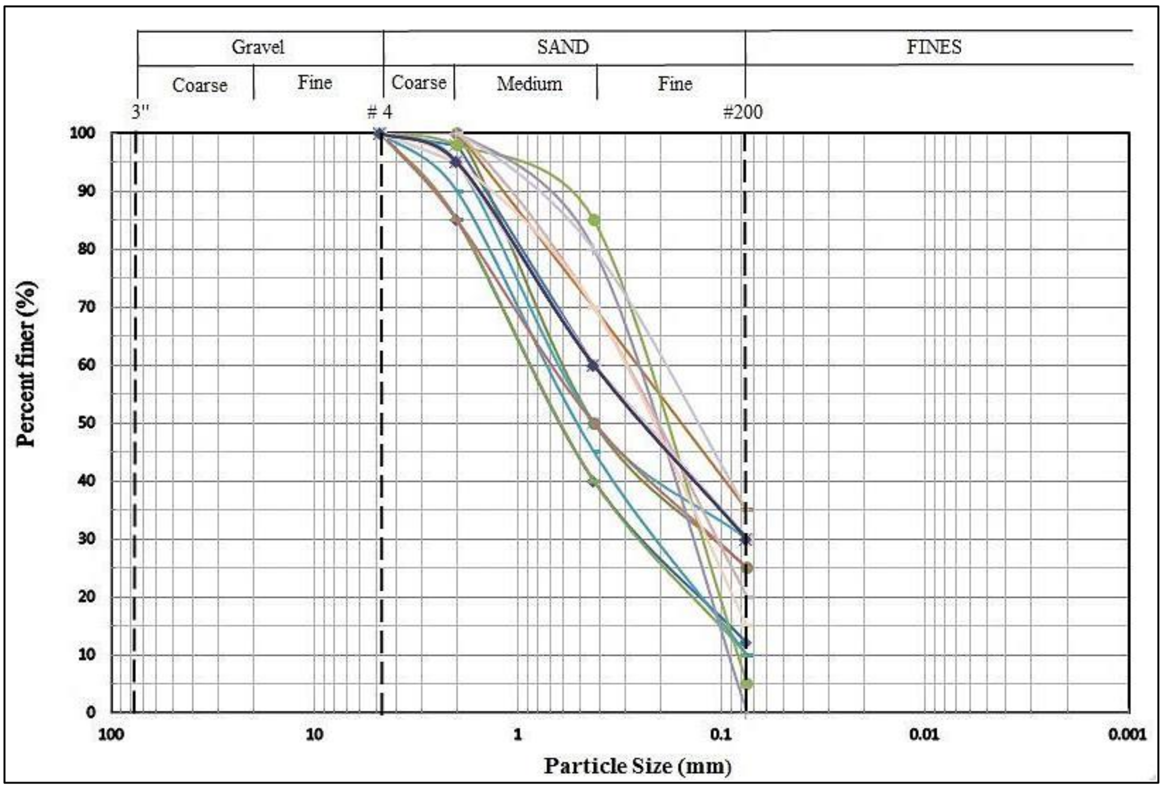

The grain size distributions were used to obtain the particle sizes which are required for the scour equations. An example of how to obtain d_{50} and d_{90} values and the values for each soil type can be seen below.

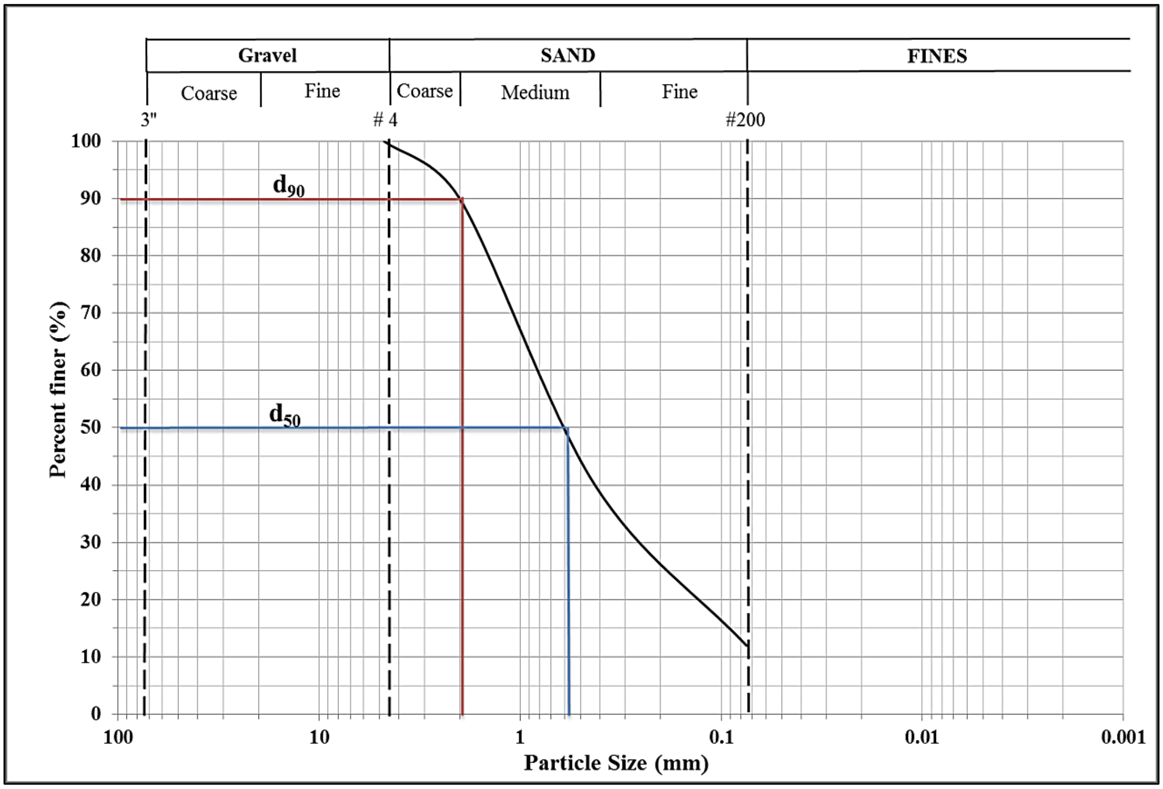
Gravel
SAND
FINES
Coarse
Fine
Coarse
Medium
Fine
3"
4
#200
d90
d50
Percent finer (%)
Particle Size (mm)
100
90
80
70
60
50
40
30
20
10
0
100
10
1
0.1
0.01
0.001

Soil Type	d_{50} (mm)	d_{90} (mm)	d_{50} (m)	d_{90} (m)
Adelphia Loam	0.25	0.00013	0.00025	0.00000013
Appoquinimink Silty loam	1.8	0.25	0.0018	0.00025
Atsion sand	0.52	2	0.00052	0.002
Berryland Sand	0.42	3.1	0.00042	0.0031
Colemantown Loam	0.25	1.5	0.00025	0.0015
Collington Loam	0.25	1.7	0.00025	0.0017
Collington Sandy Loam - urban land complex	0.25	1.7	0.00025	0.0017
Colts Neck Sandy Loam	0.42	1.6	0.00042	0.0016
Downer Loamy Sand	0.6	1.5	0.0006	0.0015
Dower Sandy Loam	0.42	1.5	0.00042	0.0015
Elkton Loam	0.17	1.2	0.00017	0.0012
Evesboro Sand/Urban land complex	0.63	2.5	0.00063	0.0025
Fallsington Loam	0.2	1.3	0.0002	0.0013
Fluvaquents Loam	1.7	1.4	0.0017	0.0014
Fort mott Loam	0.42	1.5	0.00042	0.0015
Freehold Loamy Sand	0.41	1.7	0.00041	0.0017
Freehold Sandy Loam - urband land complex/ loam	0.25	1.8	0.00025	0.0018
Hammonton Loamy Sand	0.61	2.5	0.00061	0.0025
Hammonton Sandy Loam / Urban land complex	0.42	2.5	0.00042	0.0025
Holmdel Sandy Loam/Urban land complex	0.25	1.5	0.00025	0.0015
Hooksan Sand	0.19	0.53	0.00019	0.00053
Hooksan Variant Sand	0.52	2	0.00052	0.002
Humaquepts	0.25	1.7	0.00025	0.0017
Keyport Sandy loam/Urban land Complex	0.25	1.7	0.00025	0.0017
Klej Laomy Sand/Urban land Complex	0.41	1.8	0.00041	0.0018
Klej Loamy Sand b	0.41	1.8	0.00041	0.0018
Kresson Loamy	0.41	2.8	0.00041	0.0028
Lakehurst Sand	0.43	1.8	0.00043	0.0018
Lakewood Sand	0.6	2	0.0006	0.002
Manahwkin Sand, Gravelly Sand	0.4	1.5	0.0004	0.0015
Marlton Loam/ Sandy loam	0.41	3.1	0.00041	0.0031
Pemberton Loamy sand	0.22	0.9	0.00022	0.0009
Phalanx Loamy Sand	0.6	2.5	0.0006	0.0025
Pits clay	0.25	1.15	0.00025	0.00115
Pits sand and Gravel	0.4	1.5	0.0004	0.0015
Psamments Sand	0.19	0.53	0.00019	0.00053
Sandy and Silty land	0.32	1.14	0.00032	0.00114
Sassafras Sandy Loam/Loam	0.4	3	0.0004	0.003
Sassafras Gravelly Sandy Loam	0.59	3.5	0.00059	0.0035
Shrewsbury Sandy Loam	0.25	1.6	0.00025	0.0016
Tinton Loamy Sand/Urban land complex	0.21	1.3	0.00021	0.0013
Udorthents Loam/Urban land complex	0.25	1.7	0.00025	0.0017
Woodstown Loam/Sandy Loam	0.25	1.4	0.00025	0.0014

After obtaining the d_{50} and d_{90} for each soil type then join this information with the soil map obtained from the County. Sediment density of the soil is also joined to the soil map.

Based on the literatures on sediment density, it was found that sediment density values ranges from 2.6-2.7 g/cm^3 and they are typically taken as 2.65 g/cm^3.

APPENDIX E: FEMA-MOTF DATA

Obtaining data from FEMA-MOTF database

FEMA-MOTF data was obtained from Hurricane Sandy Impact Analysis (https://www.arcgis.com/home/item.html?id=307dd522499d4a44a33d7296a5da5ea0). The data provided is in the form of ArcGIS shapefile and an example of the data is shown below.

FID	Shape *	ID	LONGITUDE	LATITUDE	STATEABBR	COUNTYNAME	STATENAME	DAMAGE	INUNDATED	DAMAGETYPE	DMG_COMB	DEPTH_COMB
0	Point	2181362	-73.997168	40.309516	NJ	Monmouth	New Jersey	No Damage	Y	INUNDATION ONLY	Minor	2.180158
1	Point	2181364	-73.987633	40.314646	NJ	Monmouth	New Jersey	No Damage	Y	INUNDATION ONLY	Major	6.41138
2	Point	2181372	-73.99702	40.30934	NJ	Monmouth	New Jersey	No Damage	Y	INUNDATION ONLY	Minor	2.046004
3	Point	2181386	-73.996875	40.309117	NJ	Monmouth	New Jersey	No Damage	Y	INUNDATION ONLY	Affected	1.682364
4	Point	2181389	-73.97448	40.36413	NJ	Monmouth	New Jersey	Minor	Y	DAMAGE AND INUNDATION	Major	5.838392
5	Point	2181394	-73.991926	40.403755	NJ	Monmouth	New Jersey	No Damage	Y	INUNDATION ONLY	Major	5.433212
6	Point	2181398	-73.974325	40.363694	NJ	Monmouth	New Jersey	Destroyed	Y	DAMAGE AND INUNDATION	Destroyed	5.770733
7	Point	2181413	-73.974798	40.364084	NJ	Monmouth	New Jersey	Destroyed	Y	DAMAGE AND INUNDATION	Destroyed	6.453705
8	Point	2181415	-73.997018	40.310054	NJ	Monmouth	New Jersey	No Damage	Y	INUNDATION ONLY	Affected	1.78614
9	Point	2181417	-73.990288	40.404553	NJ	Monmouth	New Jersey	No Damage	Y	INUNDATION ONLY	Minor	2.421611
10	Point	2181420	-73.996913	40.309917	NJ	Monmouth	New Jersey	No Damage	Y	INUNDATION ONLY	Minor	2.308371
11	Point	2181423	-73.975026	40.364041	NJ	Monmouth	New Jersey	Destroyed	Y	DAMAGE AND INUNDATION	Destroyed	6.085763
12	Point	2181429	-73.996792	40.309655	NJ	Monmouth	New Jersey	No Damage	Y	INUNDATION ONLY	Minor	2.320533
13	Point	2181432	-73.98732	40.314321	NJ	Monmouth	New Jersey	No Damage	Y	INUNDATION ONLY	Major	6.285932
14	Point	2181437	-73.99187	40.403849	NJ	Monmouth	New Jersey	No Damage	Y	INUNDATION ONLY	Major	5.685339
15	Point	2181469	-73.979102	40.323467	NJ	Monmouth	New Jersey	No Damage	Y	INUNDATION ONLY	Major	6.166275
16	Point	2181472	-73.986983	40.336585	NJ	Monmouth	New Jersey	No Damage	Y	INUNDATION ONLY	Minor	2.675529
17	Point	2181473	-73.991816	40.403923	NJ	Monmouth	New Jersey	No Damage	Y	INUNDATION ONLY	Major	5.455809
18	Point	2181477	-73.991722	40.403868	NJ	Monmouth	New Jersey	No Damage	Y	INUNDATION ONLY	Major	5.536948
19	Point	2181481	-73.97304	40.36539	NJ	Monmouth	New Jersey	Major	Y	DAMAGE AND INUNDATION	Major	-9999
20	Point	2181483	-73.996246	40.30888	NJ	Monmouth	New Jersey	No Damage	Y	INUNDATION ONLY	Affected	1.907527
21	Point	2181486	-73.986579	40.314717	NJ	Monmouth	New Jersey	No Damage	Y	INUNDATION ONLY	Minor	4.394855
22	Point	2181491	-73.989821	40.404519	NJ	Monmouth	New Jersey	No Damage	Y	INUNDATION ONLY	Minor	2.266897
23	Point	2181495	-73.991521	40.403759	NJ	Monmouth	New Jersey	No Damage	Y	INUNDATION ONLY	Major	5.406629
24	Point	2181505	-73.989863	40.404458	NJ	Monmouth	New Jersey	No Damage	Y	INUNDATION ONLY	Affected	1.743834
25	Point	2181507	-73.995767	40.309301	NJ	Monmouth	New Jersey	Affected	Y	DAMAGE AND INUNDATION	Affected	1.273359

For this study only inundation damage was extracted from the different damage type and the damage combo and depth related to that building.

REFERENCES

Arneson LA, Zevenbergen LW, Lagasse PF, Clopper PE (2012) Evaluating Scour at Bridges. Hydraulic Engineering Circular No. 18 fifth edition https://www.fhwa.dot.gov/engineering/hydraulics/pubs/hif12003.pdf

Atkinson J, Roberts H, Hagen SC, Zhou S, Bacopoulos P, Medeiros S, Weishampel J, Cobell Z (2011) Deriving Frictional Parameters and Performing Historical Validation for an ADCIRC storm surge model of the Florida Gulf Coast. Florida Watershed Journal No.4 22-27

Avinmelech Y (2001) Water content, organic carbon and dry bulk density in flooded sediments. Agricultural Engineering No.25 25-33

Banks JC, Camp JV, Abkowitz MD (2014) Scale and Resolution Considerations in the Application of HAZUS-MH 2.1 to Flood Risk Assessments Natural Hazards Earth System Sciences 12:3733–3752. doi: 10.1061/(ASCE)NH.1527- 6996. .0000160

Barkdoll BB (2000) Discussion of: Time scale for local scour at bridge piers. J. Hydraul. Eng. 126(10): 793–794. doi: 10.1061/ (ASCE)0733-9429

Blake GR, Hartge KH (1986) Particle density. In: Klute, ed. Methods of Soil Analysis, Part 1. Physical and Mineralogical Methods. American Society of Agronomy. No. 9, Madison, 363-375

Blake ES, Berg TB, Cangialosi JP, Beven JL (2013) Tropical Cyclone Report: Hurricane Sandy. Report number AL182012, National Hurricane center http://www.nhc.noaa.gov/data/tcr/AL182012_Sandy.pdf

Boyd CE (1995) Bottom Soils, Sediment, and Pond Aquaculture. Chapman & Hall, New York, p. 348

Briaud JL, Govindasamy AV, Kim D, Gardoni P, Olivera F, Chen H-C, Mathewson C, Elsbury K (2009) Simplified Method For Estimating Scour at Bridges. FHWA/TX-09/0-5505-1

Briaud JL, Ting FKF, Chen HC, Guadavalli R, Perugu S, Wei, G (1999) SRICOS: Prediction of Scour Rate in Cohesive Soils at Bridge Piers. J. Geotec. Geoenviron. Eng 125 (4): 237-246. doi: 10.1061/ (ASCE)1090-0241

Bunya S et al (2010) A High-Resolution Coupled Riverine Flow, Tide, Wind, Wind Wave, and Storm Surge Model for Southern Louisiana and Mississippi. Part I: Model Development and Validation. Monthly Weather Review 138:345–377

Chen J, Huang Z, Jiang C, Deng B, Long Y (2013) Tsunami-induced scour at coastal roadways: a laboratory study. Nat. Hazard. doi: 10.1007/s11069-013-0727-6

Coduto DP, Yeung MR, Kitch WA (2011) Geotechnical Engineering. Pearson, NJ

Das BM, Sobohan K (2006) Principles of Geotechnical Engineering. Cengage Learning

Deng L, Cai CS (2010) Bridge Scour: Prediction, Modeling, Monitoring. And Countermeasures Review Practice Periodical on Structural Design and Construction. 15:125-134.doi: 10.1061/ASCESC.1943-5576.0000041

Dietrich JC et al. (2010) A High-Resolution Coupled Riverine Flow, Tide, Wind, Wind

Wave, and Storm Surge Model for Southern Louisiana and Mississippi. Part II: Synoptic Description and Analysis of Hurricanes Katrina and Rita. Monthly Weather Review 138: 378–404.

Dietrich JC, Zijlema M, Westerink JJ, Holthuijsen LH, Dawson C, Luettich RA, Jensen R, Smith JM, Stelling GS, Stone GW (2011) Modeling hurricane waves and storm surge using integrally-coupled, scalable computations. Coastal Engineering, 58(1), 45-65

Ettema RE (1980) Scour at Bridge Piers. University of Auckland

FEMA (2009) Technical Manual HAZUS-MH MR4: Flood Model. Washington, DC, FEMA

FEMA (2013) A Year after Hurricane Sandy: New Jersey Recovery by the Numbers. http://www.fema.gov/news-release/2013/10/25/year-after-hurricane-sandy-new-jersey-recovery-numbers

FEMA (2013) Hurricane Sandy in New Jersey and New York. Mitigation Assessment Team Report http://www.fema.gov/medialibrarydata/1386850803857025eb299df32c6782fdcbb6f69b35b13/Combined_Sandy_MAT_Report_508post.pdf

FEMA-MOTF (2014) Hurricane Sandy Impact Analysis. https://www.arcgis.com/home/item.html?id=307dd522499d4a44a33d7296a5da5ea0

Ferreira, C. M.; Irish, J.; Olivera, F (2014) "Quantifying the potential impact of land cover changes due to sea-level rise on storm surge on lower Texas coast bays" Coastal Engineering, (94), 102-111

Froehlich DC (1989) Local Scour at Bridge Abutments. Proc. National Conference on Hydraulic Engineering, ASCE, New orleans, LA, pp. 13-18

Garratt JR (1977) Review of drag coefficients over oceans and continents. Monthly Weather Review 105:915–929

Govindasamy AV, Briaud JL, Kim D, Olivera F, Gardoni P, Delphia J (2013) Observation Method for Estimating Future Scour Depth at Existing Bridges. J. Geotec. Geoenviron. Eng 139(7), 1165-1175. doi: 10.1061/(ASCE)GT.1943-5606.0000838

Hallegatte S, Green C, Nicholls RJ, Morlot JC (2013) Future flood losses in major coastal cities. Nature Climate Change. doi: 10.1038/NCLIMATE1979

Hatzikyriakou A, Lin N, Gong J, Xian S, Hu X, Kennedy A (2015) Component-Based Vulnerability Analysis for Residential Structures Subjected to Storm Surge Impact from Hurricane. Sandy Nat. Hazards Rev. doi: 10.1061/ (ASCE) NH.1527-6996.0000205

Hillel D (1980) Fundamentals of Soil Physics. Academic Press, Inc., N.Y.

Holland GJ (1980) An analytic model of the wind and pressure profiles in hurricanes. Monthly Weather Review 108:1212–1218

Interagency Performance Evaluation Taskforce (IPET) (2007) Performance Evaluation of the New Orleans and South East Louisiana Hurricane Protection System. U.S. Army Corps of Engineers Final rep. vol. 4 http://biotech.law.lsu.edu/katrina/ipet/FINAL%20Vol%20IV%20The%20Storm%20-%20maintext.pdf

Jones JS (1983) Comparison of prediction equations for bridge pier and abutment scour. Transportation Research Record 950, Second Bridge Engineering Conference, vol. 2, Transportation Research board, Washington, DC

Jongman B et al. (2012) Comparitive flood damage model assessment: towards a European approach. Natural Hazards Review. doi: 10.5194/nhess-12-3733-2012

Kerr PC, Martyr RC, Donahue AS, Hope ME, Westerink JJ, Luettich Jr RA, Kennedy AB, Dietrich JC, Dawson C, Westerink HJ (2013) U.S IOOS coastal and ocean modeling testbed: Evaluation of tide, wave, and hurricane surge response sensitivities to mesh resolution and friction in the Gulf of Mexico. J. Geophys. Res. Oceans 118. doi: 10.1002/jgrc.20305

Kohli A, Hager WH (2001) Building Scour in Floodplains. Water &Maritime Engineering 148 (2):61-80

Kreibich H, Seifert I, Merz B, Thieken AH (2010) Development of FLEMOcs - A New Model for the estimation of flood losses in the commercial sector. Hydrological Science 55 (8):1302-1314.doi: 10.1080/02626667.2010.529815

Landsea C, Franklin J, Beaven J (2015) The Revised Atlantic Hurricane Database (HURDAT2). http://www.nhc.noaa.gov/data/hurdat/hurdat2-format-atlantic.pdf

Le Provost C, Genco ML, Lyard F, Vincent P, Canceil P (1994) Spectroscopy of the world ocean tides from a finite element hydrodynamic model. J. Geophys. Res. Oceans 99: 24777–24797

Liu Y, Ma X, Sun Y (2012) Flood Damage to Rural Buildings Result from Foundation Scour and Scour Protection Strategy Applied Mechanics and Materials. 166-169: 2627-2630. doi: 10.4028/ www.scientific.net/AMM.166-169.2627

Mattocks C, Forbes C (2008) A real-time, event-triggered storm surge forecasting system for the state of North Carolina. Ocean Modelling 25: 95–119

Mattocks C, Forbes C, Ran L (2006) Design and implementation of a real-time storm surge and flood forecasting capability for the State of North Carolina. UNC–CEP Technical Report 103

Melville BW, Chiew YM (1999) Time Scale for Local Scour at Bridge Piers. Journal of Hydraulic Engineering 125: 59-65. doi: 10.1061/ (ASCE)0733-9429

Nadal NC, Melby JA, Gonzalez VM, Cox AT (2015) Northern Atlantic Coast Comprehensive Study (NACCS) - Coastal Storms Hazards from Virginia to Maine. Technical Report. U.S. Army Engineer Research and Development Center, Vicksburg, MS.

Nadal NC, Zapata RE, Pagan I, Lopez R, Agudelo J (2010) Building damage due to riverine and coastal floods. J. Water Resource Planning Management 136(3):327-336. doi: 10.1061/(ASCE) WR.19435452.0000036

Penning-Rowsell E, Johnson C (2005) The benefits of Flood and Coastal Risk Management: A Manual of assessment techniques. Middlesex Univ. Press, UK

Resio DT, Westerink JJ (2008) Modeling the physics of storm surges. Physics Today 61:33-38

Richardson EV, Davis SR (2001) Evaluating Scour at Bridges. Federal Highway Agency, National Highway Institute, Hydraulic Engineering Circular 18: NHI 01-001 http://www.stream.fs.fed.us/fishxing/fplibrary/FHWA_2001_Evaluating_Scour_at_Bridges.pdf

Robertson IN, Riggs HR, Yim SCS, Young YL (2007) Lessoms from Hurricane Katrina Storm Surge on Bridges and Buildings. J. Waterway, Port, coastal, Ocean Eng. doi: 10.1061/(ASCE)0733-950X

Scawthorn C, Blais N, Seligson H, Tate E, Mifflin E, Thomas W, Murphy J, Jones C (2006) HAZUS-MH Flood Loss Estimation Methodology. I. Overview and Flow Hazard Characterization. Natural Hazards Review 7(2):60-71. doi: 10.1061/ (ASCE) 1527-6988 (2006) 7:2 (60)

Schaller J, Mattos C (2009) Gis Model Applications for Sustainable Development and Environmental Planning at the Regional Level: GeoSpatial Visual Analytics, Springer Netherlands, pp 45-57

Shen GW, Schneider VR, Karaki S (1969) Local Scour around Bridge Piers. Journal of hydraulic division 95(HY6): 1919-1940

Tate E, Munoz C, Suchan J (2014) Uncertainty and Sensitivity Analysis of the HAZUS-MH Flood Model. Natural Hazards Earth System Sciences 12:3733–3752. doi: 10.1061/ (ASCE) NH.1527-6996.0000167

Wagenaar DJ, De Bruijn KM, Bouwer LM, De Moel H (2015) Uncertainty in flood damage estimates and its potential effect on investment decisions. Nat. Hazards Earth Syst. Sci. Discuss 3:607-640. doi: 10.5194/nhessd-3-607-2015

Westerink JJ, Luettich RA, Feyen JC, Atkinson JH, Dawson C, Roberts HJ, Powell MD, Dunion JP, Kubatko EJ, Pourtaheri H (2008) A basin- to channel-scale unstructured grid hurricane storm surge model applied to southern Louisiana. Monthly Weather Review 136:833–864

Wolf J (2009) Coastal Flooding: impacts of coupled wave-surge-tide models. Nat Hazards 49:241-260.
doi 10.1007/s11069-008-9316-5

Xian S, Lin N, Hatzikyriakou A (2015) Storm surge damage to residential areas: a quantitative analysis for Hurricane Sandy in comparison with FEMA flood map. Nat. Hazards. doi: 10.1007/s11069-015-1937-x

Zevenbergen LW, Lagasse PF, Edge BL (2004) Tidal hydrology, hydraulics and bridge scour. Federal Highway Agency, National Highway Institute, Hydraulic Engineering Circular No. 25, Arlington, Va

BIOGRAPHY

Mariamawit Borga graduated from Piney Woods School, Piney woods, Mississippi, in 2010. She received her Bachelor of Science from Jackson State University in 2014.